Platelet-derived Growth Factor Receptor β Activation and Regulation in Primary Myelofibrosis

Inaugural-Dissertation

to obtain the academic degree

Doctor rerum naturalium (Dr. rer. nat.)

submitted to the Department of Biology, Chemistry and Pharmacy

of Freie Universität Berlin

by

Frederike Kramer

2019

This study was performed from January 2016 to June 2019 under supervision of Prof. Dr. Kai Kappert at Center for Cardiovascular Research (CCR), Charité - Universitätsmedizin Berlin.

ACKNOWLEDGEMENTS

TABLE OF CONTENTS

Abbreviations

AML	Acute myeloid leukemia
APS	Ammonium persulfate
BCR-ABL	Breakpoint cluster region-abelson fusion oncogene
bFGF	Basic fibroblast growth factor
bp	Basepairs
BRO1	BRO1 homology
BSA	Bovine serum albumin
Cad	Cadherin-like juxtamembrane sequence
CAH	Carbonic anhydrase-like
CALR	Calreticulin
CML	Chronic myeloid leukemia
CSF1R	Colony-stimulating factor 1 receptor
CSF3R	Colony-stimulating factor 3 receptor
DAPI	4′,6-Diamidino-2-phenylindole
DEP-1	Density-enhanced phosphatase 1
DMEM	Dulbecco's Modified Eagle Medium
DNA	Deoxyribonucleic acid
dNTP	Deoxynucleotide triphosphate
DTT	Dithiothreitol
ECM	Extracellular matrix
EDTA	Ethylenediaminetetraacetic acid
EGFR	Epidermal growth factor receptor
ER	Endoplasmic reticulum
ERK	Extracellular signal-regulated kinase
ET	Essential thrombocythemia
EtOH	Ethanol
FACS	Fluorescence-activated cell sorting
FBS	Fetal bovine serum
FDA	US Food and Drug Administration
FERM	FERM mephrin/A5/µ domain
FISH	Fluorescence *in situ* hybridization
FN	Fibronectin type III-like domain
GFP	Green fluorescent protein
Gly	Glycosylated
GO	Gene ontology
HCl	Hydrochloric acid
HD	Histidin domain
HRP	Horseradish peroxidase

HSC	Hematopoietic stem cell
IB	Immunoblot
Ig	Immunoglobulin
IHC	Immunohistochemistry
IL	Interleukin
JAK2	Janus kinase 2
KD	Knockdown
kDa	Kilodalton
KIM	Kinase-interacting motif
LDH	Lactate dehydrogenase
mAb	Monoclonal Antibody
MAM	Mephrin/A5/μ domain
Max	Maximum
MF	Myelofibrosis
mIHC	Multiplexed immunohistochemistry
Min	Minimum
MPN	Myeloproliferative neoplasm
MSC	Mesenchymal stromal cell
n/a	Not applicable
NaCl	Sodium chloride
NCBI	National Center for Biotechnology Information
NIH	National Institutes of Health
ns	Not significant
NT	Nontargeting
qPCR	Quantitative polymerase chain reaction
pAb	Polyclonal antibody
PBS	Phosphate-buffered saline
PCR	Polymerase chain reaction
PDGF	Platelet-derived growth factor
PDGFR	Platelet-derived growth factor receptor
PDGFRα	Platelet-derived growth factor receptor α
PDGFRβ	Platelet-derived growth factor receptor β
PI3K	Phosphatidylinositol 3-kinase
PLA	Proximity ligation assay
PLCγ1	Phospholipase C γ1
PLT	Platelet
PMF	Primary myelofibrosis
Pro	Proline-rich
PTP	Protein tyrosine phosphatase
PTPN	Non-receptor protein tyrosine phosphatase
PTPR	Receptor-like protein tyrosine phosphatase
PV	Polycythemia vera

PVDF	Polyvinylidene difluoride
RasGAP	GTPase activating protein of Ras
RBC	Red blood cell
RCP	Rolling circle product
RGDS	RGDS-adhesion recognition motif
RNA	Ribonucleic acid
RNAseq	RNA sequencing
SD	Standard deviation
SDS	Sodium dodecyl sulfate
SDS-PAGE	Sodium dodecyl sulfate-polyacrylamide gel electrophoresis
SEC14	SEC14/cellular retinalaldehyde-binding protein-like
SH2	Src homology 2
SHP-2	SH protein tyrosine phosphatase 2
STAT	Signal transducer and activator of transcription
TBS-T	Tris-buffered saline with Tween® 20
TC-PTP	T cell protein tyrosine phosphatase
TEMED	Tetramethylethylenediamine
TGFβ	Transforming growth factor β
UV	Ultraviolet
v/v	Volume per volume
VEGF	Vascular endothelial growth factor
vs.	*Versus*
w/v	Weight per volume
WBC	White blood cell
WHO	World Health Organization
WT	Wild type

List of tables

List of figures

[*] These figures were created using Servier Medical Art templates (licensed under a Creative Commons Attribution 3.0 Unported License).

URL: https://smart.servier.com

Abstract

Primary myelofibrosis (PMF) is a proliferative disease of the bone marrow which is characterized by the presence of somatic, acquired mutation in hematopoietic stem cells, a resulting proliferation of cells of the megakaryocytic lineage and, as the primary disease manifestation, progressive bone marrow fibrosis. The mechanisms leading to myelofibrosis are largely unknown, however, prevailing evidence suggests a decisive role of platelet-derived growth factors (PDGFs) and their cognate receptors. Using the Gata-1^{low} mouse model for PMF, this study aimed at characterizing expression, activation and regulation of PDGF receptor β (PDGFRβ) in different stages of the disease. RNAsequencing, qPCR, protein expression analyses, multiplexed immunohistochemistry and, as a novel approach in bone marrow tissue, an *in situ* proximity ligation assay (PLA) was applied to provide a detailed characterization of PDGFRβ signaling and regulation during development of myelofibrosis. Therefore, murine bone marrow was analyzed the at a pre-, an early, and an overt fibrotic stage. An increase in gene and protein expression of the PDGF signaling components in early and overt fibrotic bone marrow, and a cell-type-specific expression of the ligands and the receptors was detected. PDGFRα expression was predominantly seen in megakaryocytes, whereas PDGFRβ was expressed in fibroblast, underlining the important role of PDGFRβ in fibroblast proliferation within disease development. PDGFRβ and PDGF-B protein expression was enhanced in overt fibrotic bone marrow, along with an increase in PDGFRβ–PDGF-B interaction, analyzed by PLA. However, PDGFRβ tyrosine phosphorylation levels were not elevated. Hence, further analyses focused on regulation of PDGFRβ by protein tyrosine phosphatases (PTPs) as endogenous PDGFRβ antagonists. Gene expression analyses showed distinct expression dynamics among PDGFRβ-targeting PTPs. In particular, enhanced T-cell PTP (TC-PTP) protein expression and PDGFRβ–TC-PTP interaction was observed in early and overt fibrotic bone marrow of Gata-1^{low} mice. *In vitro*, TC-PTP (*Ptpn2*) knockdown increased PDGFRβ phosphorylation at Y^{751} and Y^{1021}, leading to enhanced downstream AKT and phospholipase C γ1 (PLCγ1) activation in fibroblasts. Further, *Ptpn2* knockdown cells showed increased growth rates when exposed to low-serum growth medium. Taken together, this study provides detailed insights into PDGF signaling during PMF development and suggests PTPs as novel, and so far unrecognized components in PMF.

Zusammenfassung

Die primäre Myelofibrose (PMF) ist eine proliferative Erkrankung des Knochen-marks, die durch Mutationen in hämatopoetischen Stammzellen verursacht wird. Als Konsequenz kommt es zur Proliferation unreifer Megakaryozytenvorläuferzellen und zur Knochenmarksfibrose. Die zugrundeliegenden Mechanismen sind bislang unklar, die Forschung der letzten Jahre deutet allerdings daraufhin, dass Wachstumsfaktoren der *Platelet-Derived Growth Factor* (PDGF) Familie, sowie ihre Rezeptoren, eine entscheidende Rolle bei der Entstehung der PMF spielen. Diese Arbeit hatte zum Ziel, die Expression, Aktivierung sowie die Regulation des PDGF Rezeptor β (PDGFRβ) mithilfe des Gata-1^{low} Mausmodells für PMF detailliert zu charakterisieren. Dabei wurden Gen- und Proteinexpressionsanalysen, *Multiplexed Immunohistochemistry*, sowie ein erstmalig im Knochenmark angewandter *Proximity Ligation Assay* (PLA) zur Analyse von Protein-Protein-Interaktion und Proteinphosphorylierung *in situ* genutzt, um Mäuse in einem prä-, einem frühen sowie einem fibrotischen Stadium zu untersuchen. Es konnte eine erhöhte Gen- und Proteinexpression von PDGF-A und PDGF-B, sowie beider Rezeptoren in einer frühen und fortgeschrittenen PMF nachgewiesen werden. Dabei wurde PDGFRβ fast ausschließlich in Knochenmarksfibroblasten detektiert. In früher sowie in der fortgeschrittenen Knochenmarksfibrose waren PDGFRβ und PDGF-B Protein-expression deutlich erhöht, und damit verbunden konnte eine erhöhte Interaktion von Rezeptor und Ligand mittels *in situ* PLA nachgewiesen werden. Eine vermehrte Tyrosin-Phosphorylierung des Rezeptors war nicht detektierbar. Die Arbeit kon-zentrierte sich daher weiterhin auf die enzymatische Gruppe der Protein-Tyrosin-Phosphatasen (PTPs), welche PDGFRβ durch Dephosphorylierung regulieren. Genexpressionsanalysen zeigten sehr unterschiedliche Expressions-dynamiken der unterschiedlichen PTPs, insbesondere konnte eine erhöhte Expression der *T cell* PTP (TC-PTP) beobachtet werden. Die Interaktion von PDGFRβ und TC-PTP war in früher und fortgeschrittener Fibrose nachweislich erhöht. *In vitro* führte TC-PTP (*Ptpn2*) *Knockdown* in Fibroblasten zu vermehrter PDGFRβ Y^{751} und Y^{1021}-Phosphorylierung, damit verbunden war eine erhöhte AKT und Phospholipase C γ1 (PLCγ1) Aktivierung. Desweiteren zeigten *Ptpn2 Knockdown* Zellen eine höhere Proliferation unter nährstofflimitierten Bedingungen. Zusammenfassend wurden in dieser Arbeit Komponenten des PDGF Systems charakterisiert, sowie PTPs als neue, bislang unberücksichtigte Komponenten in der PMF nachgewiesen.

1 INTRODUCTION

1.1 Hematopoiesis and the bone marrow

Blood cells have a limited live span and new blood cells are formed from a common precursor cell, a process referred to as hematopoiesis.[1] In adult mammals, the bone marrow is the major blood-forming organ, which resides in the medulla of axial and long bones.[2] The bone marrow consists of a wide variety of different cell types, and presents a mixture of cells in different states of differentiation (Figure 1.1). Hematopoietic stem cells (HSCs) and mesenchymal stromal cells (MSCs) are the two central cell entities which give rise to differentiated cells.

As a defining feature, HSCs are able to differentiate into all blood and immune cells and have an indefinite self-renewal capacity.[1] Importantly, HSCs can rescue effects of lethal irradiation,[3] and are thus capable of reconstituting the blood system of entire organisms. This serves as the biological base for the regeneration of blood systems by stem cell transplantation. HSCs differentiate into lymphoid precursors, with the ability to further mature into B lymphocytes, T lymphocytes and natural killer cells, and myeloid precursors, giving rise to granulocytes, erythrocytes, monocytes and megakaryocytes.[4]

MSCs can differentiate into cells that form the bone marrow stroma as a scaffold. MSCs have multipotent differentiation characteristics and can mature into adipocytes, chondrocytes, osteoblasts and myogenic cells.[5-7] Due to their stem cell-like differentiation potential, these cells have previously been referred to as 'mesenchymal stem cells'. However, there is no evidence that MSCs have unlimited self-renewal potential and MSCs do not possess transplantation characteristics that are comparable to HSCs.[8] In fact, data indicate that MSCs are a heterogeneous pool of immature progenitor cells without a clearly defined immunophenotype. Hence, it has been disputed if MSCs qualify as 'stem cells',[9,10] and 'mesenchymal stromal cells' is the preferred terminology to more accurately reflect their functional role as connective tissue and scaffolding cells.
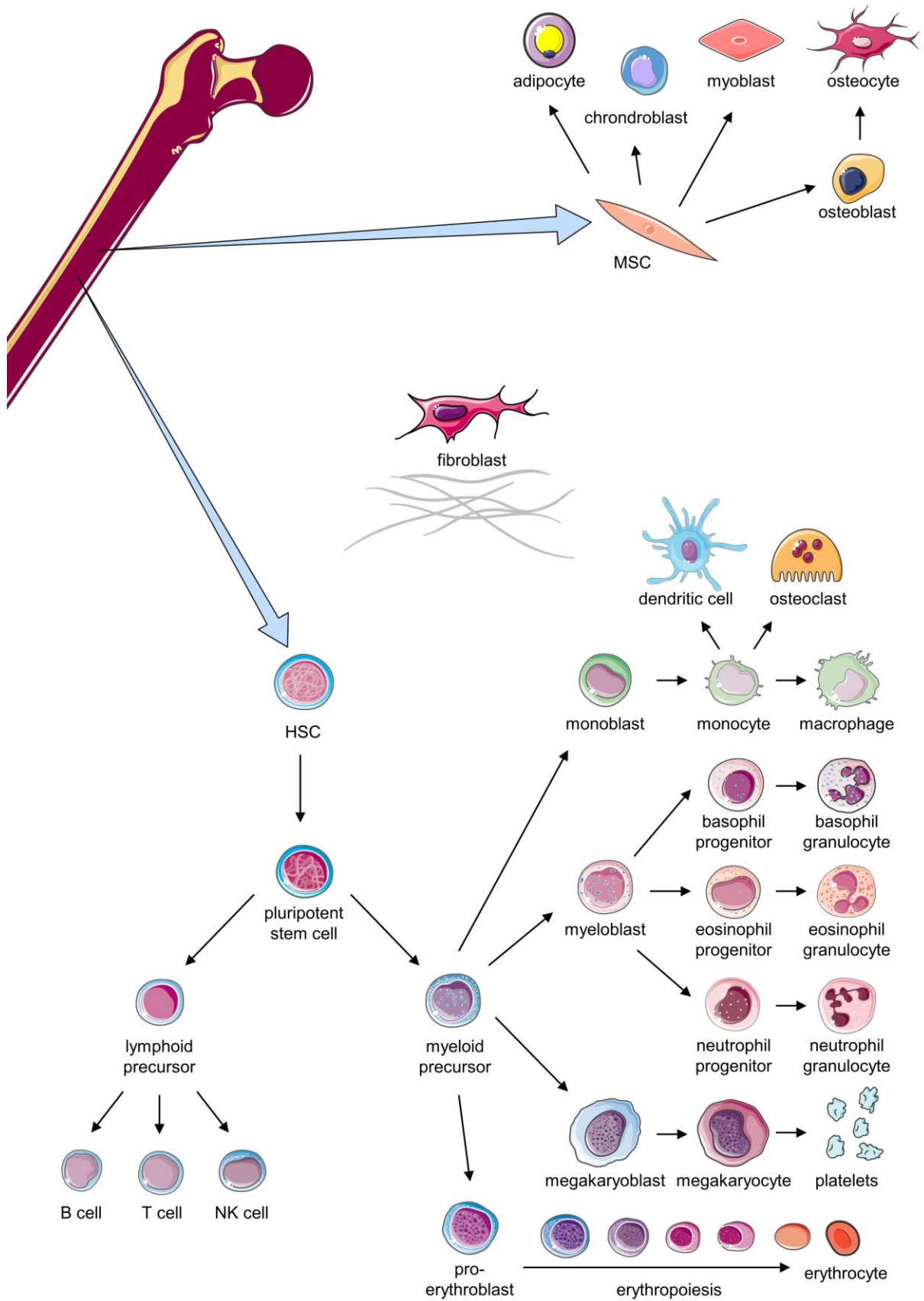
Figure 1.1: Cells within the bone marrow. Hematopoietic stem cells (HSCs) can differentiate into all mature blood cells of the lymphoid lineage (B cells, T cells and natural killer (NK) cells) and the myeloid lineage (monocytes, granulocytes, megakaryocytes and erythrocytes). Mesenchymal stromal cells (MSCs) give rise to scaffolding cells, such as osteoblasts, chondrocytes, adipocytes and myogenic cells.[*]

While both HSCs and MSCs share a mesodermal origin,[11,12] it is largely accepted that HSCs and MSCs present two distinct lineage entities. The classical model of hematopoiesis summarizes research from more than one century, since A. Maxilow postulated that blood cells are formed from one progenitor cell in 1909.[13] This monophyletic model suggests a clear hierarchy and branching lineage directions, nevertheless, the origin of many cell types is still not known. For example, it has long been assumed that MSCs, which have a fibroblast-like phenotype, and mature fibroblasts are derived from a similar lineage.[14,15] Transplantation experiments, however, indicate that fibroblasts have an HSC origin.[16] In fact, differentiation patterns are not always straight forward and additional mechanisms, such as trans-, de- and re-differentiation, might contribute to cell maturation.[17-19]

Differentiation, quiescence and self-renewal are tightly regulated processes, which rely on growth factors, cytokines, cell-cell interactions, extracellular matrix components and many other factors.[20,21] HSCs are strongly dependent on their surrounding cells and microenvironment, also referred to as their niche.[22-24] Hence, the different cells are not randomly distributed within the bone marrow but reside in specialized bone marrow niches. Undifferentiated HSCs, for example, preferably reside in the osteoblast niche or near blood vessel, referred to as the vascular niche.[25,26] A multitude of external factors establish a controlled balance between differentiation and self-renewal of HSCs, however, the disruption of this balance can result in the development of a variety of proliferative malignancies.

1.2 Myeloproliferative Neoplasms

The common defining feature of myeloproliferative neoplasms (MPNs) is the clonal expansion of at least one cell type of the myeloid lineage, leading to an impaired hematopoietic function of the bone marrow. The classification of MPNs was revised by the World Health Organization (WHO) in 2016 (Table 1.1).[27] Leukemia, characterized by the proliferation of granulocytes,[28] is represented by three MPN subtypes: chronic myeloid leukemia (CML), characterized by the presence of the breakpoint cluster region-abelson (BCR-ABL) fusion oncogene,[29] chronic neutrophilic leukemia and chronic eosinophilic leukemia. Three further MPNs have been specified: essential thrombocythemia (ET), polycythemia vera (PV) and primary

myelofibrosis (PMF). As the latter three MPNs share common driver mutations and underlying mechanisms, these three are often subgrouped as 'classical, BCR-ABL-negative MPNs' (highlighted in Table 1.1). Nevertheless, those diseases present very distinct clinical features. Whereas ET and PV are characterized by platelet and erythrocyte overproduction, respectively, PMF is marked by aberrant proliferation of cells of the megakaryocytic lineage and, as the 'primary' disease manifestation, progressive bone marrow fibrosis. Both ET and PV can evolve into 'secondary' myelofibrosis and all three MPN subtypes can transform into acute myeloid leukemia (AML).[30]

Table 1.1: Classification of myeloproliferative neoplasms (MPNs) by revised 2016 WHO criteria and frequently occurring driver mutations.

MPN	Driver mutations (frequencies)
Chronic neutrophilic leukemia	*CSF3R* (59%)[31]
Chronic eosinophilic leukemia, not otherwise specified	*ASXL1*, *CSF3R*, *SETBP1* and others[32]
Chronic myeloid leukemia (CML)	*BCR-ABL* (95%)[28]
Essential thrombocythemia (ET)	*JAK2* (52%), *CALR* (25-26%), *MPL* (4%)[29,34]
Polycythemia vera (PV)	*JAK2* (97-98%)[34,36]
Primary myelofibrosis (PMF)	*JAK2* (59-60%), *CALR* (22-34%), *MPL* (5-6%)[29,37,38]
MPN, unclassifiable	*JAK2* (72%), *CALR* (11%), *MPL* (3%)[39]

(Bracket annotations at right of table: secondary myelofibrosis[33]; leukemic transformation[35])

All MPNs are initiated by acquired, somatic mutations. Nevertheless, with the exception of BCR-ABL in CML[28] and colony-stimulating factor 3 receptor (CSF3R) in chronic neutrophilic leukemia,[31] driver mutations are not unique for the respective MPN subtypes. Especially the classical, BCR-ABL-negative MPNs cannot yet be genetically distinguished and the mechanisms directing the cells towards their specific, disease-defining phenotype remain unknown.

In the classical, BCR-ABL-negative MPNs, a driver mutation in one cell is sufficient to initiate the disease.[40] Which cell presents the malignant origin has been extensively analyzed. Acquired mutations can be detected in mature cells[41] but also in the HSCs at the top of the hierarchy,[42,43] indicating that HSCs are the original malign cells. This supports the hypothesis that an undifferentiated HSC acquires a somatic driver mutation, which consequently promotes proliferation and differentiation in a myeloid direction.[44]

1.3   Primary myelofibrosis

Fibrosis is an essential part of tissue repair processes in response to injury. Fibroblasts, myofibroblasts and pericytes play a key role in fibrosis, as they produce collagens and other extracellular matrix (ECM) proteins and respond to cytokines, chemokines, and other mediators of inflammation.[45] Fibrosis, however, is characterized by expansion of activated fibroblasts and extensive formation of ECM components, becoming irreversible and potentially leading to the loss of tissue function.[46] Chronic and slowly progressing diseases are frequently accompanied by fibrosis, and virtually any organ can be affected by fibrotic changes.[47] Anti-fibrosis treatment is typically anti-inflammatory and organ-specific; however, established treatment strategies for fibrosis are lacking.[48]

Myelofibrosis, terminologically referring to fibrosis in the bone marrow, presents a central entity within the different MPNs. Myelofibrosis can occur as a primary clinical manifestation (PMF), but both ET and PV can evolve into secondary myelofibrosis. Importantly, even though myelofibrosis is considered the 'primary' condition in PMF, biologically accurate myelofibrosis is a 'secondary' feature. Fibroblasts in PMF do not harbor driver mutations and are thus not considered malign cells.[49] Similar to other fibrotic diseases, myelofibrosis in PMF is caused by cell-extrinsic effect of malign HSCs. Hence, there is a chronic activation of fibroblasts by growth factors deriving from the clonal cells. Clinically, however, both PMF and secondary myelofibrosis present common features. This study largely concentrates on PMF, nevertheless certain aspects are conferrable to myelofibrosis as a secondary condition.

PMF is a rare disease with 0.1 - 1 per 100,000 newly diagnosed cases per year in Europe.[50] PMF, which is slightly more prevalent in men than in women, is typically diagnosed in elderly patients and median survival ranges from 1.8 years in high risk to 17.5 years in low risk patients.[51] Disease symptoms are diverse and very heterogenic among patients, common features during PMF progression are summarized in Figure 1.2. Patients typically display symptoms of ineffective hematopoiesis such as anemia, thrombocythemia, evolving into thrombocytopenia in later stages, leukocytosis and increased numbers of circulating progenitor cells. Defects in blood cell maturation result in compensative extramedullary hematopoiesis in spleen and liver. Especially splenic hematopoiesis leads to an increase in size of the spleen, referred to as splenomegaly, which causes patients discomfort. Constitutional symptoms include bone pain, fatigue, cachexia and further unspecific symptoms. The bone marrow of PMF patients shows dysplastic megakaryocytes, neoangiogenesis, osteosclerosis and, as a central pathological feature, progressive fibrosis.[52,53]
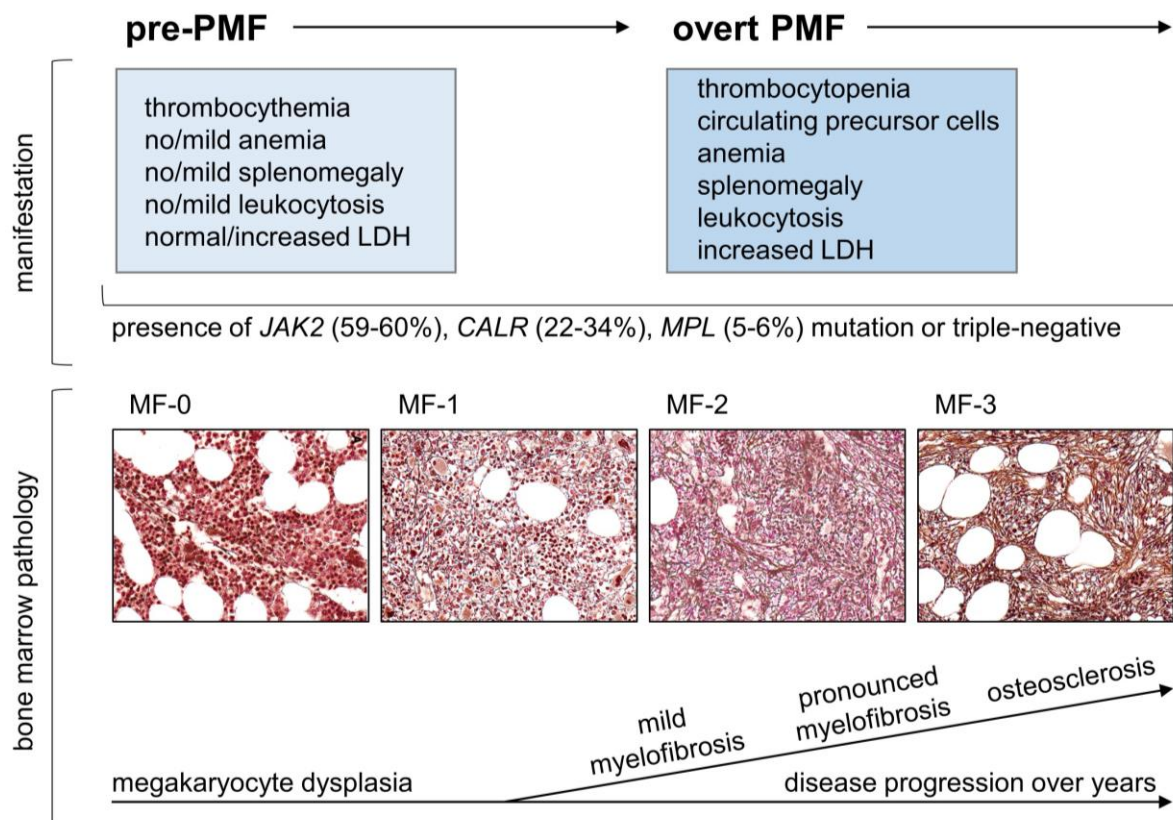
Figure 1.2: Clinical manifestation and pathological features of primary myelofibrosis (PMF) from a pre-fibrotic stage (pre-PMF) to overt PMF. LDH: lactate dehydrogenase, MF: myelofibrosis. Images for the illustration of MF grades (MF-0 to MF-3) are adopted and modified from Kvasnicka et al., 2016.[54]

Diagnosis of PMF is made according to the 2016 WHO revision on MPN classification and diagnostic criteria. These take into account clinical and laboratory features, such as blood cell counts and lactate dehydrogenase (LDH), but mainly rely on the assessment of bone marrow morphology.[27] Bone marrow fibrosis is commonly visualized using a reticulum staining with WHO myelofibrosis (MF) scoring system ranging from grade MF-0 (normal condition) to grade MF-3 (dense and extensively intersected reticulum).[54] The presence of driver mutations (*JAK2*, *CALR* and *MPL*) is supportive but not essential for diagnosis, since up to 10% of patients are triple-negative for the three driver mutations. PMF is classified either as pre-fibrotic PMF or overtly fibrotic PMF. Especially in the pre-fibrotic stage, PMF is difficult to diagnose, since the morphological features and the lack of fibrosis in pre-PMF resemble features also commonly found in ET. However, it is highly relevant to correctly distinguish these two MPNs. ET and pre-fibrotic PMF are biologically different: megakaryocytes in PMF show peculiar dysplasia, an altered differentiation, and hence differences in pro-platelet production and cytokine storage within α-granules, whereas megakaryocytes in ET display hyperproliferation with excess platelet production.[55,56] Also from a clinical point of view, prognosis and potential complications are very distinct in PMF and ET. In a cohort of 180 pre-PMF patients (formerly diagnosed with/classified as ET) and 891 ET patients, the 15-year survival for PMF and ET were 59% and 80%, respectively, and the 15-year leukemic transformation rates were 11.7% and 2.1%, respectively.[57] Still, the histopathological assessment of diagnostic criteria such as megakaryocyte morphology, size, and clustering poses major problems for hematopathologists, and reproducibility is poor.[58] The limitations in diagnostic precision and the lack of specific molecular markers for the respective MPNs emphasize the need for new diagnostic approaches.

1.3.1 Molecular alterations in primary myelofibrosis

1.3.1.1 JAK-STAT signaling

Aberrantly activated janus kinase - signal transducer and activator of transcription (JAK-STAT) signaling is central to the pathogenesis of the classical, BCR-ABL-negative MPNs and supports proliferation and differentiation of malign HSCs.[59] In

approximately 90% of PMF patients, one of three main driver mutations can be detected (see Table 1.1).

First described in 2005, the most common genetic aberration is a point mutation in janus kinase 2 (JAK2), which leads to substitution of a valine for a phenylalanine at position 617 (V617F) in the pseudokinase domain of JAK2.[60] The pseudokinase domain exerts an inhibitory function that regulates the kinase activity,[61] and mutation leads to a constitutive activation of JAK2.[62,63] In 2013, *CALR* mutations were discovered in most PMF and ET patient who do not harbor *JAK2* mutations.[64] *CALR* encodes calreticulin, a chaperone in the endoplasmic reticulum (ER), which exerts a control function for unfolded proteins.[65] Furthermore, calreticulin binds calcium ions and thus plays an important role in calcium-mediated intracellular signaling.[66] Importantly, *CALR* mutation promotes megakaryocytic differentiation, which is supportive of the fact that *CALR* mutations only occur in MPNs which affect the megakaryocytic lineage (ET and PMF).[67] In recent years it has become more clear that *CALR* mutation leads to aberrant activation of JAK-STAT signaling as well, although mechanisms seem to be substantially different from JAK2^{V617F}-mediated JAK-STAT activation.[68] The thrombopoietin receptor MPL is required for mutant calreticulin to induce MPN,[69,70] and *CALR* mutation leads to an increase in *MPL* expression.[71] These data strongly indicate that *CALR* mutation leads to JAK-STAT activation downstream of MPL. In line with these data, mutations in *MPL*, which can be detected in 4-6% of ET and PMF patients, likewise lead to JAK-STAT activation.[72]

Evidently, the main functional consequence of each of the three mutations is increased JAK-STAT signaling in HSCs. The fact that the mutations occur mutually exclusive further provides evidence for their capacity to independently activate JAK-STAT signaling in disease-causing MPN stem cells. How exactly these alterations support the cell-extrinsic capacity of malign HSCs to promote myelofibrosis, however, is not yet known.

1.3.1.2 Other mutations

Although one of the three main driver mutations alone is sufficient to initiate disease in patients and in mouse models, they are accompanied by further acquired mutations in approximately 50% of MPN patients.[73] Particularly as the disease progresses or leukemic transformation occurs, an accumulation of mutations can be

detected,[74,75] indicating that additional genetic instability contributes to disease progression. Importantly, the specific mutational landscape has a strong negative impact on prognosis.[37] Among the additional mutations, many genes are involved in RNA splicing (e.g. *SRSF2* and *U2AF1*) and epigenetic regulation (e.g. *ASXL1* and *TET2*).[38]

1.3.1.3 Chronic inflammation and the bone marrow microenvironment

The chronic inflammatory state of the bone marrow is considered a major pathophysiological component in myelofibrosis.[76] During wound healing, inflammation is an important protective mechanism to promote tissue repair. Chronic inflammation, however, promotes fibrotic changes in organs.[77] The increased expression of inflammatory cytokines in the bone marrow of PMF patients, among those, interleukin (IL)-2, IL-6, IL-8, tumor necrosis factor α and interferon γ, supports the hypothesis of chronic inflammation-driven bone marrow fibrosis.[53,78] Furthermore, transforming growth factor β (TGFβ), which is strongly associated with myelofibrosis, is crucial in tissue repair and inflammation.[79] There are multiple mechanisms by which TGFβ exerts pro-fibrotic effects and promotes fibroblasts proliferation and extracellular matrix remodeling. For example, activation of TGFβ receptor leads to downstream extracellular signal-regulated kinase (ERK) and phosphatidylinositol 3-kinase (PI3K) signaling to promote proliferation of TGFβ receptor expressing cells.[80,81] Furthermore, TGFβ induces expression of platelet-derived growth factor (PDGF)-B[82] and ErbB ligands.[83] The hypothesis of a chronically inflamed bone marrow is also in line with the concept that myelofibrosis is caused by corrupted crosstalk between the defective microenvironment and HSCs, also referred to as the 'bad seeds in bad soil' concept.[84,85] The importance of the complex cell-cell interactions within the bone marrow is further emphasized by the fact that normal megakaryocyte function is required for HSC quiescence.[86]

1.3.1.4 Pro-fibrotic cytokines and growth factors

The transformation from malign proliferation of hematopoietic cells to myelofibrosis seen in PMF has been ascribed to the overproduction of pro-fibrotic cytokines and growth factors by HSCs. PDGF signaling components have evolved as central mediators of myelofibrosis.[87,88] Expression of the PDGF ligands, as well as PDGF receptor α (PDGFRα) and PDGF receptor β (PDGFRβ) expression is increased in

the bone marrow of PMF patients, regardless of driver mutations.[89,90] Moreover, increased expression of basic fibroblast growth factor (bFGF),[91] TGFβ,[92,93] and vascular endothelial growth factors (VEGFs)[94,95] can be detected, which promote fibroblast proliferation and neo-angiogenesis in the bone marrow.

1.3.2 Current treatment options for primary myelofibrosis

To date, allogeneic hematopoietic stem cell transplantation (HSCT) remains the only curative therapy for myelofibrosis. However, HSCT is associated with substantial morbidity and mortality, and is only suitable for a subset of PMF patients.[96,97] All other therapies are palliative and are not able to improve or reverse bone marrow fibrosis.

The discovery of JAK-STAT-associated mutations led to efforts in the development of JAK inhibitors. However, only one JAK inhibitor is approved by the US Food and Drug Administration (FDA) so far. Since its approval in 2011, the JAK1/2 inhibitor ruxolitinib (Jakavi®) has become part of combined standard therapy for PMF patients. Ruxolitinib treatment is not limited to patients harboring JAK2 mutations but shows equal efficacy in patients with other driver mutations.[98,99] Long-term treatment with ruxolitinib reduces spleen size and prolongs the overall survival of PMF patients.[100] However, there is no improvement or reversal of bone marrow fibrosis. Furthermore, efficacy of ruxolitinib is limited by drug resistances[101] and JAK inhibition does not abrogate clonal proliferation.[102] Moreover, studies show that ruxolitinib treatment does not suppress PDGF-AA and -BB production, and PDGFRα signaling remains active in splenocytes after ruxolitinib treatment in an MPN mouse model.[103]

The most common symptomatic treatment strategies aim at rendering anemia (erythropoiesis-stimulating agents, androgens, immunomodulators, blood transfusions) and splenomegaly (ruxolitinib, hydroxyurea, radiation therapy, splenectomy).[104] The limitations in efficient treatment of myelofibrosis clearly emphasizes the needs for new therapeutic approaches.

1.4 PDGFs and their cognate receptors

PDGFs and their cognate receptors have been identified as crucial mediators in bone marrow fibrosis. PDGFs are disulfide-bonded, dimeric proteins which were first described in 1974 for their ability to stimulate the growth of different cell types.[105-107] There are four PDGF isoforms, denoted PDGF-A, -B, -C and -D.[108] PDGF-A and -B can either form homodimers (PDGF-AA and PDGF-BB) or heterodimers (PDGF-AB), which are processed intracellularly and then excreted as functional dimers.[109-113] PDGF-C and -D, which were first described in 2000 and 2001, are synthesized as homodimers (PDGF-CC and PDGF-DD). In contrast to the other PDGF dimers, PDGF-CC and -DD are released from cells as inactive precursors and are proteolytically cleaved by extracellular serine proteases.[114,115]

PDGFs can bind two cognate receptors, PDGFRα and PDGFRβ, which have distinct ligand-binding specificities (Figure 1.3). PDGF-A binding is exclusive to the PDGFRα chain, but PDGF-B can bind both PDGFRα and PDGFRβ.[116] Hence, depending on ligand dimers, PDGF receptors can form both homodimers and, if co-expressed, heterodimers. PDGF-CC can bind PDGFRα homo- and heterodimers,[117] whereas PDGF-DD primarily binds PDGFRβ homodimers and, with lower affinity, receptor heterodimers.[114,116] Depending on co-expression, ligands can act on their receptors in a paracrine or an autocrine manner.[118]
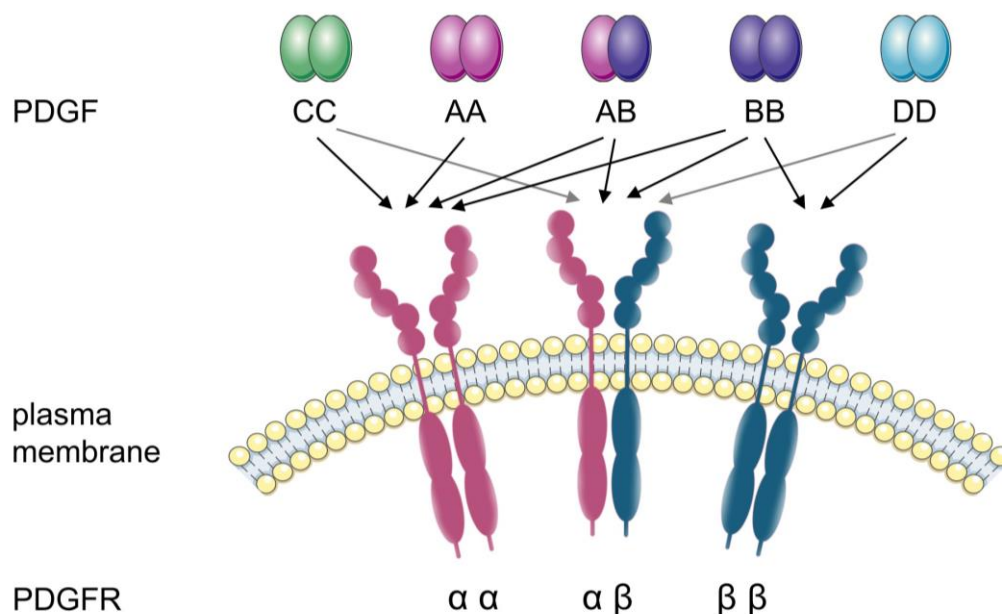
Figure 1.3: Schematic illustration of platelet-derived growth factor (PDGF) isoforms and binding specificities of the ligand dimers towards transmembranous PDGF receptor (PDGFR) α and β homo- and heterodimers.[*]

PDGF-A is mainly expressed in epithelial, myogenic, and neuronal progenitor cells. PDGF-B expression can also be detected in endothelial and neuronal cells, enabling heterodimerization with PDGF-A. The largest share of PDGF-B, however, derives from megakaryocytes, where PDGF-B is stored in the growth factor-storing granules of platelets, referred to as α-granules. PDGF-C expression overlaps with PDGF-A expression, and PDGF-D can be detected in fibroblasts and smooth muscle cells, possibly acting on PDGFRβ in an autocrine manner.[116,119] PDGF receptors are predominantly expressed by cells of mesenchymal origin. Within the bone marrow, PDGFRα is expressed in endosteal and endothelial cells, but highest expression is observed in megakaryocytes.[89] PDGFRβ, in contrast, is almost exclusively expressed in fibroblasts, but can also be detected in vascular smooth muscle cells and pericytes.[90,116]

The PDGF system plays a crucial role in embryonal development, as highlighted by several mouse studies. PDGF-B and PDGFRβ knockout is perinatally lethal, and mice show severe cardiovascular, renal and hematopoietical deficiencies.[120-122] Mice lacking PDGF-A die either pre- or postnatally showing alveolar septation defects,[123] and PDGFRα knockout mice die during embryonic development displaying incomplete cephalic closure.[124] Knockout of PDGF-C is perinatally lethal and mice display respiratory defects,[125] whereas PDGF-D knockout mice are viable with a mild vascular phenotype.[126]

1.4.1 PDGF receptor structure and signaling

PDGF receptors are transmembrane receptor tyrosine kinases (RTKs) which have an extracellular part, consisting of five Immunoglobulin (Ig)-like domains that contain the ligand binding site (see Figure 1.4, exemplary for PDGFRβ structure). Receptors are further constituted of a transmembrane domain, followed by a juxtamembrane domain, an intracellular tyrosine kinase domain and a C-terminal tail.[127] Upon PDGF-binding, receptors dimerize and cross-phosphorylate intracellular tyrosine residues, which serve as binding sites for downstream signaling components.[128]

The major share of PDGFRβ tyrosine phosphorylation sites are located near the intracellular protein kinase domain of the receptor (Figure 1.4) and phosphorylated by autocatalysis, however, some tyrosine sites can be phosphorylated by ABL non-

receptor tyrosine kinases[129] or Src.[130] The receptor contains an activation loop including the Y^{857} phosphorylation site, hence autophosphorylation at Y^{857} is necessary for full activation of PDGFRβ.[131] Most other phosphorylated tyrosine residues provide docking sites for Src homology 2 (SH2) domain containing adapter proteins, such as Src and Grb2.[132] Since these proteins have distinct preferences in amino acid sequence adjacent to the phosphotyrosine binding site, the different PDGFRβ tyrosine phosphorylation sites are bound by specific proteins. Two autophosphorylation sites in the juxtamembrane region (Y^{579} and Y^{581}) mediate binding to Src.[133] The Y^{740} and Y^{751} sites are required for PI3K activation, which is bound to PDGFRβ via its p85 subunit,[134,135] and hence phosphorylation at Y^{751} is necessary for downstream AKT activation.[136] Phosphorylated Y^{716} and Y^{775} sites mediate binding to Grb2 and activate downstream ERK signaling.[137,138] Phosphorylation at Y^{771} serves as a binding site for GTPase activating protein of Ras (RasGAP), counteracting the activation of ERK signaling.[135,139,140] While PDGFRα and PDGFRβ largely share common signaling mechanisms, PDGFRα-induced ERK signaling is not regulated by RasGAP-binding.[141] Phosphorylation at sites Y^{1009} and Y^{1021} activates phospholipase C γ1 (PLCγ1) and protein lipase C-mediated calcium signaling.[142,143] Together, the activated pathways promote proliferation, survival, migration and differentiation of cells.[128]

The kinase domain sequences of human PDGFRα and PDGFRβ share 65% amino acid sequence homology. The C-terminal tail, in contrast, only displays 32% homology (sequences collected from UniProt database and aligned using NCBI blastp® tool), and hence, differences in PLCγ1 activation intensity have been observed.[144] Nevertheless, both receptors activate the same signaling pathways. Differences in function of the two receptors have mainly been attributed to different PDGFR expression patterns in cells and tissues. The question whether there are different signaling mechanisms of the receptor isoforms has been addressed by replacing the intracellular domain of PDGFRα with the PDGFRβ intracellular domain, and *vice versa*. These experiments revealed a large functional overlap, demonstrated by a substantial rescue, although fusion with the intracellular PDGFRα domain did not rescue PDGFRβ without vascular defects.[145] This indicates physiologically relevant differences in α and β receptor signaling in normal tissue development.
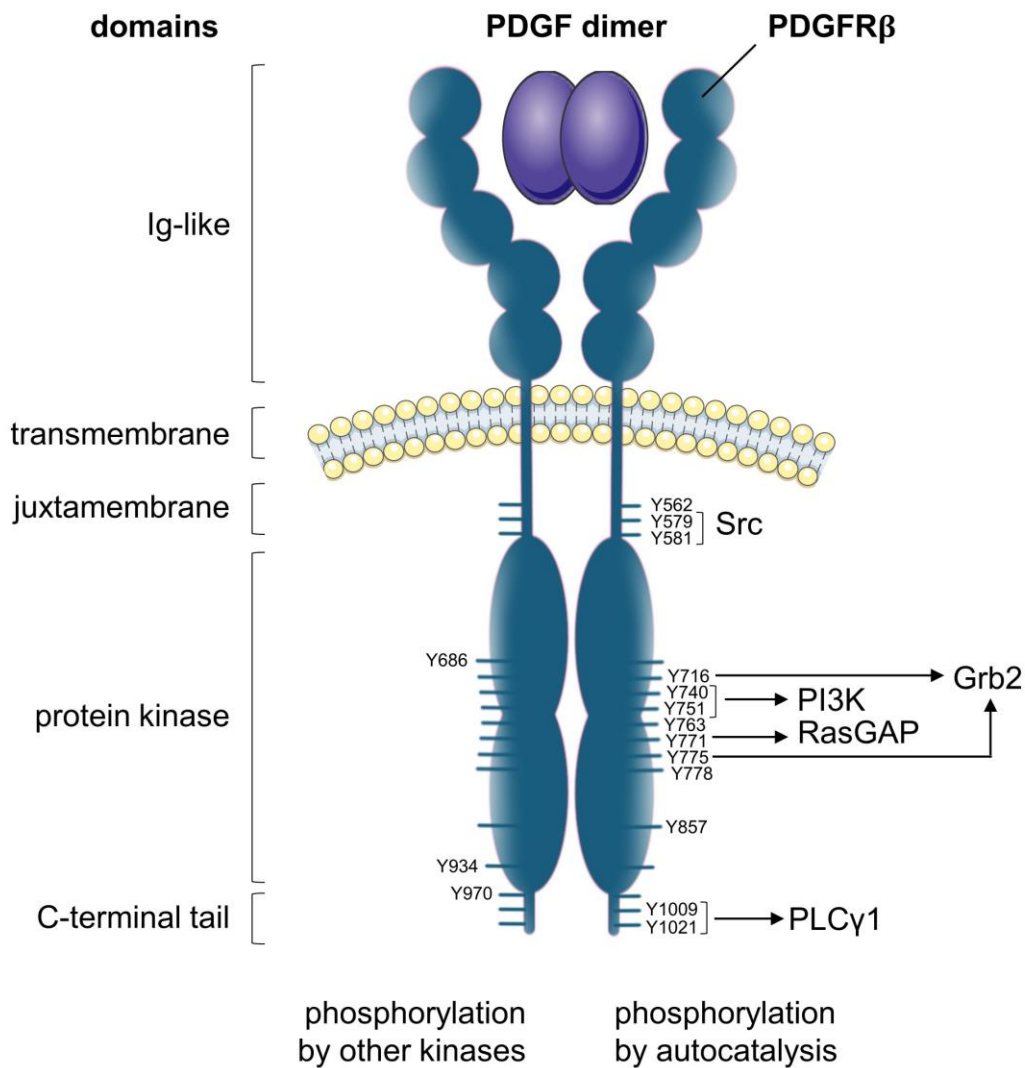
Figure 1.4: Schematic illustration of platelet-derived growth factor receptor β (PDGFRβ) structure, tyrosine phosphorylation sites and activated signaling pathways. Ig-like: immunoglobulin-like domain, PI3K: phosphatidylinositol 3-kinase, PLCγ1: phospholipase C γ1, RasGAP: GTPase activating protein of Ras.[*]

1.4.2 The PDGF system in proliferative diseases, cancer and fibrosis

The PDGF system has been implicated in various proliferative diseases and tissue remodeling processes, e.g. pulmonary arterial hypertension[146,147] and neointima formation.[148,149] Further, dysregulation of PDGF signaling is involved in different types of cancer, as summarized in Table 1.2. For example, mutations in PDGFRα can be detected in 5-10% of glioblastoma patients[150-152] and in 5% of patients with gastrointestinal stromal tumors.[153] PDGF receptor fusion proteins are associated with certain types of leukemia[154,155] and in dermatofibrosarcoma protuberans, a rare skin cancer, expression of a collagen 1A1–PDGF-B fusion protein is evident in 100% of patients.[156,157] Further, PDGF signaling components are often differentially

expressed, e.g. in many types of breast, brain, liver, lung and prostate cancer. Often, but not always,[158] increased PDGF receptor expression negatively correlates with prognosis.[159-161]

Table 1.2: Implication of platelet-derived growth factor (PDGF) ligands and receptors in proliferative diseases and cancer. CML: chronic myeloid leukemia, PMF: primary myelofibrosis.

Proliferative disease/cancer type	Mutation/consequence
Artery intimal sarcomas	PDGFRα (overexpression)[162]
Breast cancer	PDGFRα (overexpression)[159]
CML with hypereosinophilia	FIP1L1-PDGFRα fusion protein[155]
Chronic myelomonocytic leukemia	TEL-PDGFRβ fusion protein[154]
Dermatofibrosarcoma protuberans	COL1A1-PDGF-B translocation, overexpression[156,157]
Esophageal squamous cell carcinoma	PDGFRα (overexpression)[163]
Gastrointestinal stromal tumors	PDGFRα (activating mutation D842V)[153]
Glioblastoma	PDGFRα (exon 8, 9 deletion, overexpression)[150-152]
Hepatocellular carcinoma	PDGF-A, PDGFRα, PDGFRβ (overexpression)[164]
Non-small cell lung cancer	PDGF-A (overexpression), PDGFRα (mutation, overexpression)[160,165]
Oligodendrogliomas	PDGFRα (overexpression)[166,167]
PMF	PDGF-A, PDGF-B, PDGFRα, PDGFRβ (overexpression)[89,90]
Prostate cancer	PDGF-D, PDGFRβ (overexpression)[168,169]

In addition to the clear implication of PDGF signaling components in clonal cells, they often play a crucial role in the tumor microenvironment. Malign cells largely depend on the tumor stroma, hence fibroblasts, pericytes and other stromal cells support tumorgenesis.[170,171] Whereas cancer cells often aberrantly express PDGFRα, stromal cells in the tumor microenvironment are frequently associated with PDGFRβ expression.[172,173] Importantly, the PDGF signaling components also have a strong implication in organ fibrosis. Fibrosis is characterized by fibroblast proliferation in response to cytokines and growth factors and the production of ECM components. As PDGFs and their receptors mediate proliferation of mesenchymal cells, it seems conclusive that the PDGF system has evolved as a central mediator of organ fibrosis. For example, PDGF-A, -B and PDGFRα expression is induced in lung fibrosis.[174-176] In liver fibrosis, PDGFRβ plays a pivotal role, with simultaneous increase in PDGF-A, -B and -D expression.[177-179] Further, PDGF-B is highly induced in renal fibrosis[180,181] and scleroderma.[182,183] Additionally, PDGFRβ activation by PDGF-DD has been attributed an important role in renal fibrosis.[184] Similar observations can be found in most types of organ fibrosis.[185,186] Myelofibrosis, classified as a proliferative disease (HSCs) and therefore listed in Table 1.2, but with fibrosis as a central feature, is likewise driven by induced expression of PDGF components. Expression of PDGF-A and -B, as well as expression of the two receptors, is increased in the bone marrow of PMF patients.[89] Importantly, PDGFRβ expression in PMF is almost exclusively detected in bone marrow fibroblasts, and expression in activated fibroblasts correlates with the grade of myelofibrosis.[90] Further studies suggest that PDGFRβ expression is enhanced in early stages of bone marrow fibrosis and that increased PDGFRβ expression precedes fiber accumulation. Conclusively, immunohistochemical staining of PDGFRβ in bone marrow of PMF patients has been suggested as a marker for PMF progression.[90,187,188]

1.4.3 Therapeutic targeting of PDGF signaling components

Due to their implication in various cancers, tumor microenvironment and fibrosis, PDGFs and their receptors have increasingly gained interest as therapeutic targets. Several kinase inhibitors are applicable as PDGF receptor antagonists, e.g. cediranib, nilotinib, imatinib, pazopanib, sorafenib and sunitinib.[189] Especially imatinib, a tyrosine kinase inhibitor which inhibits the BCR-ABL fusion protein and is

commonly used for CML treatment,[190] has substantial relevance in context of MPNs and myelofibrosis. In CML patients with hypereosinophilia expressing the FIP1L1-PDGFRα fusion protein, as well as in patients with chronic myelomonocytic leukemia expressing the TEL-PDGFRβ fusion protein, imatinib treatment showed clinical efficacy and disease remission.[191,192] There have been different reports on imatinib treatment in patients with myelofibrosis: in one study including 23 patients, imatinib caused side effects without remarkable benefits for patients;[193] a second study with 11 patients reported a similar outcome;[194] in a third study including 18 patients, responses were positive but marginal.[195] However, none of these studies included PDGFRβ expression analyses in the bone marrow of patients. Hence, PDGF targeting treatment or kinase inhibition could potentially be more efficient in patients who have been screened for PDGF receptor expression or activation status. A number of patients might respond to and benefit from treatment, nevertheless, appropriate *in situ* methods to detect the receptor activation status for diagnostics are not yet established.

Most tyrosine kinases inhibitors function by blocking the ATP-binding site of RTKs, and hence lack specificity. None of the inhibitors mentioned above is specific for one PDGF receptor, but inhibit both PDGFRα and PDGFRβ. Furthermore, these inhibitors do not only target PDGF receptor but have other primary targets such as ABL, VEGF receptors or Kit.[189] To overcome the limitations caused by the lack of specificity, other approaches aim at blocking PDGF-binding to the receptors. Monoclonal antibodies or antibody fragments targeting the ligands or receptors are being evaluated.[196-198] One example is the PDGFRα-targeting monoclonal antibody olaratumab, which prolongs survival in soft tissue sarcoma patients when administered in combination with the chemotherapeutic agent doxorubicin.[198] Furthermore, a vaccine prepared from PDGF‑B polypeptides coupled to carrier proteins was investigated for the treatment of hepatic fibrosis and showed anti-fibrotic effects in a mouse model.[199]

1.5   Protein tyrosine phosphatases

Different mechanisms are involved in the regulation of PDGF signaling, e.g. injury and pro-inflammatory cytokines affect expression of the ligands and receptors.[185] Similar to most transmembrane RTKs, PDGF receptors are internalized upon ligand binding and either recycled to the cell surface, or ubiquitinated and degraded.[200] Nevertheless, ligand-induced endocytosis is not solely a negative regulation, since receptor signaling continues after internalization, and endocytosis is required for full activation of downstream signaling pathways.[201,202] The most relevant regulatory components for PDGF receptors are protein tyrosine phosphatases (PTPs), which dephosphorylate intracellular tyrosine residues and are thus regulatory modulators of RTKs.[203,204]

Virtually every signaling event within and between cells relies on phosphorylation of proteins and hence, phosphorylation is of paramount importance for transcriptional and translational processes, cell proliferation, migration and differentiation.[205] To date, 107 genes coding for PTPs have been identified and therefore outnumber the 90 RTKs encoded within the human genome.[206,207] PTPs are very selective in substrate specificity and require defined amino acid sequences for their catalytic activity.[208] However, most PTPs dephosphorylate more than only one RTK. Conclusively, PTPs are equally important for the cellular phosphorylation status, compared to RTKs.[209] The 107 PTPs are structurally divided into four groups: class I PTPs (38 classical PTPs and 61 dual-specific phosphatases), class II PTPs (low molecular weight (LMW)-PTP, one member), class III PTPs (CDC25 phosphatases, three members) and class IV PTPs (EYA, four members).[210] Based on their location, the 38 classical PTPs are further classified as transmembranous, receptor-like PTPs (PTPRs, 21 members) and cytosolic, non-receptor PTPs (PTPNs, 17 members).[207] In addition to cell-type specific expression, the structural diversity of PTPRs and PTPNs (Figure 1.5) largely determines their function, substrate specificity and activity.[207]
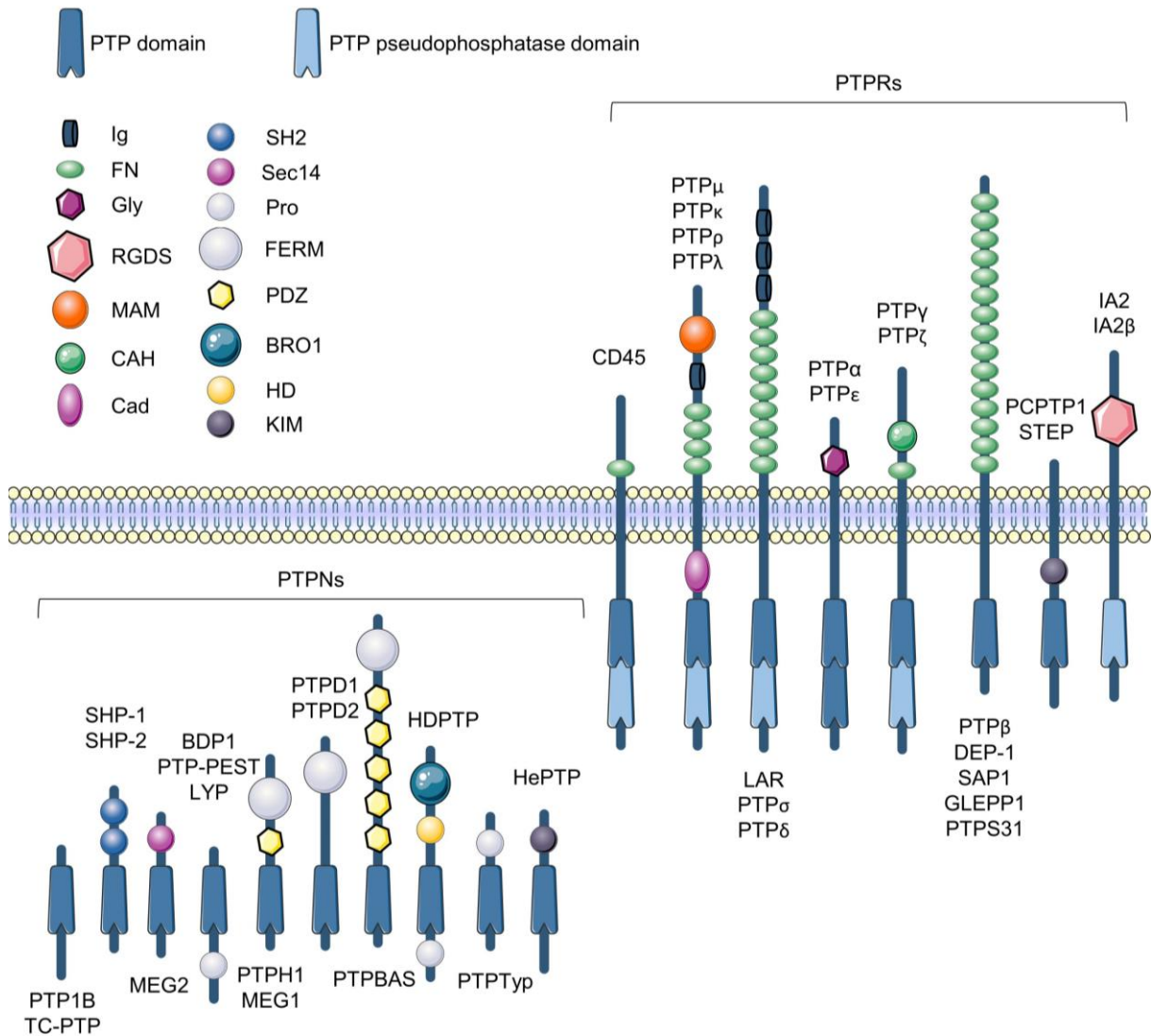
Figure 1.5: Structural diversity of class I classical protein tyrosine phosphatases (PTPs), subgrouped as non-receptor PTPs (PTPNs) and receptor-like PTPs (PTPRs). BRO1: BRO1 homology, CAH: carbonic anhydrase-like, Cad: cadherin-like juxtamembrane sequence, FERM: FERM mephrin/A5/µ domain, FN: fibronectin type III-like domain, Gly: glycosylated, HD: histidin domain, Ig: immunoglobulin domain, KIM: kinase-interacting motif, MAM: mephrin/A5/µ domain, Pro: proline-rich, RGDS: RGDS-adhesion recognition motif, SEC14: SEC14/cellular retinalaldehyde-binding protein-like, SH2: Src homology 2. Adopted and modified from Tonks, 2006.[207],[*]

Several PTPs have been identified as PDGFRβ-targeting enzymes (Table 1.3). Among these, six PTPs belong to the class I classical PTP-subgroup (five cytosolic PTPNs and one transmembranous PTPR). PTEN is a dual-specific phosphatase, which, in addition to tyrosine residues, dephosphorylates serine and threonine residues. Furthermore, the class II LMW-PTP has been identified to dephosphorylate PDGFRβ.

Table 1.3: Platelet-derived growth factor receptor β (PDGFRβ)-targeting protein tyrosine phosphatases (PTPs) and targeted tyrosine phosphorylation sites.

Gene	Protein	PDGFRβ tyrosine phosphorylation site	References
PTPN1	PTP1B	Y^{716}, Y^{751}	118,211-213
PTPN2	TC-PTP	preferably Y^{1021} and Y^{771}	212,214
PTPN6	SHP-1	n/a	215,216
PTPN11	SHP-2	Y^{751}, Y^{740}, Y^{763}, Y^{771}, Y^{1009}, Y^{1021}	212,217-221
PTPN12	PTP-PEST	Y^{1021}	212,222
PTPRJ	DEP-1	preferably Y^{1021}	148,223
PTEN	PTEN	n/a	224
ACP1	LMW-PTP	Y^{857}	225

Most of these PTPs negatively regulate PDGFRβ, nevertheless, SHP-2 is a PTP which has been ascribed positive effects on signaling.[220,221] For instance, SHP-2 serves as an adapter protein for Grb2 and thus promotes ERK signaling.[226] Reversely, not all phosphorylation sites are associated with receptor activation. Phosphorylation on serine residues, for example, inhibit the tyrosine kinase activity of PDGFRβ.[227] Thus, the PDGFRβ phosphorylation and activation status is refined by multiple components.

1.6 Aim of the study

PMF is a fatal disease with perspicuous limitations in early diagnosis and a scarcity in adequate treatment options. PDGFs and their receptors are linked to myelofibrosis based on their increased expression in the bone marrow of PMF patients.[89,90] However, the mechanisms of transformation from malign clonal proliferation of HSCs to myelofibrosis and the involvement of the PDGF system are not fully understood. Especially the time-dependent expression dynamics of PDGF receptors, the interaction with the PDGF ligands, and the regulation by PTPs during the development of bone marrow fibrosis have not been thoroughly addressed. Using a mouse model for PMF, this study therefore concentrated on PDGFRβ and its relevance in fibroblast proliferation.

In particular, this study aimed at:

(1) Analyzing the expression dynamics and localization of PDGF signaling components during PMF development

(2) Comprehensively evaluating the PDGFRβ activation status in bone marrow fibrosis by analyzing receptor-ligand interaction and receptor phosphorylation using a novel *in situ* proximity ligation assay (PLA)

(3) Evaluating PLA as a novel diagnostic method in the bone marrow

(4) Assessing the expression of PTPs and evaluating the regulation of PDGFRβ by PTPs during PMF development

(5) Investigating the regulation of PDGFRβ by candidate PTPs in fibroblasts *in vitro*

For a detailed characterization in the time-dependent development of PMF in mice, the bone marrow of Gata-1^{low} mice was assessed in a **pre-**, an **early** and an **overt fibrotic stage** to create in-depth analyses of expression, activation and regulation of PDGFRβ during the development of bone marrow fibrosis.

2 MATERIALS AND METHODS

2.1 Materials

2.1.1 Equipment

Agarose gel electrophoresis equipment	Baacklab
Analytical balance (SE 523i)	VWR
Centrifuge for conical tubes (Universal 32 R)	Hettich
Centrifuge for multiwell plates (5810 R)	Eppendorf
CO_2 incubator (HeraCell 150)	Heraeus
Cooling plate for histology (EG1130)	Leica
Epifluorescence microscope (BZ-9000)	Keyence
Film processor (Curix 60)	AGFA
Heating block (ThermoMixer®)	Eppendorf
Hematology analyzer (K4500)	Sysmex
Histology staining jars	Fisher Scientific
Incubator (BE 400)	Memmert
Laminar flow hood (LaminAir 1.2)	Heto-Holten
Live cell imaging system (IncuCyte®)	Essen Bioscience
Magnetic stirrer (RET basic)	IKA
Microcentrifuge (PerfectSpin)	Peqlab
Micropipettes (Pipet-Lite XLS, 2, 10, 100, 200, 1000 µl)	Rainin
Microscope (DM IL)	Leica
Microtome (HM 325 rotary microtome)	Thermo Scientific
Microwave (Continent MW800)	GGV
Mixing device (Vortex Genie 2)	Scientific Industries
Multispectral Imager (Vectra® Polaris™)	Perkin Elmer
PCR cycler (PTC-100™)	MJ Research
pH meter (accumet® AE150)	Fisher Scientific
Pipette controller (accu-jet® pro)	Brand
Platform shaker (PMR-30)	Grant Instruments
Protein gel electrophoresis equipment	Bio-Rad
Real time PCR cycler (Mx3000P)	Stratagene

Spectrophotometer (NanoDrop® ND-1000)   Peqlab

Tissue embedding station (EC 350-1)   Thermo Scientific

Tissue processor (Shandon Citadel 1000)   Thermo Scientific

Waterbath, floating, for histology   Enno Vieth

Waterbath for cell culture   Memmert

2.1.2 Consumables

Barrier pen, hydrophobic (PAP pen)   Daido Sangyo

Blood collection needles (S-Monovette®, 20Gx1")   Sarstedt

Blood collection tubes (S-Monovette®, 1.2 ml, EDTA) Sarstedt

Blotting paper   Bio-Rad Laboratories

Cell culture flasks (75 cm^2, Falcon®)   Corning

Cell scraper (Costar®)   Corning

Chamber slides (Lab-Tek®II)   Thermo Fisher Scientific

Chemiluminescence detection films (Hyperfilm ECL) Amersham, GE Healthcare

Coverslips (24x40 mm, 24x60 mm, Menzel™)   Fisher Scientific

Microscope slides (SuperFrost®Plus)   VWR

Microtome blades (A35)   FEATHER Safety Razor

Multiwell plates (6, 96 well, Falcon®)   Corning

Pipet tips (10, 200, 1000 µl)   Sarstedt

Pipets, serological (5, 10, 25, 50 ml, Falcon®)   Corning

Polyvinylidene difluoride (PVDF) blotting
membrane (Amersham Hybond™-P)   GE Healthcare

qPCR plates (96 well)   Sarstedt

qPCR plate sealing tape   Sarstedt

Reaction tubes (0.2 ml) for PCR   Sarstedt

Reaction tubes (1.5, 2 ml, SafeSeal)   Sarstedt

Reaction tubes, conical (15, 50 ml, Falcon®)   Corning

Scalpels   FEATHER Safety Razor

Tissue cassettes   Simport

2.1.3 Chemicals, reagents and solvents

Acetic acid	J.T.Baker
Acrylamide/bis solution (30%)	Serva
Agarose	Serva
Ammonium persulfate (APS)	VWR
Autofluorescence inhibitor reagent	Merck
β-Mercaptoethanol	AppliChem
Bovine serum albumin (BSA), blotting grade	AppliChem
Bradford dye reagent	Bio-Rad Laboratories
Bromphenol blue sodium salt	Merck
Chemiluminescence detection reagent (Amersham™)	GE Healthcare
Chloroform	J.T.Baker
Deoxycholic acid sodium salt	Serva
Developer and fixation solution (G153 and G354)	Agfa
4′,6-Diamidino-2-phenylindole dihydrochloride (DAPI)	Perkin Elmer
DNA ladder (GeneRuler™, 100 bp)	Thermo Fisher Scientific
Ethanol (EtOH) ≥ 99.8%, 96%, 70%	Roth
Ethidium bromide solution (1%)	Roth
Ethylenediaminetetraacetic acid (EDTA)	Sigma-Aldrich
Glycerol	Sigma-Aldrich
Glycine	Roth
Hydrochloric acid (HCl, 32%)	Labochem international
Isopropanol	Merck
Milk, powdered, blotting grade	Roth
Mounting medium, anhydrous (Neo-Mount®)	Merck
Mounting medium (ProLong™ Diamond Antifade)	Thermo Fisher Scientific
Mounting medium with DAPI (Fluoroshield™)	Abcam
Methanol	Merck
Neo-Clear® (xylene substitute)	Merck
Paraffin type 6	Thermo Scientific
Paraffin type 9	Thermo Scientific
Phosphatase inhibitor tablets (PhosSTOP™)	Roche
Phosphate-buffered formaldehyde (4%)	Labochem international
Protease inhibitor tablets (cOmplete™ Mini)	Roche

Protein ladder (PageRuler™, prestained)   Thermo Fisher Scientific

Sodium chloride (NaCl)   Merck

Sodium dodecyl sulfate (SDS)   Roth

Sodium hydroxide (NaOH)   VWR

Sodium pyrophosphate   Sigma-Aldrich

Tetramethylethylenediamine (TEMED)   Roth

TRI reagent®   Sigma-Aldrich

Tris   Roth

Tris-HCl   Roth

Trisodium citrate dihydrate   Merck

Triton™ X-100   Sigma-Aldrich

Tween® 20   Serva

2.1.4 Enzymes and kits

GoTaq® G2 DNA polymerase, buffer and deoxy-   Promega
nucleotide triphosphates (dNTPs)

High Capacity RNA-to-cDNA Kit   Applied Biosystems

Duolink® *in situ* Detection Reagents Orange   Sigma-Aldrich

SYBR® Green PCR Master Mix   Applied Biosystems

2.1.5 Buffers and solutions

Water quality is essential for many experimental procedures and different water purity grades were used in this study. Water purity grades are indicated as follows:

Tab water   -   tab water

H_2O -   distilled water

pure H_2O -   low endotoxin, DNase- and RNase-free water (Biochrom)

Antigen Retrieval buffer   10 mM Sodium citrate
                                      0.05% (v/v) Tween® 20
                                      in H_2O, pH 6

APS stock solution   10% (w/v) APS
                                      in pure H_2O

Decalcification solution	10% (w/v) EDTA in H_2O, pH 7.4
DNA extraction solution I	25 mM NaOH 0.2 mM EDTA in pure H_2O
DNA extraction solution II	40 mM Tris-HCl in pure H_2O, pH 5.5
Lysis buffer	150 mM NaCl 20 mM Tris 10 mM EDTA 7.5 mM Sodium pyrophosphate 0.5% (w/v) Deoxycholic acid 0.5% (v/v) Triton™ X-100 in pure H_2O, pH 7.5
Protein loading buffer (6x)	350 mM Tris-HCl 10% (w/v) SDS 36% (w/v) Glycerol 5% (v/v) β-Mercaptoethanol 0.025% (w/v) Bromphenol blue in pure H_2O, pH 6.8
SDS-polyacrylamide gel electrophoresis (SDS-PAGE) buffer	25 mM Tris 192 mM Glycine 0.05% (w/v) SDS in H_2O
SDS stock solution	10% (w/v) SDS in pure H_2O
Separation gel buffer	1.5 M Tris-HCl in H_2O, pH 8.8
Stacking gel buffer	0.5 M Tris-HCl in H_2O, pH 6.8
Stripping buffer	200 mM Glycine 0.1% (w/v) SDS 1% (v/v) Tween® 20 in H_2O, pH 2.2
Transfer buffer	25 mM Tris 192 mM Glycine 0.05% (w/v) SDS 20% (v/v) Methanol in H_2O

Tris-Acetate-EDTA (TAE) buffer	40 mM Tris
	20 mM Acetic acid
	1 mM EDTA
	in H_2O, pH 8.4
Tris-buffered saline with Tween® 20 (TBS-T)	150 mM NaCl
	20 mM Tris
	0.1% (v/v) Tween® 20
	in H_2O, pH 7.4
Wash buffer	100 mM NaCl
	200 mM Tris
	in H_2O, pH 7.5

2.1.6 Staining solutions, dyes and kits

Giemsa staining solution	Dr. K. Hollborn & Söhne
May-Grünwald staining solution	Dr. K. Hollborn & Söhne
Reticulum Stain Kit	Abcam
Opal™ fluorophores	PerkinElmer

2.1.7 Primers

All primers used for this study were purchased from Invitrogen (Thermo Fisher Scientific), diluted with pure H_2O to obtain a 10 µM concentration and stored at -20°C.

Primer sequences for mouse genotyping by polymerase chain reaction (PCR) originate from the Jackson Laboratory standard protocol:

Gata-1[low] forward	5'–GACCCATCCATCTCCTTTCC–3'
Gata-1[low] reverse	5'–GTGTGAGAGTGGCTATGTGC–3'
Wild type forward	5'–ACTCTTGCTCTCTTTTGCAG–3'
Wild type reverse	5'–AATCAGGAATGCAACATCTC–3'

All primers used for quantitative polymerase chain reaction (qPCR) analyses were designed to be specific to the target gene in the mouse genome using Primer-BLAST tool.[228] If applicable for the individual gene structure, amplicons span at least one intron to avoid amplification in genomic DNA. Primer sequences used for qPCR are listed below.

Col1a1 forward	5'–CTGACGCATGGCCAAGAAGA–3'
Col1a1 reverse	5'–ATACCTCGGGTTTCCACGTC–3'
Col3a1 forward	5'–CTGGTCCTGCTGGAAAGGAT–3'
Col3a1 reverse	5'–TCCATTGCGTCCATCAAAGC–3'
Pdgfa forward	5'–TTGTAACACCAGCAGCGTCA–3'
Pdgfa reverse	5'–CTCCACTTTGGCCACCTTGA–3'
Pdgfb forward	5'–CGGCCTGTGACTAGAAGTCC–3'
Pdgfb reverse	5'–GAGCTTGAGGCGTCTTGG–3'
Pdgfra forward	5'–AGTGGCTACATCATCCCCCT–3'
Pdgfra reverse	5'–CCGAAGTCTGTGAGCTGTGT–3'
Pdgfrb forward	5'–ACGGCATGGACTTCTTAGCC–3'
Pdgfrb reverse	5'–ATCTTGACCAGCTTGCCCTC–3'
Ptpn1 forward	5'–CGGGAGGTCAGGGACCTT–3'
Ptpn1 reverse	5'–GGGTCTTTCCTCTTGTCCATCA–3'
Ptpn2 forward	5'–GCTACGACGGCTCAGAAGGT–3'
Ptpn2 reverse	5'–TGTCTGTCAATCTTGGCCTTTTT–3'
Ptpn6 forward	5'–CGTACCCTCCCGCTGTGA–3'
Ptpn6 reverse	5'–TTTTCGTACACCTCCTCCTTGTG–3'
Ptpn11 forward	5'–CCTCAACACAACTCGTATCAATGC–3'
Ptpn11 reverse	5'–TGTTGCTGGAGCGTCTCAAA–3'
Ptpn12 forward	5'–GAGTCGCCTCCTCCTTTACC–3'
Ptpn12 reverse	5'–TGGAAGTTCATGCCACTCAGG–3'
Ptprj forward	5'–GCAGTGTTTGGATGTATCTTTGGT–3'
Ptprj reverse	5'–CTTCATTATTCTTGGCATCTGTCCTT–3'
Hprt forward	5'–TGCTGACCTGCTGGATTACA–3'
Hprt reverse	5'–TATGTCCCCCGTTGACTGAT–3'

2.1.8 Antibodies and antibody-conjugates

All antibody-based approaches in this study were preceded by blocking of non-specific binding sites. Different blocking reagents were used for the following applications:

Multiplexed immunohistochemistry:	Serum-free protein block solution (Dako)
PLA and immunofluorescence:	Duolink® blocking solution (Sigma-Aldrich)

Immunoblotting: 3% milk in TBS-T for pPDGFRβ Y^{751}

5% BSA in TBS-T for all other antibodies

All primary antibodies used for this study are listed in Table 2.1 below. A list of secondary antibodies and antibody-conjugates is summarized in Table 2.2.

Table 2.1: Primary antibodies used in this study, including species/clonality, catalog#, supplier and dilutions for the respective applications. IB: Immunoblot, IF: immunofluorescence, Ig: immunoglobulin, mIHC: multiplexed immunohistochemistry, PLA: proximity ligation assay, mAb: monoclonal antibody, pAb: polyclonal antibody.

Antibody	Species/ Clonality	Catalog#	Supplier	Application/ Dilution
Akt	Rabbit pAb	9272	Cell Signaling Technology	IB: 1:1000
pAkt S^{473}	Rabbit mAb	4060	Cell Signaling Technology	IB: 1:2000
β-Actin	Mouse mAb	sc-81178	Santa Cruz	IB: 1:500
Erk1/2	Rabbit pAb	9102	Cell Signaling Technology	IB: 1:1000
pErk1/2 T^{204}/Y^{204}	Rabbit mAb	4370	Cell Signaling Technology	IB: 1:2000
GAPDH	Mouse mAb	MAB374	Millipore	IB: 1:50000
Pan-pY pY100	Mouse mAb	9411	Cell Signaling Technology	PLA: 1:500
Pan-pY pY20	Mouse mAb	ab10321	Abcam	PLA: 1:900
Pan-pY 4G10	Mouse mAb	05-321	Merck Millipore	PLA: 1:1000
PDGFRα D1E1E	Rabbit mAb	3174	Cell Signaling Technology	mIHC: 1:80 PLA: 100
PDGFRβ 28E1	Rabbit mAb	3169	Cell Signaling Technology	IB: 1:1000
PDGFRβ 42G12	Mouse mAb	NBP1-19191	Novus Biologicals	PLA: 1:50
PDGFRβ Y92	Rabbit mAb	ab32570	Abcam	mIHC: 1:50 PLA: 1:50
pPDGFRβ Y^{751}	Mouse mAb	3166	Cell Signaling Technology	IB: 1:1000
pPDGFRβ Y^{1021}	Rabbit pAb	ab16868	Abcam	IB: 1:2000
PDGF-A	Mouse mAb	sc-9974	Santa Cruz	mIHC: 1:50 PLA: 1:50
PDGF-B	Rabbit pAb	ab21234	Abcam	mIHC: 1:80 PLA: 1:50
PLCγ1	Rabbit pAb	#2822	Cell Signaling Technology	IB: 1:1000
pPLCγ1 Y^{783}	Rabbit pAb	#2821	Cell Signaling Technology	IB: 1:1000
TC-PTP F-8	Mouse mAb	sc-373835	Santa Cruz	IB: 1:100 mIHC: 1:100 PLA 1:50
Negative control	Mouse IgG1	X0931	Dako	PLA: 1:50
Negative control	Rabbit IgG fraction	X0903	Dako	PLA: 1:10000

Table 2.2: Secondary antibodies and secondary antibody-conjugates used in this study, including species/clonality, catalog#, supplier and dilutions for the respective applications. IB: Immunoblot, IF: immunofluorescence, HRP: horseradish peroxidase, mIHC: multiplexed immunohistochemistry, PLA: proximity ligation assay, mAb: monoclonal antibody, pAb: polyclonal antibody.

Antibody-conjugate	Species/ Clonality	Catalog#	Supplier	Application/ Dilution
Anti-mouse-Alexa Fluor 568	Goat pAb	A11004	Thermo Fisher Scientific	IF: 1:1000
Anti-rabbit-Alexa Fluor 488	Goat pAb	A11008	Thermo Fisher Scientific	IF: 1:500
Anti-mouse-HRP	Rabbit pAb	P0260	Dako	IB: 1:2000
Anti-rabbit-HRP	Swine pAb	P0217	Dako	IB: 1:1000
ImmPRESS® anti-mouse-HRP	Horse IgG	MP-7402	Vector Laboratories	mIHC: ready-to-use
ImmPRESS® anti-rabbit-HRP	Horse IgG	MP-7401	Vector Laboratories	mIHC: ready-to-use
Duolink® *in situ* PLA probe anti-mouse PLUS	Donkey IgG	DUO92001	Sigma Aldrich	PLA: 1:5
Duolink® *in situ* PLA probe anti-mouse MINUS	Donkey IgG	DUO92004	Sigma Aldrich	PLA: 1:5
Duolink® *in situ* PLA probe anti-rabbit PLUS	Donkey IgG	DUO92002	Sigma Aldrich	PLA: 1:5
Duolink® *in situ* PLA probe anti-rabbit MINUS	Donkey IgG	DUO92005	Sigma Aldrich	PLA: 1:5

2.1.9 Mice

Gata-1^{low} mice were purchased from Jackson Laboratory (Bar Harbour, ME, USA).

2.1.10 Cell line, cell culture, transfection and stimulation materials

NIH-3T3 fibroblasts were purchased from American Type Culture Collection (ATCC®). All cell culture reagents were sterile, suitable for use in cell culture and handled aseptically under laminar air flow.

Dulbecco's modified eagle medium (DMEM)   Gibco
4.5g/L D-glucose, L-glutamine, 110 mg/L sodium pyruvate

Fetal bovine serum (FBS)   Gibco, Lot: 0861360K

Lipofectamine™ 2000   Invitrogen

Opti-MEM® reduced serum medium   Gibco

Dulbecco's phosphate buffered saline (PBS)   Gibco

PDGF-BB, human recombinant   Peprotech

Penicillin/streptomycin   Merck

siRNA, nontargeting (NT) control no. 1 (Ambion®)   Thermo Fisher Scientific

siRNA, mouse *Ptpn2* (Ambion®, id 150390)   Thermo Fisher Scientific

Trypsin/EDTA solution   Merck

2.1.11 Software and online tools

Table 2.3: Software, version, developer and application used in this study. mIHC: multiplexed immunohistochemistry, PLA: proximity ligation assay, qPCR: quantitative polymerase chain reaction.

Software	Version	Developer	Application
BLASTP	2.9.0+	National Center for Biotechnology Information (NCBI)	Protein sequence alignment
Duolink® ImageTool	1.0.1.2	Sigma-Aldrich	Quantification of PLA signals
EndNote	X8.2	Clarivate Analytics	In-text citations
Gene Ontology (GO)/ PANTHER	Release dates 2018-08-09/ 2017-12-05	Gene Ontology Consortium	Enrichment analysis of RNA sequencing data
GraphPad Prism	6.01	GraphPad Software Inc.	Graphs and statistics
ImageJ	1.52n	National Institutes of Health (NIH)	Image merging, cropping, maximum filter for PLA signals
IncuCyte® 2018A	20181.2.0.0	Essen Bioscience	Live cell imaging of NIH-3T3 cells
InForm®	2.4.6781.17769	Perkin Elmer	mIHC image analyses
Microsoft Office Professional Plus 2016	16.0.4266.1001	Microsoft	Tables and calculations (Excel), generation of figures (PowerPoint) and text documents (Word)
MxPro Mx3000P	4.10	Stratagene	qPCR analyses
PhenoChart™	1.0.9	Perkin Elmer	mIHC image visualization and region selection
Primer-BLAST	n/a	National Center for Biotechnology Information (NCBI)	Design of qPCR primer sequences

2.2 Methods

2.2.1 Mouse studies

Gata-1^{low} mice have originally been generated by targeted mutation in the promotor region for the *Gata1* gene which results in impaired expression of the transcription factor Gata-1 in megakaryocytes.[229] While Gata-1 expression is reduced, megakaryocytes retain a high proliferation rate, remain immature and release reduced platelet numbers. Further, Gata-1^{low} mice develop fibrosis in the bone marrow that resembles the development of myelofibrosis in PMF patients.[230] The *Gata1* gene is located on the X chromosome, hence breeding of Gata-1^{low} mice aimed at generating homozygous females and hemizygous males. A breeding colony was started by crossing two heterozygous female Gata-1^{low} mice with two male wild type (WT) littermates. Mice were maintained according to standard protocols at the animal facility at Center for Cardiovascular Research at Charité – Universitätsmedizin (Berlin, Germany). 3 weeks after birth, mice received ear notches for identification and to provide tissue for genotyping.

2.2.1.1 Genotyping

For DNA isolation, ear punches were placed in 75 µl DNA extraction solution I and incubated at 98°C for 1 h. After cooling, 75 µl DNA extraction solution II were added for neutralization. The samples were centrifuged at 4000xg for 3 min and the DNA solution was transferred to a new tube. All littermates were genotyped by PCR according to the standard protocol provided by Jackson Laboratory. The following duplex PCR reaction was used:

5.5 µl	Pure H$_2$O		
2.4 µl	5x GoTaq® buffer		
0.24 µl	dNTPs		
0.6 µl	Primer Gata-1^{low} forward	previously prepared in an upscaled premix	∑ 12 µl
0.6 µl	Primer Gata-1^{low} forward		
0.3 µl	Primer WT forward		
0.3 µl	Primer WT reverse		
0.06 µl	GoTaq® polymerase		
2 µl	DNA		

PCR products were amplified using the following temperature program:

94°C	3 min	
94°C	30 sec	
58°C	1 min	35 cycles
72°C	1 min	
72°C	2 min	
10°C	up to 12 h	

The PCR products were subsequently separated by agarose gel electrophoresis, using 1% agarose in TAE buffer containing 5 µl ethidium bromide solution per 100 ml agarose gel. A DNA ladder was loaded on the gel as a size marker. Visualization by ultraviolet (UV) light enabled detection of a 220 basepair (bp) product in WT mice, a 370 bp product in Gata-1^{low} mice, or both PCR products in heterozygous mice (exemplarily shown in Figure 2.1).
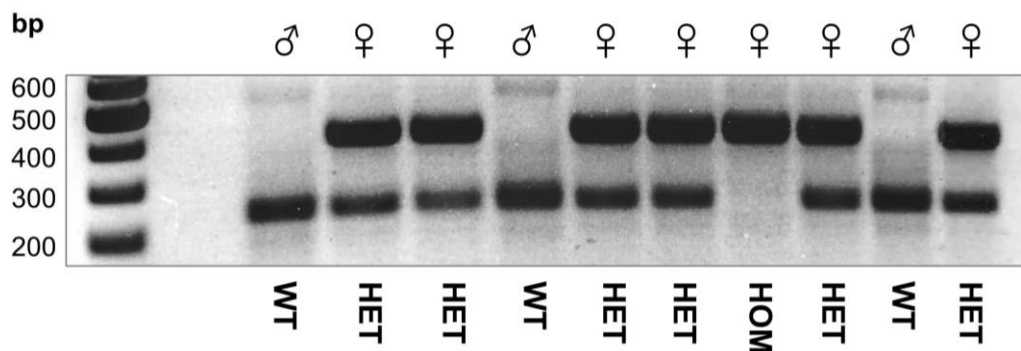
Figure 2.1: Visualization of polymerase chain reaction (PCR) products from genotyping of a mouse cohort, separated on a 1% agarose gel. The wild type (WT) gene generates a 220 basepair (bp), the Gata-1^{low} mutation a 370 bp PCR product. HET: heterozygous, HOM: homozygous.

For experiments, Gata-1^{low} mice and age-matched WT littermates were sacrificed by isoflurane overdose at 5, 10 and 15 months of age. Whole blood was collected *post mortem*, and femurs were dissected and frozen in liquid nitrogen for RNA isolation, or fixed in 4% phosphate-buffered formaldehyde for histological procedures.

2.2.2 Blood cell counts

Murine blood was collected directly *post mortem* from cardiac puncture into 1.2 ml EDTA tubes. The tubes were inverted to mix and whole blood was analyzed within 6 h from sample collection using a hematology analyzer.

2.2.3 Gene expression analyses

2.2.3.1 RNA isolation

Total RNA was obtained from whole murine femurs by pulverizing the frozen bone with a cooled pestle. The pulverized, frozen tissue was dissolved in 1.5 ml TRI reagent® and incubated for 5 min at room temperature. 300 µl chloroform were added to the mixture, inverted and incubated for 3 min at room temperature. The mixture was centrifuged for 15 min at 12,000xg at 4°C and the upper, RNA containing aqueous phase was transferred to a new tube. 700 µl isopropanol were added to the aqueous phase, inverted, and incubated for 10 min at room temperature. The sample was centrifuged for 10 min at 12,000xg at 4°C to pellet the precipitated RNA and the supernatant was subsequently discarded. The pellet was washed twice with 1.5 ml 75% EtOH, followed by centrifugation for 5 min at 7,500xg at 4°C. After discarding the washing solution, the RNA pellet was air-dried and resuspended in 30 µl pure H_2O. All further RNA handling steps were carried out on ice, and RNA concentration was determined by spectrophotometric analyses using NanoDrop®.

2.2.3.2 RNA sequencing

Total RNA from whole femurs of 10-month-old mice (n=3 Gata-1^{low} vs. n=3 WT) was used for RNA sequencing (RNAseq) analyses. RNAseq and bioinformatics were performed by Microsynth AG (Balgach, Switzerland) and hence, devices and reagents for RNAseq are not listed in the 'Materials' section. In brief, RNA quality was evaluated by Microsynth on Agilent 2100 BioAnalyzer (Santa Clara, Ca, USA), library preparation including poly(A) enrichment was done using Illumina stranded TruSeq RNA library including poly(A) enrichment (San Diego, CA, USA). Sequencing was conducted with 1x75 bp reads and 30 million reads per sample. Reads were mapped to the mouse genome, counts were normalized and analyzed for differential expression. Genes of interest were plotted using GraphPad Prism. Significantly upregulated genes were further used for gene ontology (GO) enrichment analysis.[231] PANTHER overrepresentation test using the GO molecular function annotation data set and Fisher's exact test were applied.

2.2.3.3 cDNA synthesis

1 µg RNA per sample was diluted up to 9 µl with pure H_2O and used as template for reverse transcription. One reaction included:

9 µl   diluted RNA (1 µg)

10 µl   2x buffer

1 µl   reverse transcriptase   previously prepared in an upscaled premix   ∑ 20 µl

A separate reaction included diluted RNA and buffer, omitting reverse transcriptase, serving as a negative control in primer validation experiments ('–RT control'). The reactions were prepared in PCR reaction tubes and cDNA was synthesized in a PCR cycler running a program of 1 h at 37°C, followed by 5 min enzyme inactivation at 95°C. The 20 µl reaction was finally diluted up to a final volume of 100 µl with pure H_2O.

2.2.3.4 Quantitative polymerase chain reaction

To analyze the expression levels of specific genes, qPCR was performed using SYBR® Green. Primers were used at a final concentration of 100 nM, each reaction contained:

10 µl SYBR® Green

0.2 µl Primer forward (10 µM)

0.2 µl Primer forward (10 µM)   previously prepared in an upscaled premix for each gene   ∑ 20 µl

8.6 µl Pure H_2O

1 µl   cDNA

Gene amplification was measured using a quantitative real-time PCR cycler applying the following temperature program:

50°C	2 min
95°C	10 min
95°C	15 sec
60°C	1 min
95°C	1 min
55°C	30 sec
95°C	30 sec

40 cycles (applied to the 95°C 15 sec / 60°C 1 min steps)

Each gene was measured in triplicates. All primer pairs were tested using cDNA dilutions series (1:4, 1:16, 1:64) to evaluate amplification efficiency and each primer pair was tested for amplification of genomic DNA in –RT controls. Every experiment further included a template-omitting negative control to rule out detection of primer dimers or nucleic acid contaminations. mRNA levels were calculated in relative units using the $2^{-\Delta\Delta Ct}$ method[232] with *Hprt* as a reference gene for normalization. Values observed in age-matched WT control mice served as reference.

2.2.4 *In situ* methods

Murine femurs were fixed in 4% phosphate-buffered formaldehyde for 6 h and decalcified in decalcification solution for 7 days with daily changes of the solution. Femurs were further processed in a citadel allowing dehydration, clearing and paraffin infiltration using the following program:

70% EtOH	1 h
80% EtOH	1 h
96% EtOH	1 h
100% EtOH (1)	1 h
100% EtOH (2)	1 h
Neo-Clear® (1)	40 min
Neo-Clear® (2)	40 min
Paraffin type 6	1 h
Paraffin type 9	up to 12 h

Femurs were afterwards paraffin-embedded and cooled paraffin blocks were cut into 1 µm sections using a microtome. The cut sections were then floated onto a water bath to eliminate wrinkles and transferred to microscopic slides. The tissue slides were dried at 60°C for 90 min and subsequently stored at -20°C to ensure optimal preservation of epitope integrity.

2.2.4.1 May-Grünwald Giemsa staining

For histological evaluation of blood and progenitor cells in the bone marrow, a combination of May-Grünwald and Giemsa staining was used. Tissue slides were deparaffinized in Neo-Clear® (2x5 min), followed by rehydration in graded EtOH (100%, 96%, 80%, 70%) for 3 min each, transferred to H_2O and immersed in methanol for 5 min. The slides were incubated in May-Grünwald staining solution for 5 min and directly transferred into Giemsa staining solution for 45 min. 1% acetic acid solution was used to destain the tissue, which was afterwards rinsed in H_2O. Finally, slides were dehydrated in 96% EtOH, 100% EtOH and Neo-Clear® for 3 min each, and mounted using anhydrous mounting medium.

2.2.4.2 Reticulum staining

In order to visualize fibrotic changes in the bone marrow of Gata-1^{low} mice, femur sections were stained for reticulum fibers. All solutions used for the staining were part of a Reticulum Stain Kit listed in 2.1.6. Slides were deparaffinized and rehydrated in graded EtOH as described above. The tissue slides were then transferred to H_2O and placed in potassium permanganate solution for 10 min. The slides were quickly rinsed in three changes of H_2O, differentiated in potassium metabisulfite solution and again rinsed in three changes of H_2O. Slides were transferred to ferric ammonium sulfate solution for 10 min and rinsed in two changes of H_2O. Tissue sections were then stained in ammoniacal silver solution for 3 min, washed in three changes of H_2O, followed by 1 min incubation in formalin solution. After washing in three changes of H_2O, the slides were transferred to a gold chloride solution for 5 min. To remove unreduced silver, the slides were placed in sodium thiosulfate solution for 2 min and rinsed in tab water for 2 min. Nuclei were counterstained with fast red solution for 3 min, quickly rinsed in tab water followed by H_2O. The tissue was finally dehydrated in three changes of 100% EtOH and mounted with anhydrous mounting medium.

2.2.4.3 Multiplexed immunohistochemistry

In order to detect multiple epitopes within the bone marrow, multiplexed fluorescence staining of femur sections was performed using tyramide fluorophores (Opal™ fluorophores), which form a stable fluorescent precipitate after catalyzation by horseradish peroxidase (HRP).[233] Hence, proteins can be detected using primary antibodies and HRP-conjugated secondary antibodies *in situ*. Both antibodies can be removed from the tissue after staining, whereas the stable, heat-resistant fluorophore-precipitate is not affected by the antibody removal procedure. This allows the consecutive staining of multiple proteins, without the need of using different antibody species.

Slides were deparaffinized and rehydrated in graded EtOH as described above, transferred to antigen retrieval buffer and heated in a microwave. The slides were then kept simmering in a microwave for 20 min. All other staining steps were carried out at room temperature, all washing steps were carried out under agitation. Slides were washed in two changes of TBS-T for 5 min each and the tissue was sectioned using a hydrophobic barrier pen. Unspecific binding sites were blocked for 10 min, followed by incubation with primary antibody for 30 min. Slides were washed in three changes of TBS-T, 5 min each, and incubated with HRP-conjugated secondary antibodies for 10 min. Slides were again washed in three changes of TBS-T and incubated with Opal™ fluorophores for 10 min, followed by washing in TBS-T. The antigen retrieval step was subsequently repeated to remove primary and secondary antibodies. This procedure was repeated for staining of other targets. Nuclei were counterstained with DAPI for 5 min, the slides were finally washed in three changes of TBS-T and mounted with ProLong™ Diamond Antifade mounting medium. Imaging was performed with the Vectra® Polaris™ system. Hereby, a whole slide scan was first acquired at ×10 magnification to image the whole bone and region selection for multispectral imaging was performed using Phenochart™ software. Ten multispectral images at ×40 magnification were acquired. Autofluorescence elimination, spectral unmixing, generation of pseudo-brightfield IHC images and quantification was performed with inForm® software.

2.2.4.4 Proximity Ligation Assay

PLA is an antibody-based, sensitive means which can be used to quantify protein expression, protein-protein-interactions and protein phosphorylation. Hereby, two oligonucleotide-coupled secondary antibodies (PLA probes) detect a single or two different primary antibodies. Through ligation, PLUS and MINUS oligonucleotides are joined to a circle when in close proximity and serve as template for polymerization. A polymerase replicates the DNA using fluorescently labeled nucleotides and a concatemeric product is generated. The resulting rolling circle product (RCP) can be visualized and quantified as a distinct, fluorescent dot.
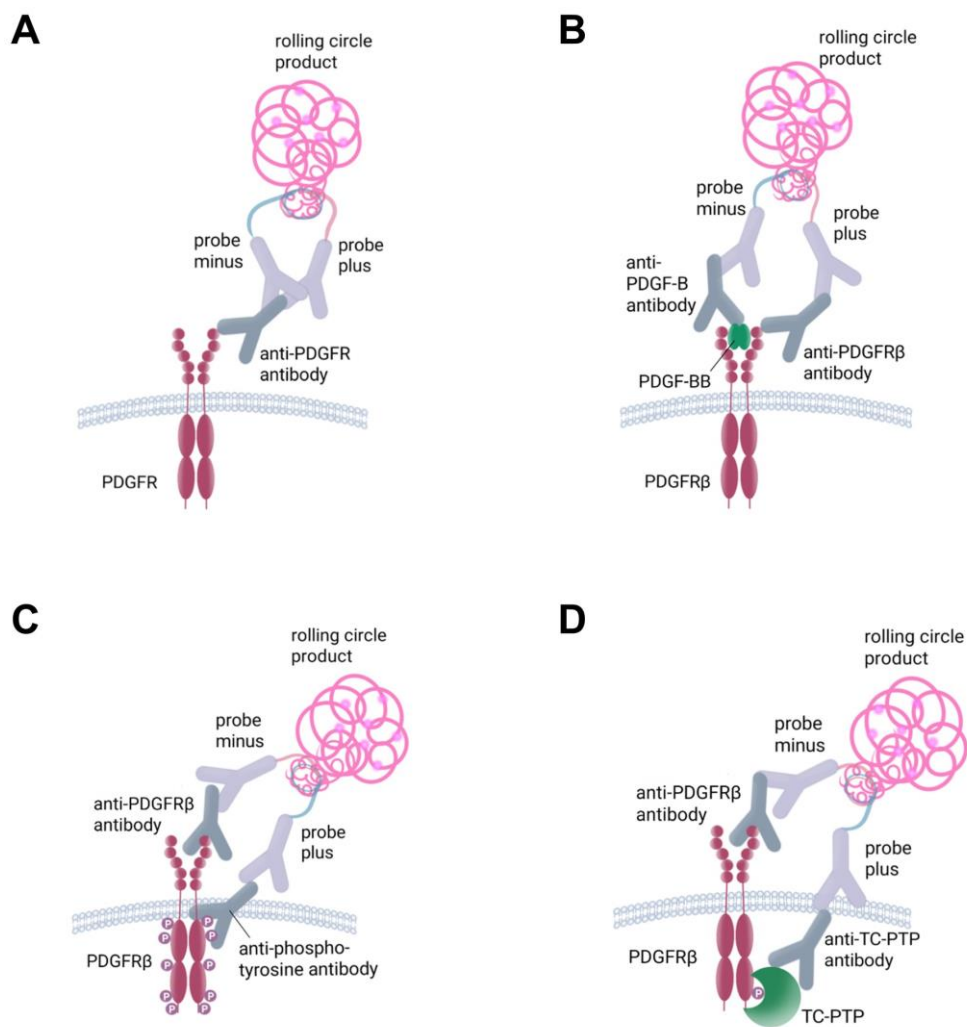
Figure 2.2: Schematic illustration of proximity ligation assay (PLA) approaches used in this study for the analysis of **A** Platelet-derived growth factor receptor (PDGFR) expression, **B** PDGFRβ–PDGF-B interaction, **C** PDGFRβ phosphorylation and **D** PDGFRβ–TC-PTP interaction. Each assay uses primary antibodies, which are bound by specific oligonucleotide-conjugated secondary antibodies (PLA probes). Oligonucleotides are ligated when both probes are in close proximity, and a rolling circle product is generated in an amplification reaction using fluorescent nucleotides. The rolling circle product can be detected *in situ* as a fluorescent dot.

In this study, PLA was used to quantify protein expression in a single recognition approach (Figure 2.2A) as well as protein-protein-interactions (Figure 2.2B and D) and protein phosphorylation (Figure 2.2C).

All solution and reagents used, if not otherwise stated, were part of the Duolink® PLA kits. Slides were deparaffinized and rehydrated in graded EtOH as described above. Tissue areas were sectioned using a hydrophobic barrier pen and autofluorescence elimination reagent was incubated on the tissue for 20 min. The tissue slides were then rinsed in 70% EtOH and transferred to H_2O. Slides were transferred to antigen retrieval buffer and heated to boiling in a microwave for 5 min. Slides were allowed to cool down for 45 min, followed by washing in three changes of TBS-T. Nonspecific binding sites were blocked for 60 min and the sections were incubated with antibodies at 4°C over night. Primary antibodies and dilutions are listed in Table 2.1 and the antibody combinations for the different assays are listed in Table 2.4 below. Unbound antibodies were removed by washing the slides in two changes of TBS-T for 5 min each, and the slides were incubated with oligonucleotide-conjugated secondary antibodies (PLA probes) for 1 h at 37°C. Subsequently, slides were washed twice in TBS-T for 5 min. A ligation mixture was incubated on the slides for 30 min at 37°C. Slides were washed in two changes of TBS-T and then incubated with the diluted amplification mixture for 100 min at 37°C. After amplification, the slides were washed in two changes of wash buffer, 10 min each, and rinsed in H_2O for 1 min. The slides were mounted using Fluoroshield™ mounting medium with DAPI to stain the nuclei. Cells were visualized using an epifluorescence microscope (BZ-9000, Keyence) with filters for DAPI and TRITC and a 60x objective. RCPs were quantified using Duolink® Image Tool. For clarity in printing, images shown where processed with ImageJ software using a maximum filter (3 pixels) for the PLA channel.

Table 2.4: Antibody combinations used in the different proximity ligation assay (PLA) approaches for the analysis of protein-protein interactions and protein phosphorylation.

Assay	Rabbit primary antibodies	Mouse primary antibodies
PDGFRβ–PDGF-B interaction	PDGF-B	PDGFRβ 42G12
PDGFRβ tyrosine phosphorylation	PDGFRβ Y92	Pan-pY pY100 Pan-pY pY20 Pan-pY 4G10
PDGFRβ–TC-PTP interaction	PDGFRβ Y92	TC-PTP F-8

2.2.5 *In vitro* methods

NIH-3T3 fibroblasts were maintained in DMEM containing 10% FBS and 1% penicillin/streptomycin in a 5% CO_2 atmosphere at 37°C. Cells were routinely split 1:5 by washing the cells with pre-warmed PBS and detaching the cells using trypsin/EDTA before reaching a confluence greater than 90%.

2.2.5.1 Immunofluorescence staining

NIH-3T3 fibroblasts were seeded into chamber slides and the following day, cells were placed on ice, washed with ice-cold PBS and fixed with 4% buffered formalin for 10 min at room temperature. Cells were washed in three changes of PBS, 5 min each, and permeabilized with 0.1% Triton™ X-100 for 10 min. Cells were again washed in three changes of PBS and unspecific binding sites were blocked for 1 h. Cells were then incubated with primary antibodies at 4°C over night. Slides were washed in three changes of PBS and incubated with secondary antibodies for 1 h at room temperature. The cells were washed in three final changes of PBS, the chamber was removed from the slide and cells were mounted using Fluoroshield™ mounting medium with DAPI. Cells were visualized using an epifluorescence microscope (BZ-9000, Keyence) with filters for DAPI, green fluorescent protein (GFP) and TRITC, and a 60x objective.

2.2.5.2 Transfection and PDGF-BB treatment

For transfection, cells were seeded into 6 well plates, grown to reach 40-50% confluence and then changed to Opti-MEM® transfection medium. In two separate reaction tubes, 75 pmol siRNA and 5 μl Lipofectamine were diluted up to 150 μl with

Opti-MEM®, respectively. The dilutions were incubated for 5 min at room temperature, then combined and incubated for 20 min at room temperature. The diluted siRNA-lipid complexes (∑300 µl per well) were added to the cells, the final concentration of siRNA in the medium was 30 nM. After 16-20 h, cells were changed to normal growth medium.

48 h after transfection, nontargeting control and *Ptpn2* knockdown cells were growth-arrested for 24 h in serum-free DMEM with 100 µg/ml BSA. 72 h after transfection, cells were treated with 50 ng/ml PDGF-BB in DMEM for 5 min, the medium in control wells was changed to fresh DMEM containing 100 µg/ml BSA. Immediately after stimulation, cells were placed on ice and washed with three changes of ice-cold PBS. Remaining PBS was removed and 150 µl lysis buffer containing protease and phosphatase inhibitors were added to each well. The cells were detached from the wells using a cell scraper and the lysate was transferred to a reaction tube. All subsequent protein handling steps were carried out on ice. The lysates were centrifuged for 20 min at 12,000xg at 4°C to pellet cell debris and the lysate was transferred to a new tube. Concentrations of the protein solutions were determined using Bradford assay by measuring extinction of the protein-dye complexes at 595 nm.[234] Concentrations were determined by generating a standard curve with BSA dilution series (0-2 mg/ml). Protein lysates were stored at -20°C (short term, <7 days) or at -80°C (long term, >7 days).

2.2.5.3 Sodium dodecyl sulfate-polyacrylamide gel electrophoresis

20 µg protein per lane were diluted with protein loading buffer, denatured at 95°C for 5 min and separated using SDS-PAGE. 3.9% stacking gels and a 10% separation gels were composed as follows:

	Separation gel	Stacking gel
Pure H_2O	4 ml	3 ml
Buffer	2.5 ml (1.5 M Tris-HCl, pH 8.8)	1.25 ml (0.5 M Tris-HCl, pH 6.8)
10% SDS solution	100 µl	50 µl
Acrylamide/bis (30%)	3.3 ml	0.65 ml
10% APS solution	50 µl	50 µl
TEMED	5 µl	6 µl

PageRuler™ prestained protein ladder served as molecular weight estimate. The gels were run in electrophoresis buffer, initially at 80 V to allow proteins to pass the stacking gel, and subsequently at 120 V for protein separation.

2.2.5.4 Immunoblotting

After complete separation, proteins were transferred to a membrane for immunoblot (IB) analyses. The gels were washed in transfer buffer and proteins were transferred to a PVDF membrane by tank blotting. Prior to blotting, the PVDF membrane was activated with methanol and positioned on top of the gel between two blotting papers and two sponges to stack a blotting 'sandwich', which was placed in blotting cassettes inside a blotting chamber filled with transfer buffer and an ice container. The transfer was run at 100 V for 1 h and the membranes were washed in three changes of TBS-T for 5 min each. Membranes were subsequently cut into stripes containing the molecular weight region of interest and unspecific binding sites were blocked for 1 h before incubation with primary antibodies at 4°C over night. Membrane stripes were then washed in three changes of TBS-T, 5 min each, and incubated with HRP-conjugated secondary antibodies for 1 h at room temperature. The membrane stripes were finally washed in three changes of TBS-T, 10 min each, and proteins of interest were detected using chemiluminescence for visualization. For immunodetection, films optimized for chemiluminescence signal detection were used. After visualization, membranes were washed in three changes of TBS-T, and, if applicable, antibodies were stripped from the membranes by incubation in three changes of stripping buffer, 20 min each. Membranes were washed in three changes of TBS-T and the blocking and antibody incubation steps were repeated. For protein quantification, densitometric analyses were performed using ImageJ software. β-Actin and GAPDH served as reference proteins for normalization. For phosphorylation site-specific antibodies, signals were normalized to the protein expression of the cognate protein.

2.2.5.5 Proliferation assay

NIH-3T3 fibroblasts were transfected as described in 2.2.5.2. 48 h after transfection, cells were seeded into 96 well plates at 1000 cells/well. 6 h after cell seeding, cells were growth-arrested for 24 h in DMEM with 100 µg/ml BSA before changing to the indicated culture media. Proliferation was monitored using IncuCyte® Live-Cell

Imaging system. Four phase contrast images per well at 10x magnification were acquired in 3 h intervals for six days. Proliferation was analyzed using IncuCyte® software and results are shown as occupied area in percent confluence over time with standard error.

2.2.6 Statistics

All results that are presented as boxplots show the median with whiskers representing minima and maxima, the number of mice (n) per group are displayed as individual points within the boxes. Bar graphs show mean and standard deviation. Statistical differences between a Gata-1^{low} and the age-matched WT control group were determined using unpaired Student's t test. For comparison of multiple groups, analysis of variance with posthoc Tukey correction was used. Statistical analyses were performed using GraphPad Prism. $P < 0.05$ was considered significant; significant differences are indicated as asterisks:

* $P < 0.05$

** $P \leq 0.01$

*** $P \leq 0.001$

**** $P \leq 0.0001$

Absence of asterisks indicates non-significance.

3   RESULTS

3.1   Development of myelofibrosis in Gata-1^{low} mice

Gata-1^{low} mice have an impaired Gata-1 expression in megakaryocytes and phenotypically resemble characteristics of PMF patients.[230,235] This study aimed at characterizing Gata-1^{low} mice at three stages of disease development: 5 months, 10 months and 15 months of age. The X-linked inheritance of the mutation led to a surplus in hemizygous males during breeding. In accordance with the literature, Gata-1^{low} mice of both sexes were viable, fertile and did not show any apparent abnormalities. While the literature suggests that Gata-1^{low} mice reach normal life expectancy, higher mortality was observed in homozygous females compared to heterozygous males. Three homozygous females intended for analysis at 15 months of age died between 8 and 13 months of age, only one homozygous female reached the age of 15 months. The reduced survival of female mice suggests a harsher or potentially earlier onset of the disease in homozygous females. Hence, blood cell counts of male and female mice were compared to reveal potential sex-specific discrepancies (Table 3.1). However, the small number of female, homozygous Gata-1^{low} mice partly impeded conclusive statistical analyses, and for female, homozygous Gata-1^{low} mice at 15 months of age (n=1), statistical analysis was not applicable. However, there were slight, but statistically significant differences in blood cell counts of both sexes in 10-month-old Gata-1^{low} mice (red blood cell counts, P=0.0489) and 15-month-old WT mice (red blood cell counts, P=0.0491; white blood cell counts P=0.0218; and platelet counts, P=0.0022). In addition to potential differences in disease progression in female Gata-1^{low} mice, the sex-specific discrepancies in WT mice indicate noticeable, age-dependent biological variations in hematological parameters in male and female mice.

Table 3.1: Blood cell counts from wild type (WT) and Gata-1^{low} mice of both sexes at 5 months (5 M), 10 months (10 M) and 15 months (15 M) of age. Highlighted cells indicate significant differences between male and female mice. RBC: red blood cell counts, WBC: white blood cell counts, PLT: platelet counts, min: minimum value, max: maximum value, SD: standard deviation.

	sex	n	RBC [x10^6/µl]		WBC [x10^3/µl]		PLT [x10^3/µl]	
			mean (min-max)	SD	mean (min-max)	SD	mean (min-max)	SD
5 M WT	♂	7	8.60 (7.35 – 9.52)	0.82	4.84 (2.2 – 8.4)	2.00	1257.57 (868 – 1966)	416.68
	♀	4	8.87 (8.36 – 9.27)	0.39	2.78 (2.0 – 3.6)	0.67	1265.75 (1151 – 1445)	125.86
5 M Gata-1^{low}	♂	8	7.14 (5.72 – 8.19)	0.85	6.75 (2.4 – 12.4)	3.05	94.63 (39 – 345)	101.94
	♀	3	7.90 (7.14 – 8.32)	0.66	8.37 (6,4 – 10.2)	1.90	227.00 (41 – 584)	309.26
10 M WT	♂	10	8.66 (8.18 – 9.32)	0.43	4.37 (3.2 – 6.7)	1.21	1537.40 (999 – 1914)	270.05
	♀	5	8.25 (7.56 – 8.83)	0.48	3.64 (2.2 – 5.3)	1.22	1241.60 (1084 – 1648)	232.47
10 M Gata-1^{low}	♂	8	6.46 (5.21 – 7.09)	0.63	8.70 (5.9 – 17.4)	4.36	83.13 (34 – 285)	84.33
	♀	3	7.35 (7.08 – 7.56)	0.25	7.30 (4.7 – 9.8)	2.55	145.00 (63 – 308)	141.16
15 M WT	♂	9	8.71 (8.14 – 9.20)	0.49	5.73 (3.3 – 11.9)	2.64	1610.00 (1239 – 1849)	194.72
	♀	6	8.00 (6.87 – 8.74)	0.74	2.87 (2.4 – 3.6)	0.46	1097.50 (560 -1597)	330.26
15 M Gata-1^{low}	♂	10	6.37 (5.53 – 7.20)	0.56	9.63 (4.2 – 14.1)	3.03	82.91 (23 – 336)	88.11
	♀	1	5.70	n/a	12.10	n/a	18.00	n/a

To minimize heterogeneity in this age-dependent study, especially in the advanced disease stage (15 months), all experiments shown were carried out using male, hemizygous Gata-1^{low} and male, age-matched WT control mice.

Male Gata-1^{low} mice of all ages were normal in body weight (Figure 3.1A). As early as 5 months of age, Gata-1^{low} mice developed a pronounced splenomegaly (Figure 3.1B). However, liver weight remained normal at all ages (Figure 3.1C), suggesting that the spleen is the main site of extramedullary hematopoiesis. Gata-1^{low} mice developed time-dependent, progressive anemia, as indicated by a steady decrease in red blood cells (Figure 3.1D). Further, an increase in white blood cells implied a moderate leukocytosis starting at month 10 (Figure 3.1E). The number of platelets was massively reduced in Gata-1^{low} mice at all ages (Figure 3.1F).
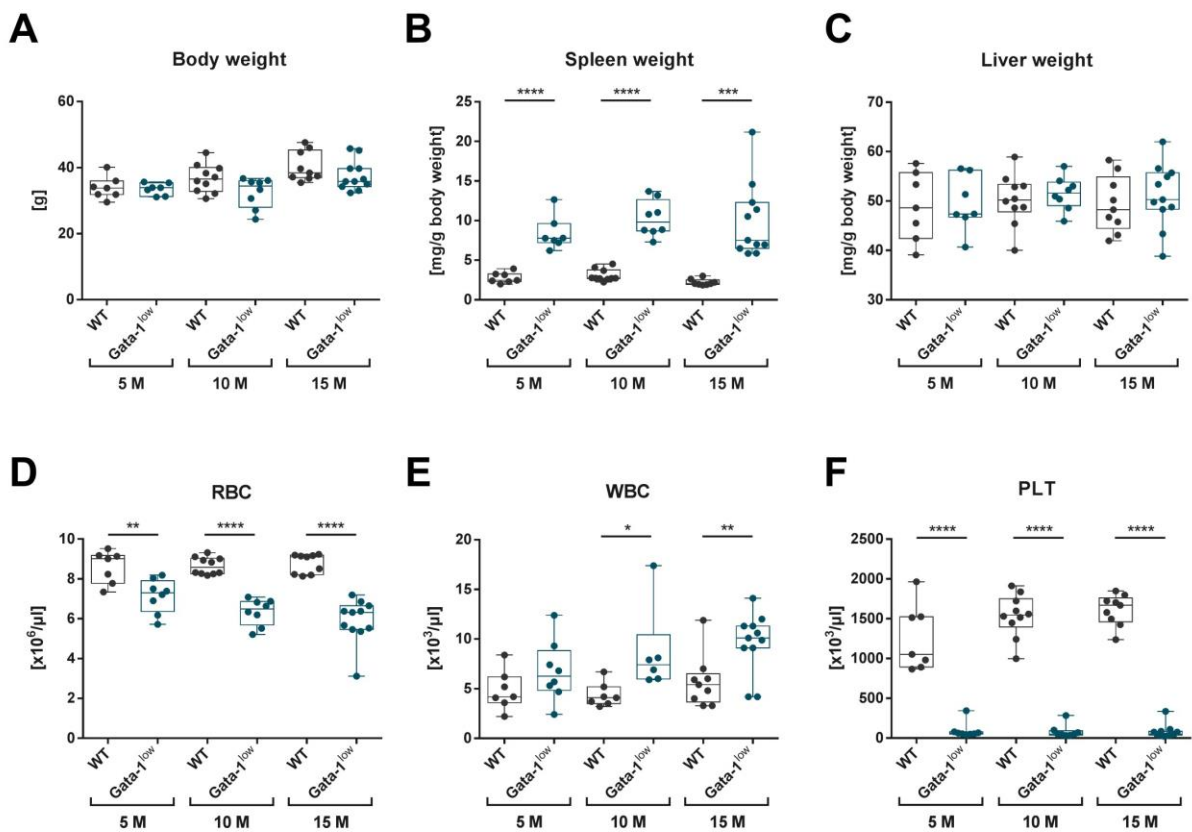
Figure 3.1: Characteristics of the Gata-1^{low} mouse model for primary myelofibrosis at 5 months (5 M), 10 months (10 M) and 15 months (15 M) of age. **A** Body weight of Gata-1^{low} mice and age-matched wild type (WT) controls. **B** Spleen weight per g body weight. **C** Liver weight per g body weight. **D** Red blood cell (RBC) counts. **E** White blood cell (WBC) counts **F** Platelet (PLT) counts.

In order to specify the time range which is signified by collagen production in the bone marrow of Gata-1^{low} mice, type I collagen *Col1a1* (Figure 3.2A) and type III collagen *Col3a1* (Figure 3.2B) gene expression were analyzed by qPCR. There was a significant decrease of *Col1a1* gene expression in the bone marrow of 5-month-old Gata-1^{low} mice. However, a marked increase in gene expression of the two collagens was detected in 10-month-old and remained increased in 15-month-old Gata-1^{low} mice.
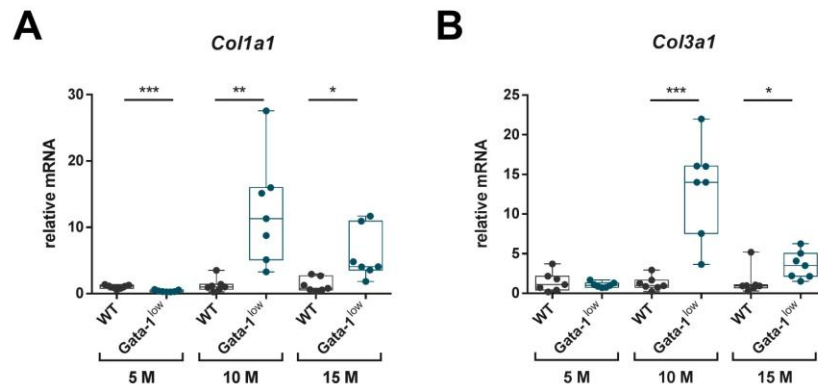
Figure 3.2: Gene expression of collagens in the bone marrow of Gata-1^{low} mice at 5 months (5 M), 10 months (10 M) and 15 months (15 M) of age. qPCR analyses of **A** type I collagen *Col1a1* and **B** type III collagen *Col3a1* in the bone marrow of Gata-1^{low} mice and age-matched wild type (WT) controls.

In order to evaluate pathological changes in the bone marrow of Gata-1^{low} mice, cells within the femoral bone marrow were visualized using May-Grünwald Giemsa staining (Figure 3.3, upper panel). As indicated by black arrows, high numbers of dysplastic megakaryocytes were found in the bone marrow of Gata-1^{low} mice at all ages. To determine fibrotic stages in Gata-1^{low} mice, bone marrow was stained for reticulum fibers (Figure 3.3, lower panel). No apparent accumulation of reticulum fibers was observed in the bone marrow of Gata-1^{low} mice at month 5, but there was an increased deposition of stained fibers at month 10. At 15 months of age, a pronounced accumulation of reticulum fibers was detected in the bone marrow (red arrowheads). Hence, month 5 was defined as a **pre-fibrotic**, month 10 as an **early fibrotic**, and month 15 as an **overt fibrotic** stage in Gata-1^{low} mice.
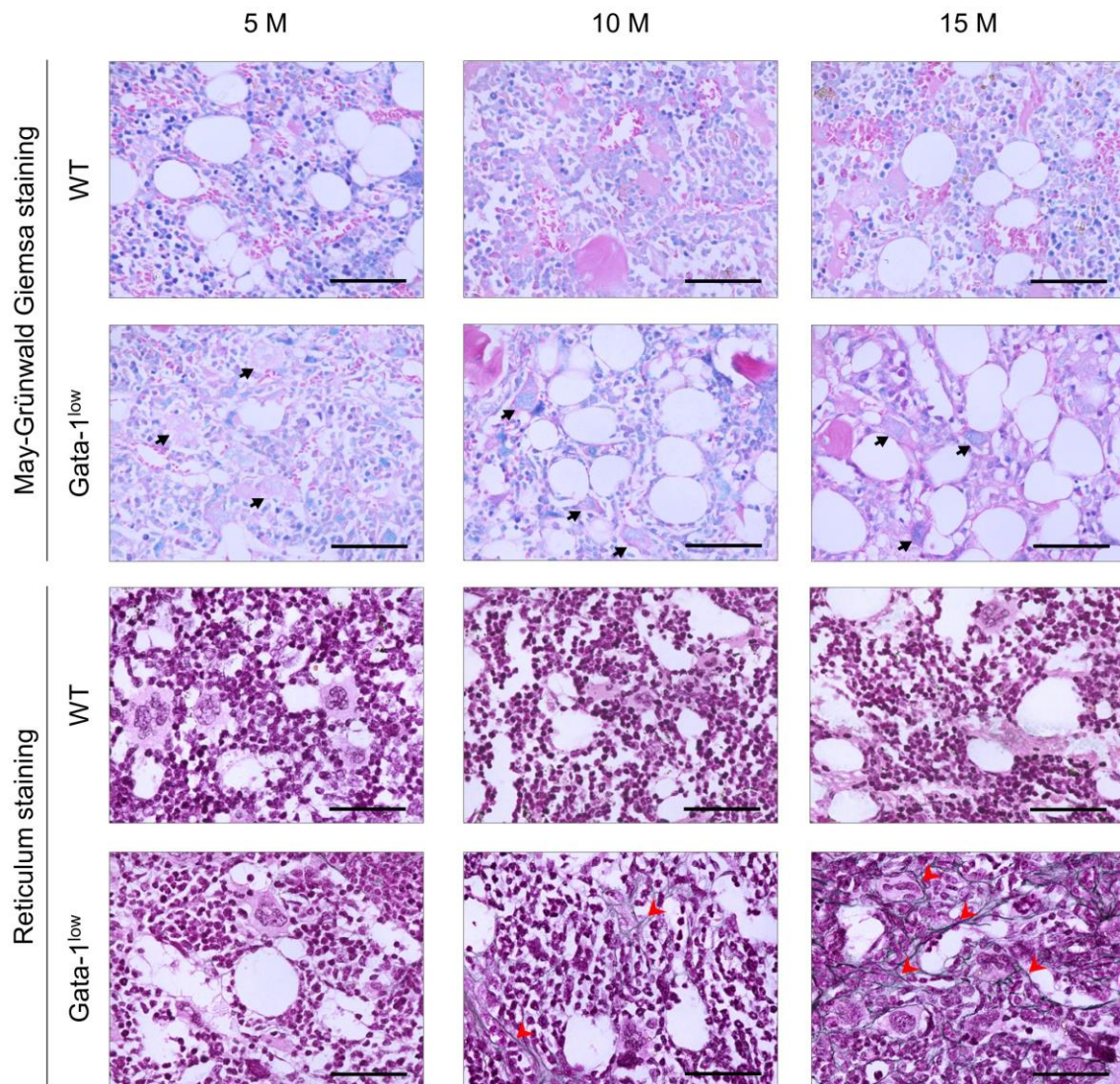
Figure 3.3: Representative images of the femoral bone marrow of Gata-1^{low} mice and wild type (WT) controls at 5 months (5 M), 10 months (10 M) and 15 months (15 M) of age. May-Grünwald Giemsa staining showing dysplastic megakaryocytes (upper panel, black arrows) and reticulum staining showing increasing amount of reticulum fibers (lower panel, red arrowheads) in the bone marrow of Gata-1^{low} mice. Scale bars = 50 μm.

3.2 Transcriptome analyses in early fibrotic bone marrow

It has previously been observed that collagen gene expression was highly upregulated in early fibrotic bone marrow of Gata-1^{low} mice at 10 months of age. Hence, transcriptomic changes in this very stage were investigated by whole transcriptome RNAseq. Differential gene expression analyses of n=3 Gata-1^{low} vs. n=3 WT mice revealed a total of 1503 upregulated and 1604 downregulated genes. Since RTKs and RTK-activating ligands have been attributed an important role in myelofibrosis, it was further focused on transcriptomic changes of RTKs (Figure

3.4A) and their cognate ligands (Figure 3.4B). Interestingly, a high number of RTKs showed a significant increase in gene expression, among those, *Flt1*, *Fgfr1*, *Ptk7*, *Tie1* and the PDGF receptors *Pdgfra* and *Pdgfrb*. Only three RTKs showed significant decrease in gene expression (*Epha7*, *Fgfrl1* and *Mertk*). Although many ligands were not significantly regulated in early fibrotic bone marrow of Gata-1^{low} mice, an induction of *Angpt2*, *Angpt4*, *Efna2*, *Efnb1*, *Igf2*, *Pgf* and *Ptn* was observed. Gene expression of three ligands (*Figf*, *Igf1*, *Kitl*,) was decreased.
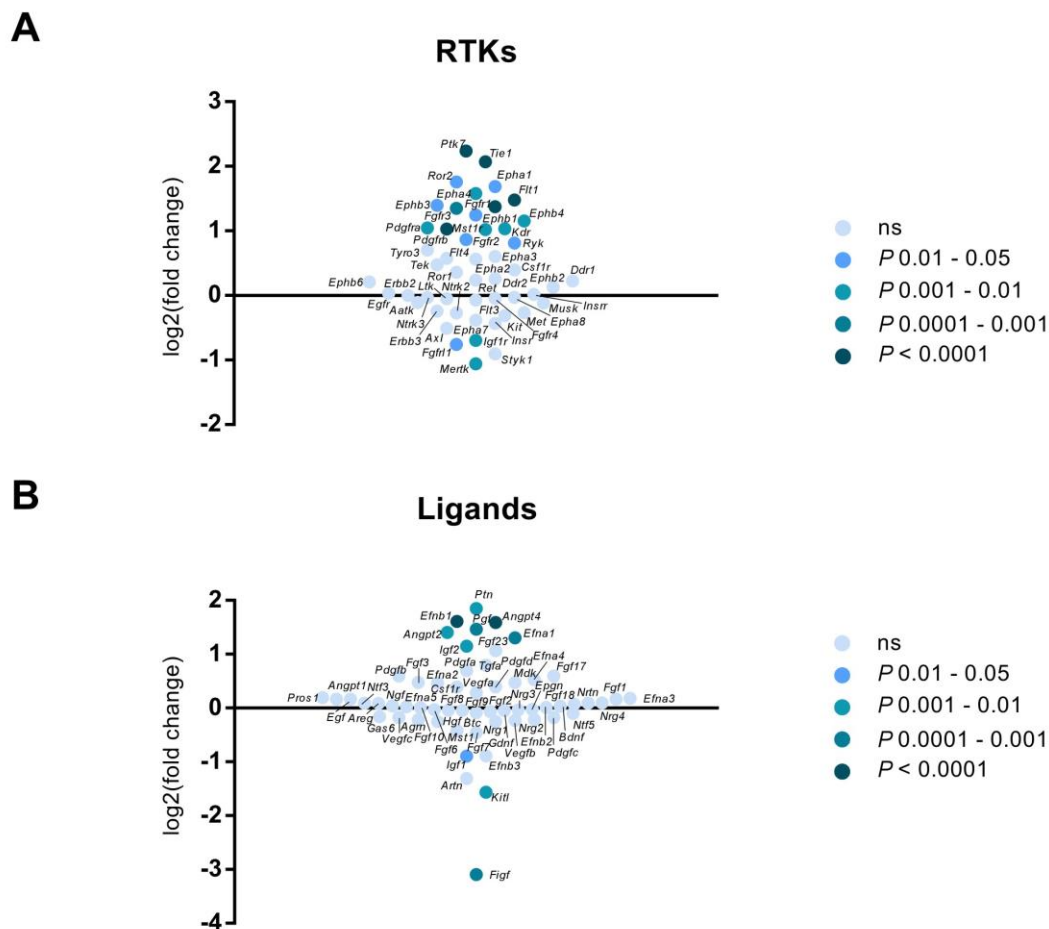
Figure 3.4: RNA sequencing analyses showing differential gene expression of receptor tyrosine kinases (RTKs) and their ligands. Total RNA from femoral bone marrow of mice at 10 months of age (n=3 Gata-1^{low} vs. n=3 wild type mice) was analyzed. **A** Differential gene expression of RTKs. **B** Differential gene expression of their cognate ligands. ns: not significant.

In order to classify all transcriptionally upregulated genes to their biological function, GO enrichment analyses were performed. These analyses aimed at identifying biological pathways of genes, which were statistically enriched within the gene expression data set. GO enrichment analyses revealed different implications of the 1503 upregulated genes (Figure 3.5). Interestingly, genes implicated in PDGF binding were most overrepresented within the upregulated genes. As per GO

molecular function annotation data set, the term 'PDGF binding' includes all selectively and non-covalently PDGF-interacting gene products (i.e. PDGF ligands, receptors and type I - VI collagens). These were followed by ECM structural constituents and genes involved in collagen binding.
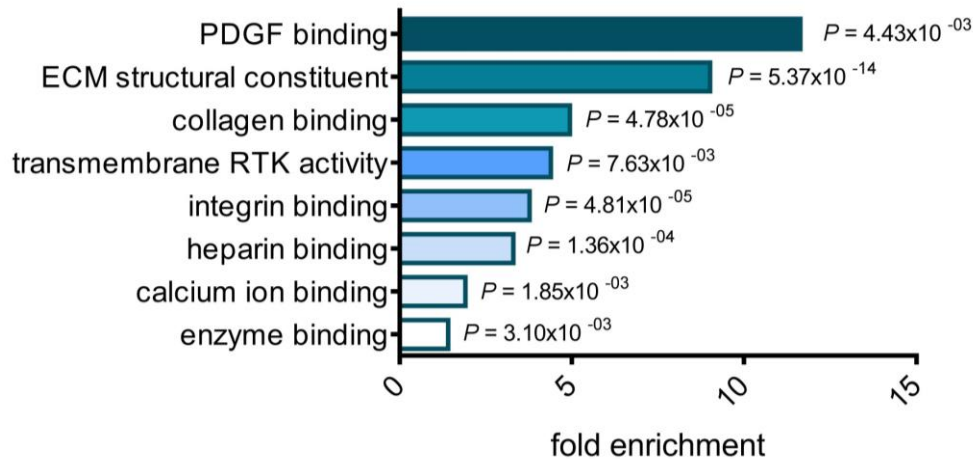
Figure 3.5: Gene ontology (GO) enrichment analysis of overexpressed genes. Results are based on RNA sequencing data from femoral bone marrow of mice at 10 months of age (n=3 Gata-1^{low} vs. n=3 wild type mice). PDGF: platelet-derived growth factor, ECM: extracellular matrix, RTK: receptor tyrosine kinase.

3.3 Expression of PDGFs and their receptors in the bone marrow

In order to characterize the expression dynamics of PDGF signaling components in different stages of bone marrow fibrosis, gene expression of the receptor and ligand genes in the bone marrow Gata-1^{low} mice were analyzed by qPCR (Figure 3.6). Here, highly induced gene expression of both receptor genes *Pdgfra* and *Pdgfrb* was observed in early fibrotic bone marrow from Gata-1^{low} mice at 10 months of age and remained increased in overt fibrotic bone marrow of 15-month-old Gata-1^{low} mice (Figure 3.6A and B). Interestingly, *Pdgfrb* gene expression was significantly decreased in pre-fibrotic bone marrow of 5-month-old Gata-1^{low} mice, as previously detected for *Col1a1* gene expression in that very stage. qPCR analyses of the ligand genes *Pdgfa* and *Pdgfb* revealed a major increase in ligand gene expression at the early fibrotic stage (Figure 3.6C and D). Again, a decrease in *Pdgfa* gene expression in pre-fibrotic bone marrow was observed, whereas *Pdgfa* gene expression was increased in early and overt fibrotic bone marrow. *Pdgfb* gene expression was significantly upregulated only in early fibrotic bone marrow and remained nearly at a baseline level in pre-fibrotic and overt fibrotic bone marrow of Gata-1^{low} mice.
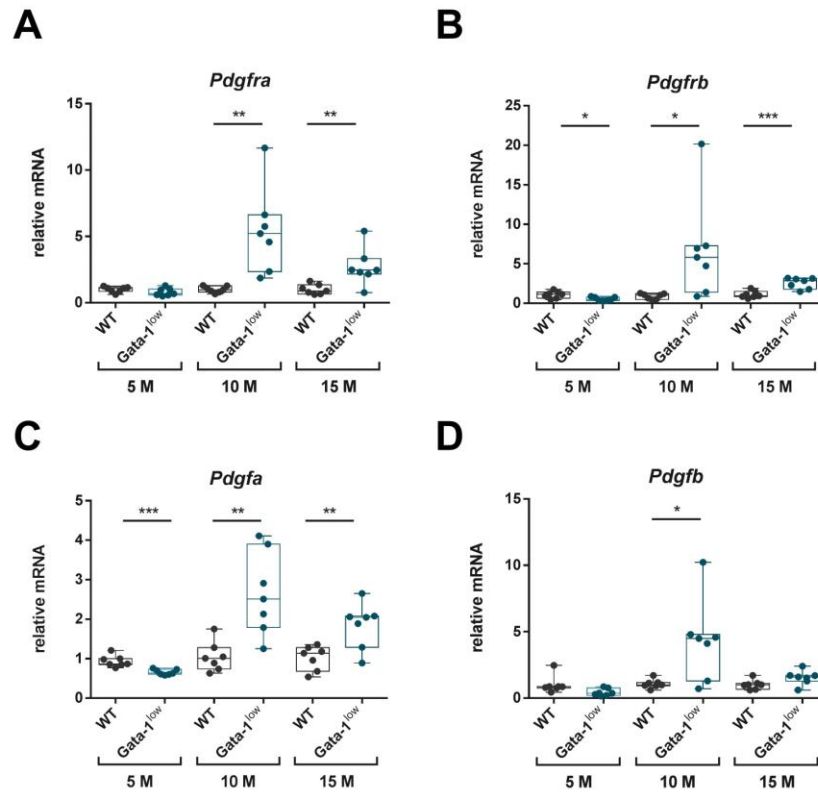
Figure 3.6: Gene expression of platelet-derived growth factors (PDGFs) and their receptors in the bone marrow of Gata-1low mice and age-matched wild type (WT) controls at 5 months (5 M), 10 months (10 M) and 15 months (15 M) of age. qPCR analyses of **A** *Pdgfra*, **B** *Pdgfrb*, **C** *Pdgfa* and **D** *Pdgfb*.

To visualize the expression of the PDGF signaling components within the bone marrow, multiplexed IHC staining of the PDGF signaling components was performed (Figure 3.7). This technique uses fluorescent tyramide HRP substrates, which form stable complexes that allow for staining of multiple proteins in one tissue section. Multispectral imaging was used for the detection of signals, which were subsequently unmixed to generate pseudo-single stained images. The multiplexed images within this work hence show staining of the different proteins in one and the same tissue section, and for a comprehensive comparison between the detected proteins, images show the same acquired image section within the tissue.
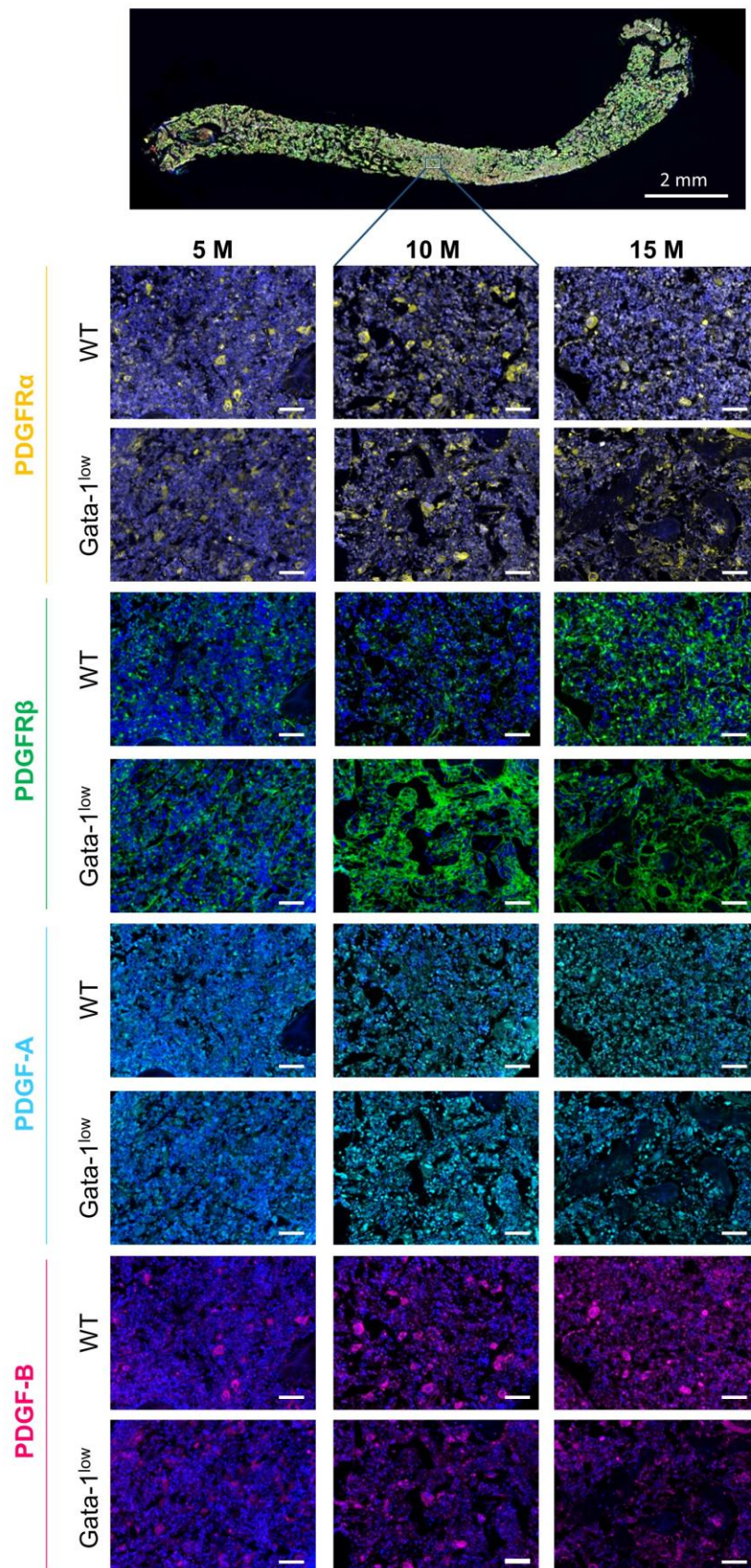
Figure 3.7: Multiplexed immunohistochemical (IHC) staining of platelet-derived growth factors (PDGFs) and their receptors in the bone marrow of Gata-1^{low} mice at 5 months (5 M), 10 months (10 M) and 15 months (15 M) of age. Representative images showing femoral bone marrow of Gata-1^{low} mice and wild type (WT) control mice stained for PDGF receptor α (PDGFRα, yellow), PDGF receptor β (PDGFRβ, green), PDGF-A (cyan) and PDGF-B (magenta). Nuclei were counterstained with DAPI (blue), scale bars in lower panels = 50 μm.

PDGFRα expression (yellow) was detected predominantly in megakaryocytes, both in WT and in Gata-1^{low} mice. PDGFRβ staining (green) was seemingly increased in early and overt fibrotic bone marrow of Gata-1^{low} mice and marked spindle-shaped cells, which typically represent stromal cells, such as fibroblasts. Staining of the ligand PDGF-A (cyan) showed expression in a wide variety of different hematopoietic cells, whereas PDGF-B (magenta) mainly derived from megakaryocytes both in WT and in Gata-1^{low} mice, suggesting a mostly paracrine effect of PDGF-B on PDGFRβ in the bone marrow.

To evaluate the cell-specific expression of PDGF receptors and ligands more clearly, the unmixed imaging data from multiplexed IHC were used to generate pseudo-brightfield IHC images (Figure 3.8). Exemplarily, bone marrow sections from 10-month-old Gata-1^{low} mice was used to include fibrosis-associated PDGFRβ-positive staining. These higher magnification images visualize more explicitly the megakaryocyte-specific expression of PDGF-A, -B and PDGFRα (black arrows). PDGF-A expression, although in low intensity, was seen more widely in other hematopoietic cells compared to PDGF-B expression, which was strongest in megakaryocytes. Megakaryocytes were clearly negative for PDGFRβ expression, but PDGFRβ staining was positive in long and spindle-like cells with elongated nuclei (black arrowhead).
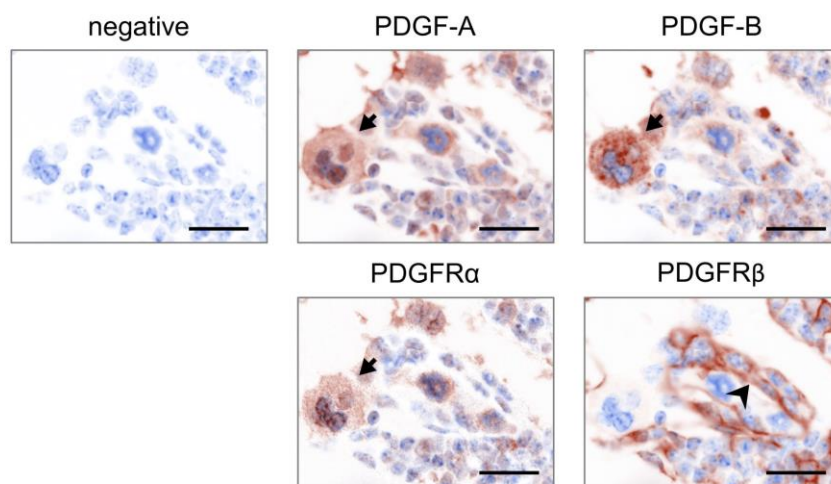
Figure 3.8: Pseudo-brightfield immunohistochemistry (IHC) images of platelet-derived growth factors (PDGFs) and their receptors in the bone marrow of Gata-1^{low} mice. PDGF-A, PDGF-B and PDGF receptor α (PDGFRα) expression in megakaryocytes is indicated by black arrows and PDGFRβ expression in spindle-shaped stromal cells is indicated by black arrowhead. Images are exemplary from bone marrow of a Gata-1^{low} mouse at 10 months of age. Scale bars = 20 μm.

Although primary antibodies detect the different isoforms specifically, it must be notes that PDGF ligands are synthesized as dimers (PDGF-AA and -BB homo-, and PDGF-AB heterodimers) and do not exist as functional protein monomers. The antibodies used in this study, however, detect peptide sequences within protein monomers, and hence might detect homo- as well as heterodimers. Consequently, the notations within antibody-based detection methods in this study refer to the PDGF ligands, physiologically inapplicable, as 'PDGF-A' and 'PDGF-B'.

The data acquired by multiplexed IHC provide a solid means to quantify protein expression of the different PDGF signaling components. In order to apply an even more sensitive method for protein quantification, an *in situ* PLA in a single recognition approach was used (see Figure 2.2A in the 'Methods' section for assay principle). The assay is based on proximity-mediated ligation of two probes and an amplification reaction which results in the creation of signals. These signals, also referred to as rolling circle products (RCPs), are detectable and quantifiable in the tissue as distinct, fluorescent dots. In the PLA single recognition approaches, the tissue sections were incubated with single, specific primary antibodies. Technical negative controls were generated by incubation with normal mouse and rabbit IgG (Figure 3.9). All negative controls within this study utilized tissue that typically yields highest signal strengths for the respective method, hence bone marrow section from 15-month-old Gata-1^{low} mice was used for negative controls in antibody-based assays. In PLA negative controls, 1-2 false-positive signals (RCPs) per 100 cells were typically detected.
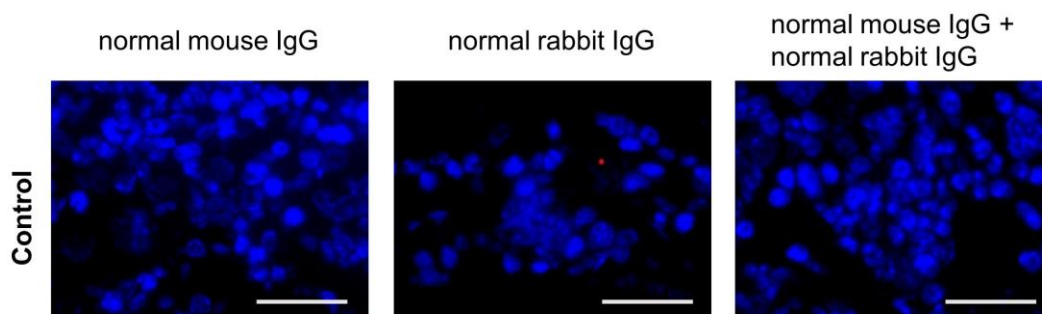
Figure 3.9: Technical negative control for the different proximity ligation assay (PLA) approaches. Bone marrow from Gata-1^{low} mice at 15 months of age were incubated with normal mouse, normal rabbit immunoglobulin G (IgG), or a combination of both. Scale bars = 20 μm.

For methodical validation of the quantitative analysis by PLA, PDGFRβ and PDGF-B protein expression was analyzed by single recognition PLA. The acquired PLA data were directly compared to quantified protein expression data from multiplexed IHC (Figure 3.10A). Comparing PDGFRβ protein expression data from multiplexed IHC (Figure 3.10B) to PDGFRβ protein expression data from PLA (Figure 3.10C), very good conformity of results was seen. Representative images of quantified RCPs are depicted in the upcoming protein expression analyses section. When comparing PDGF-B protein expression data from multiplexed IHC (Figure 3.10D) to PDGF-B protein expression data from PLA (Figure 3.10E), some discrepancy in quantification was observed in pre-fibrotic bone marrow of Gata-1^{low} mice. For a validation of the PLA for PDGFRβ–PDGF-B interaction analysis (see Figure 2.2B in the 'Methods' section for assay principle), data from a PLA was compared to colocalization data gathered from multispectral imaging (Figure 3.10F and G). The data acquired by PLA were generally in good agreement with data acquired by multiplex staining as another antibody-based method. However, colocalization and PLA interaction analyses rely on principally different detection mechanisms, and minor differences were to be expected when juxtaposing both methods.
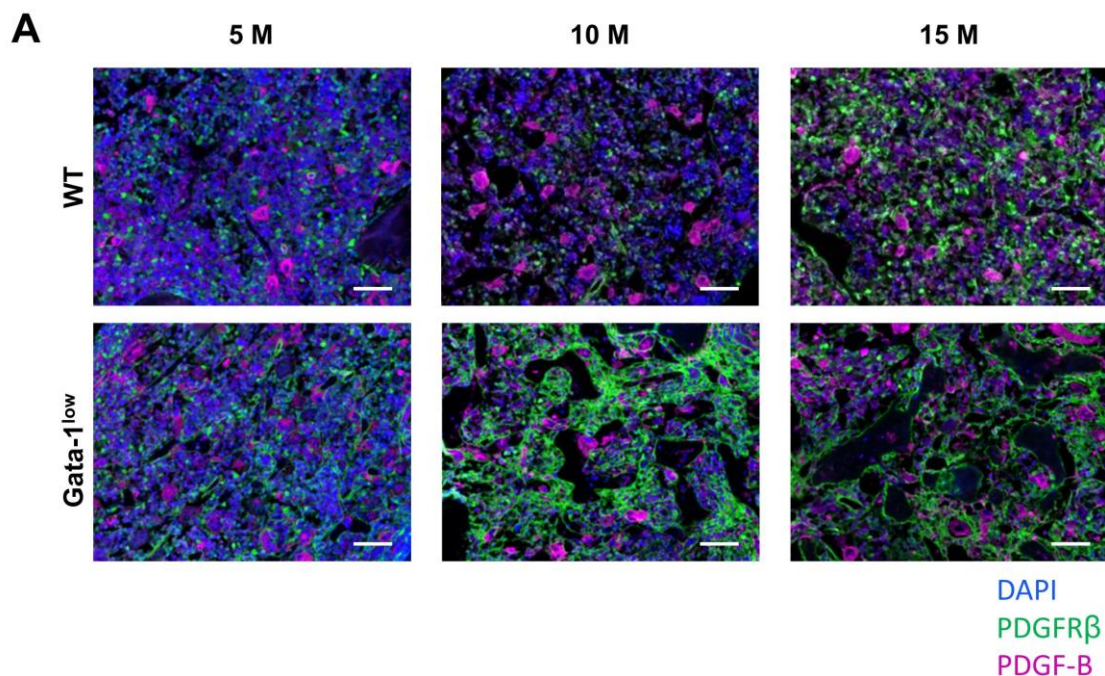
Figure 3.10: Continued on page 57.
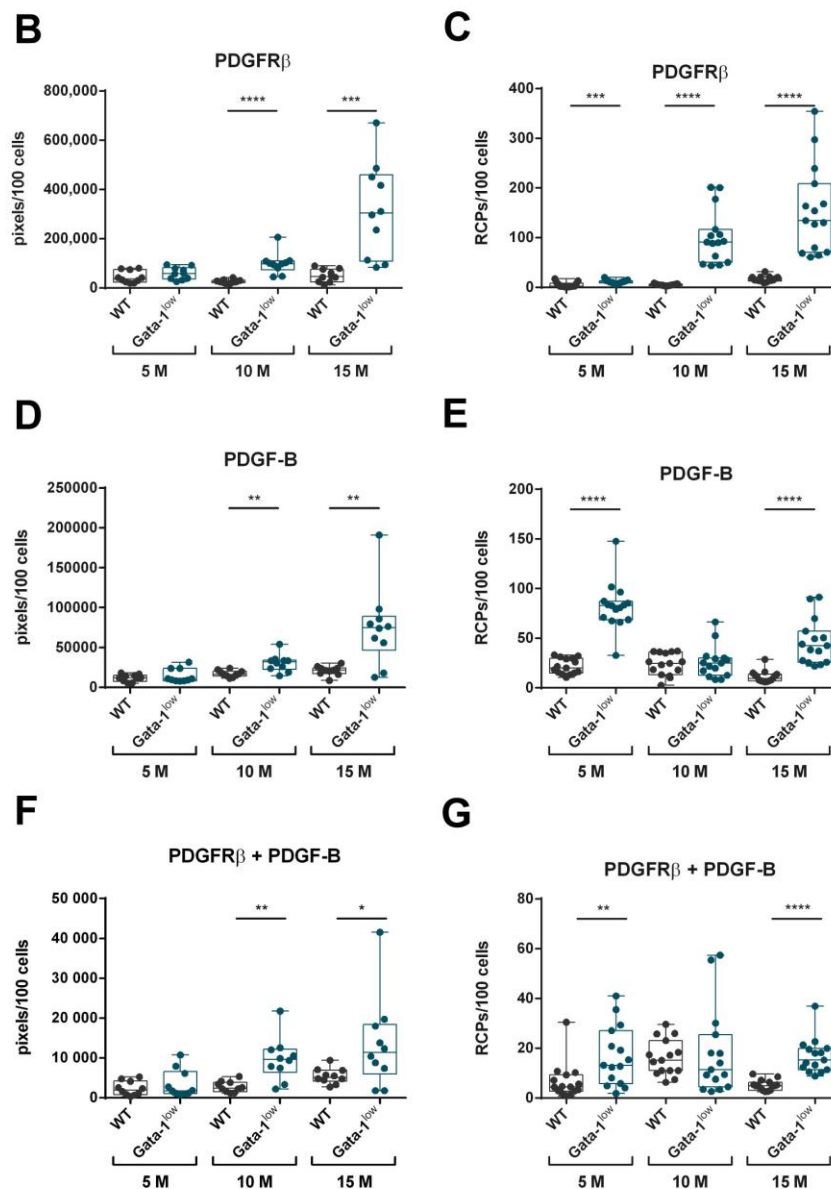
Figure 3.10: Multiplexed immunohistochemical (IHC) staining of platelet-derived growth factor (PDGF)-B and PDGF receptor β (PDGFRβ), and *in situ* protein quantification by imaging and by single recognition proximity ligation assay (PLA) in the bone marrow of Gata-1^{low} mice at 5 months (5 M), 10 months (10 M) and 15 months (15 M) of age. **A** Representative images showing femoral bone marrow of Gata-1^{low} mice and WT control mice stained for PDGFRβ (green) and PDGF-B (magenta). Nuclei were counterstained with DAPI (blue), scale bars = 50 μm. Images show the same sections which are depicted in Figure 3.7. **B** Quantification of PDGFRβ protein expression using the acquired imaging data. **C** Quantification of PDGFRβ protein expression using single recognition PLA. **D** Quantification of PDGF-B protein expression using the acquired imaging data. **E** Quantification of PDGF-B protein expression using single recognition PLA. **F** Quantification of PDGFRβ–PDGF-B colocalization using the acquired imaging data. **G** Quantification of PDGFRβ–PDGF-B interaction using PLA. All quantification plots show exemplary data from one and the same mouse, respectively, per group.

After methodical validation, the single recognition PLA was applied to quantify protein expression of the PDGF signaling components within the mouse cohorts (Figure 3.11 and Figure 3.12). Although a heterogeneity in protein expression was observed in Gata-1^{low} mice, there was a steady increase in PDGF receptor protein expression during the development of myelofibrosis, whereas expression in WT mice remained steady (Figure 3.11). However, only increases in PDGFRα protein expression in pre-fibrotic bone marrow (Figure 3.11C) and in PDGFRβ protein expression in overt fibrotic bone marrow (Figure 3.11D) reached statistical significance. When analyzing PDGF-A and PDGF-B protein expression by single recognition PLA, high heterogeneity among age-matched Gata-1^{low} mice was observed (Figure 3.12). There was a particularly high signal strength when detecting PDGF-A protein expression by single recognition PLA (Figure 3.12A), still, there was no significant increase in PDGF-A expression in Gata-1^{low} mice compared to WT controls (Figure 3.12C). However, PDGF-B protein expression was significantly increased in overt fibrotic bone marrow of 15-month-old Gata-1^{low} mice compared to WT animals (Figure 3.12B and D).
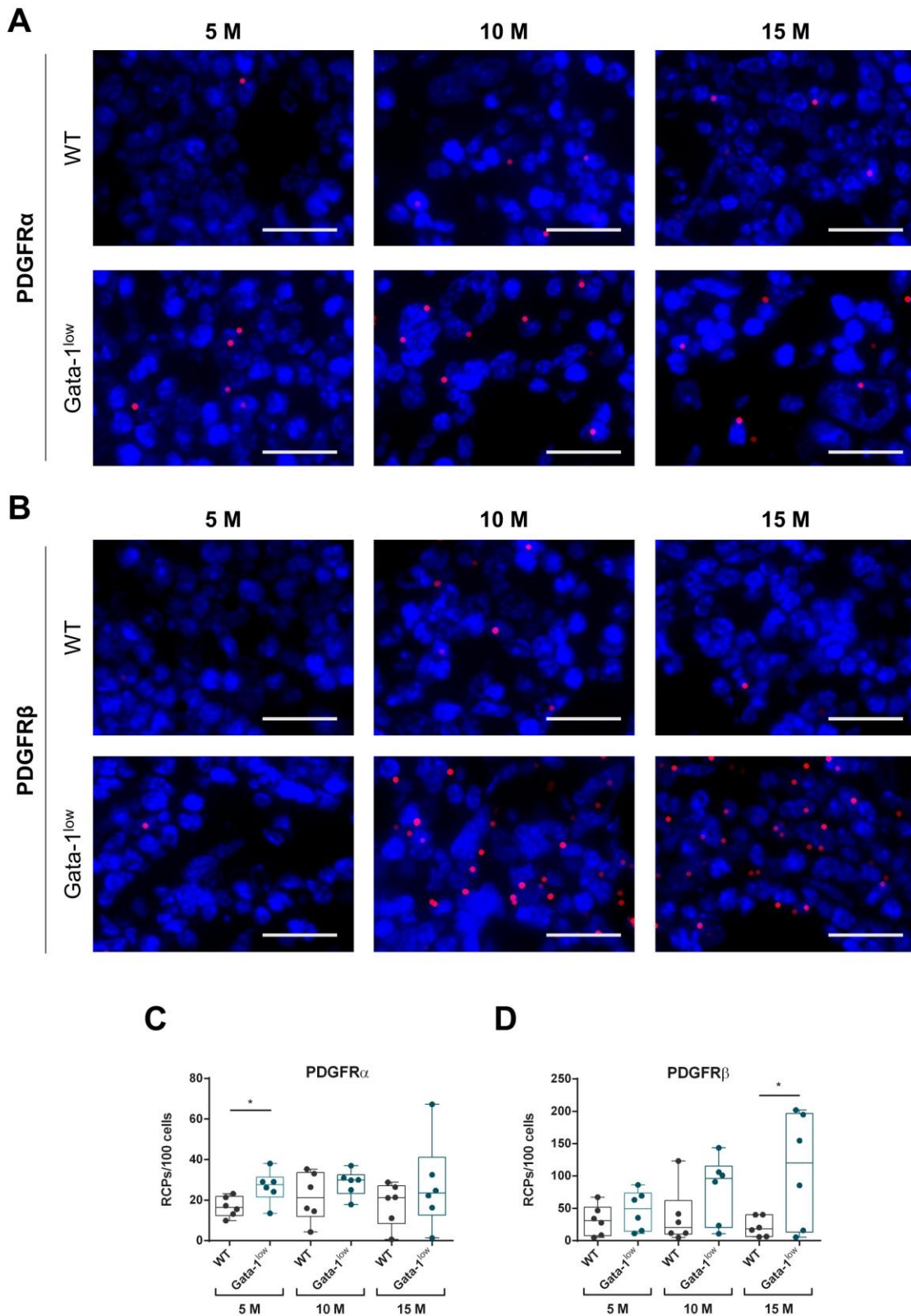
Figure 3.11: Protein expression of platelet-derived growth factor receptors (PDGFRs) in the bone marrow of Gata-1low mice at 5 months (5 M), 10 months (10 M) and 15 months (15 M) of age. Representative images of single recognition proximity ligation assay (PLA) approaches for analyses of **A** PDGFRα and **B** PDGFRβ protein expression in the bone marrow of Gata-1low mice and age-matched wild type (WT) controls. **C** Quantitative analyses of PDGFRα and **D** PDGFRβ protein expression by single recognition PLA. Scale bars = 20 μm, RCPs: rolling circle products.
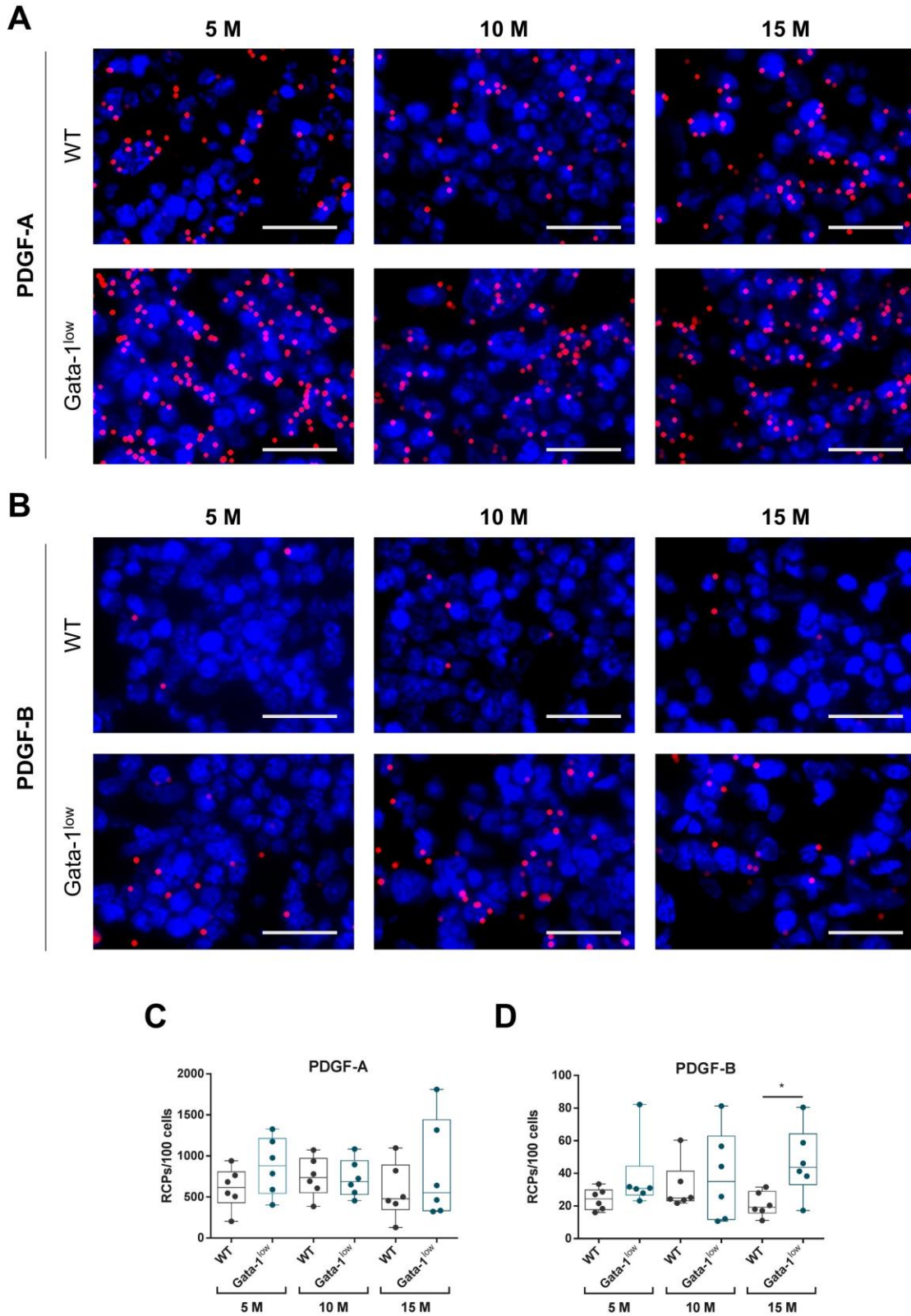
Figure 3.12: Protein expression of platelet-derived growth factors (PDGFs) in the bone marrow of Gata-1low mice at 5 months (5 M), 10 months (10 M) and 15 months (15 M) of age. Representative images of single recognition proximity ligation assay (PLA) approaches for analyses of **A** PDGF-A and **B** PDGF-B protein expression in the bone marrow of Gata-1low mice and age-matched wild type (WT) controls. **C** Quantitative analyses of PDGF-A and **D** PDGF-B protein expression by single recognition PLA. Scale bars = 20 µm, RCPs: rolling circle products.

3.4 PDGFRβ–ligand interaction and phosphorylation in the bone marrow

Whereas megakaryocyte dysplasia and proliferation is a defining feature of PMF, fibroblast proliferation leading to a progressive fibrosis is the key pathological aspect of PMF. Given the distinct expression of PDGFRβ in stromal cells in early and overt fibrotic bone marrow, shown by multiplexed IHC (Figure 3.7 and Figure 3.8), this study further concentrated on the dynamics of PDGFRβ and its ligand PDGF-B. The increased protein expression of PDGFRβ and its ligand PDGF-B in overt myelofibrosis, analyzed by single recognition PLA (Figure 3.11 and Figure 3.12), prompted to investigate the interaction of both signaling components *in situ*. In order to analyze PDGFRβ–PDGF B binding, a PLA using combined primary antibodies detecting PDGFRβ and PDGF-B was performed. PLA analyses of PDGFRβ–PDGF-B interaction revealed an increased interaction of receptor and ligand in overt fibrotic bone marrow of 15-month-old Gata-1^{low} mice (Figure 3.13A and C). This is in accordance with enhanced protein expression of both PDGFRβ and PDGF-B in overt fibrotic bone marrow of Gata-1^{low} mice and also suggests an increased activation of intracellular signaling in the overt fibrotic stage. To further analyze the activation status of the receptor, a PLA combining PDGFRβ and phosphotyrosine-targeting primary antibodies was applied in order to analyze PDGFRβ phosphorylation *in situ* (see Figure 2.2C in the 'Methods' section for assay principle). Surprisingly, no increased PDGFRβ tyrosine phosphorylation was observed at any stage of myelofibrosis in Gata-1^{low} mice (Figure 3.13B and D), suggesting the presence of mechanisms which counter-regulate PDGFRβ tyrosine phosphorylation.
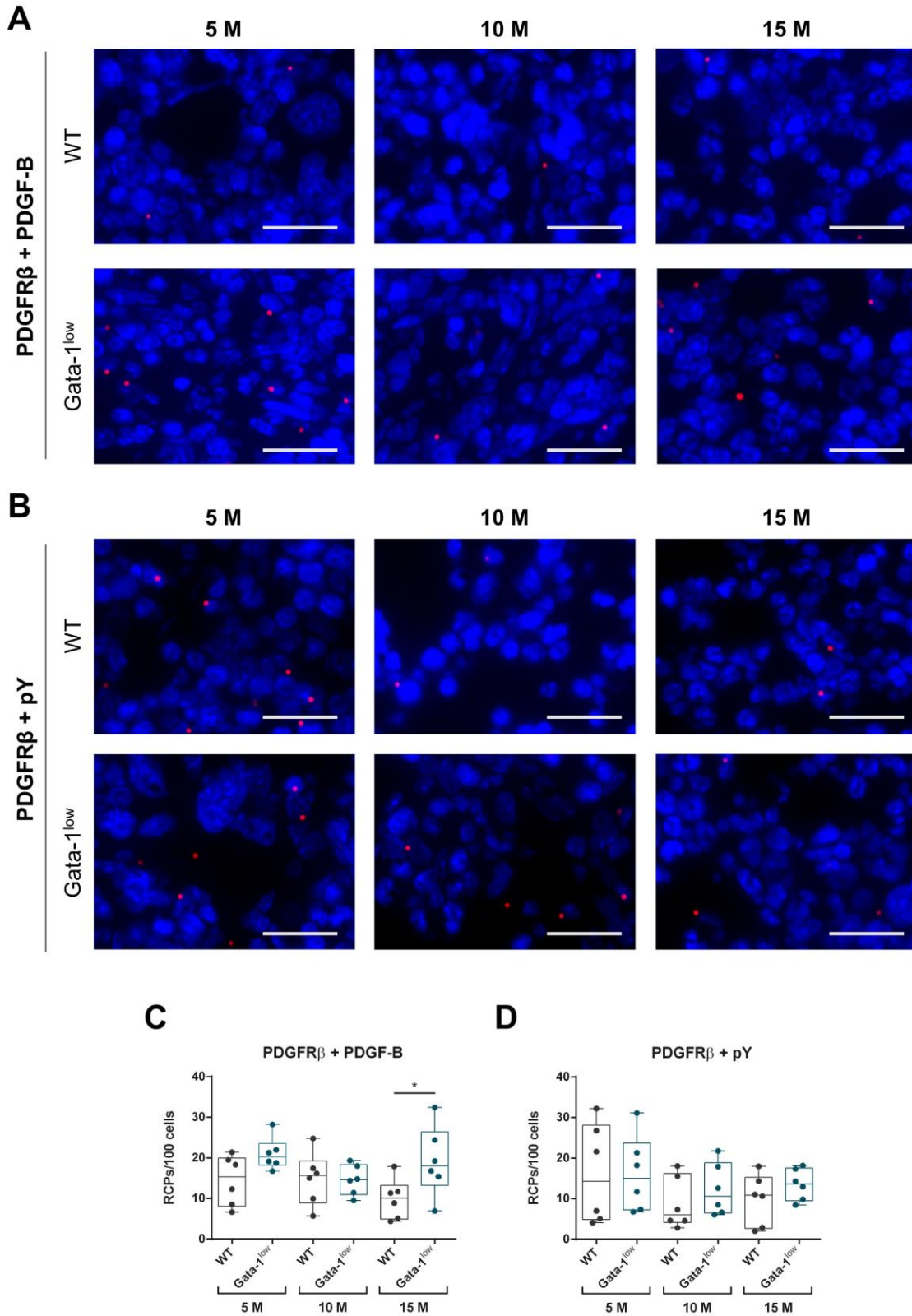
Figure 3.13: Analyses of platelet-derived growth factor receptor β (PDGFRβ) interaction with platelet-derived growth factor (PDGF)-B and PDGFRβ tyrosine phosphorylation in the bone marrow of Gata-1low mice and wild type (WT) controls at 5 months (5 M), 10 months (10 M) and 15 months (15 M) of age. Representative images showing a proximity ligation assay (PLA) for the analysis of **A** PDGFRβ–PDGF-B interaction and **B** PDGFRβ tyrosine phosphorylation in femoral bone marrow of Gata-1low mice and WT controls. **C** Quantitative analyses of PDGFRβ–PDGF-B interaction and **D** PDGFRβ tyrosine phosphorylation. Scale bars = 20 μm, RCPs: rolling circle products.

3.5   Expression of PTPs in the bone marrow

PTPs represent key regulators of RTK phosphorylation and altered PTP expression can have profound effects on cellular function.[207] Although the experiments within this study demonstrated increased protein expression, as well as interaction of PDGFRβ and PDGF-B, PDGFRβ phosphorylation was not enhanced. Therefore, differential gene expression of PTPs was examined using RNAseq data from early fibrotic bone marrow of Gata-1^{low} mice (Figure 3.14). The majority of PTPs was not differentially regulated in this stage of bone marrow fibrosis, nevertheless, there was a significant increase in *Ptprk* and *Ptprs*, and a decrease in *Ptpre*, *Pten* and *Ptprc* expression.

Figure 3.14: RNA sequencing analyses showing differential gene expression of protein tyrosine phosphatases (PTPs). Total RNA from femoral bone marrow of 10-month-old mice (n=3 Gata-1^{low} vs. n=3 wild type mice) was analyzed. ns: not significant.

Within these data, PDGFRβ-dephosphorylating PTPs were not differentially expressed (see Table 1.3 in the 'Introduction' section for a list of PDGFRβ-targeting PTPs). However, RNAseq data was only available from 10-month-old mice with n=3 mice per group. For a more refined investigation of PDGFRβ-dephosphorylating PTPs, gene expression of the six classical, class I PTPs, which are known to target PDGFRβ, was analyzed by qPCR (Figure 3.15A-F). Very distinct expression dynamics among gene expression of *Ptpn1* (encoding PTP1B), *Ptpn2* (encoding TC-PTP), *Ptpn6* (encoding SHP-1), *Ptpn11* (encoding SHP-2), *Ptpn12* (encoding

PTP-PEST) and *Ptprj* (encoding DEP-1) were observed. Overall, the data generated by qPCR from early fibrotic bone marrow of 10-month-old Gata-1^{low} mice again displayed heterogeneity in gene expression, possibly contributing to the lack of significance within the RNAseq analyses from these mice.

Interestingly, *Ptpn1* and *Ptprj* gene expression, analyzed by qPCR, was downregulated in pre-fibrotic bone marrow, a phenomenon that has previously been observed for *Col1a1*, *Pdgfrb* and *Pdgfa* gene expression. *Ptpn2*, *Ptpn6*, *Ptpn11* and *Ptpn12* were not differentially expressed in pre-fibrotic bone marrow. However, all analyzed PTPs, measured by median, show tendencies towards an upregulation in early fibrotic bone marrow of 10-month-old Gata-1^{low} mice. Still, only the increased expression of *Ptpn11* and *Ptpn12* reached significance. In overt fibrotic bone marrow, *Ptpn1*, *Ptpn6*, *Ptpn12* and *Ptprj* gene expression was not different in Gata-1^{low} mice and WT controls, but there was a significant increase in *Ptpn2* and *Ptpn11* gene expression in overt fibrotic bone marrow.
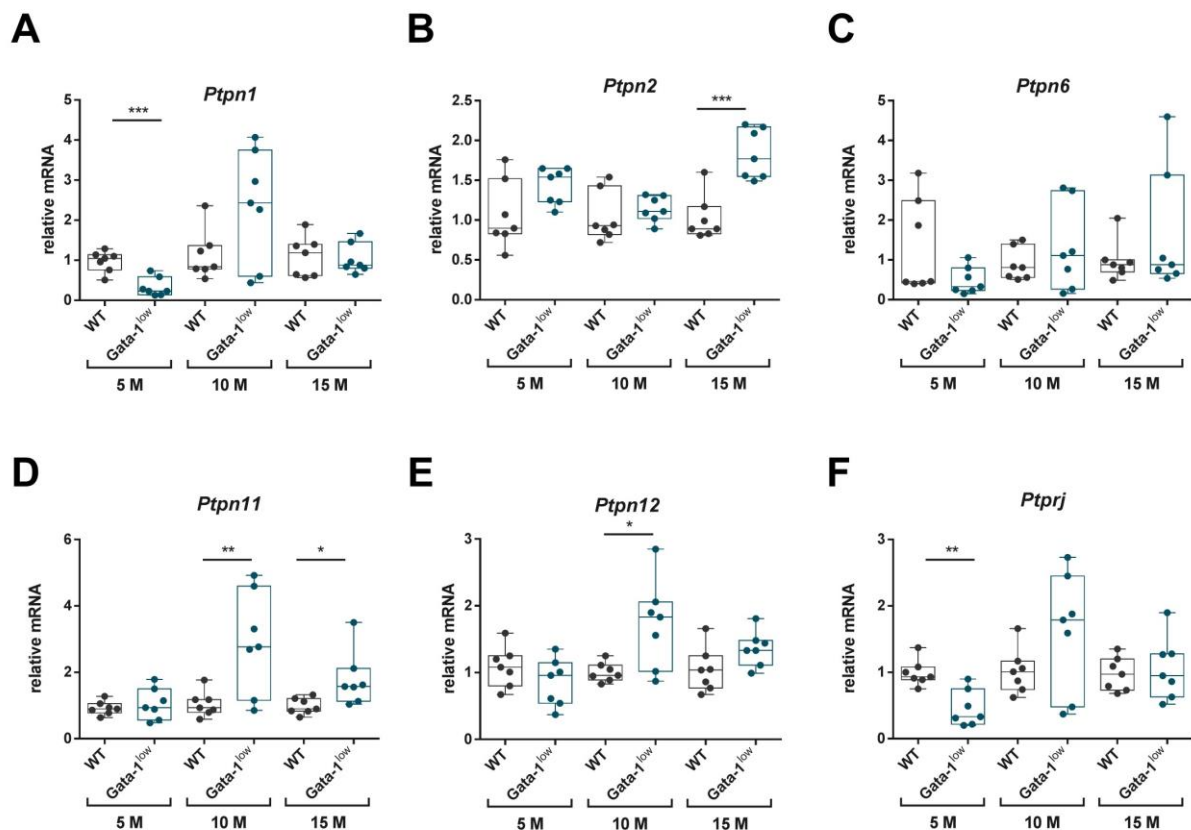
Figure 3.15: Gene expression analyses of platelet-derived growth factor receptor β (PDGFRβ)-targeting protein tyrosine phosphatases (PTPs) in the bone marrow of Gata-1^{low} mice and wild type (WT) controls at 5 months (5 M), 10 months (10 M) and 15 months (15 M) of age. qPCR analyses of **A** *Ptpn1*, **B** *Ptpn2*, **C** *Ptpn6*, **D** *Ptpn11*, **E** *Ptpn12* and **F** *Ptprj*.

An increased PTP expression in the bone marrow of 15-month-old Gata-1^{low} mice might be a possible explanation for previous observations regarding the lack of PDGFRβ phosphorylation in the overt fibrotic stage. Especially induction of *Ptpn2,* encoding T cell PTP (TC-PTP), was highly significant in overt fibrotic bone marrow. Given the conclusive increase in *Ptpn2* gene expression and the vital role of TC-PTP in normal hematopoietic function,[236,237] this study further focused on the role of TC-PTP as a possible contributor to PDGFRβ regulation.

3.6 TC-PTP expression and interaction with PDGFRβ in the bone marrow

In order to visualize and evaluate the expression patterns of TC-PTP in the bone marrow of Gata-1^{low} mice, multiplexed IHC was used (Figure 3.16). Staining of TC-PTP (red) revealed ubiquitous expression in the bone marrow of both WT and Gata-1^{low} mice of all ages. There was a slight but visible increase in TC-PTP staining intensity in the bone marrow of 10-month-old and 15-month-old Gata-1^{low} mice.
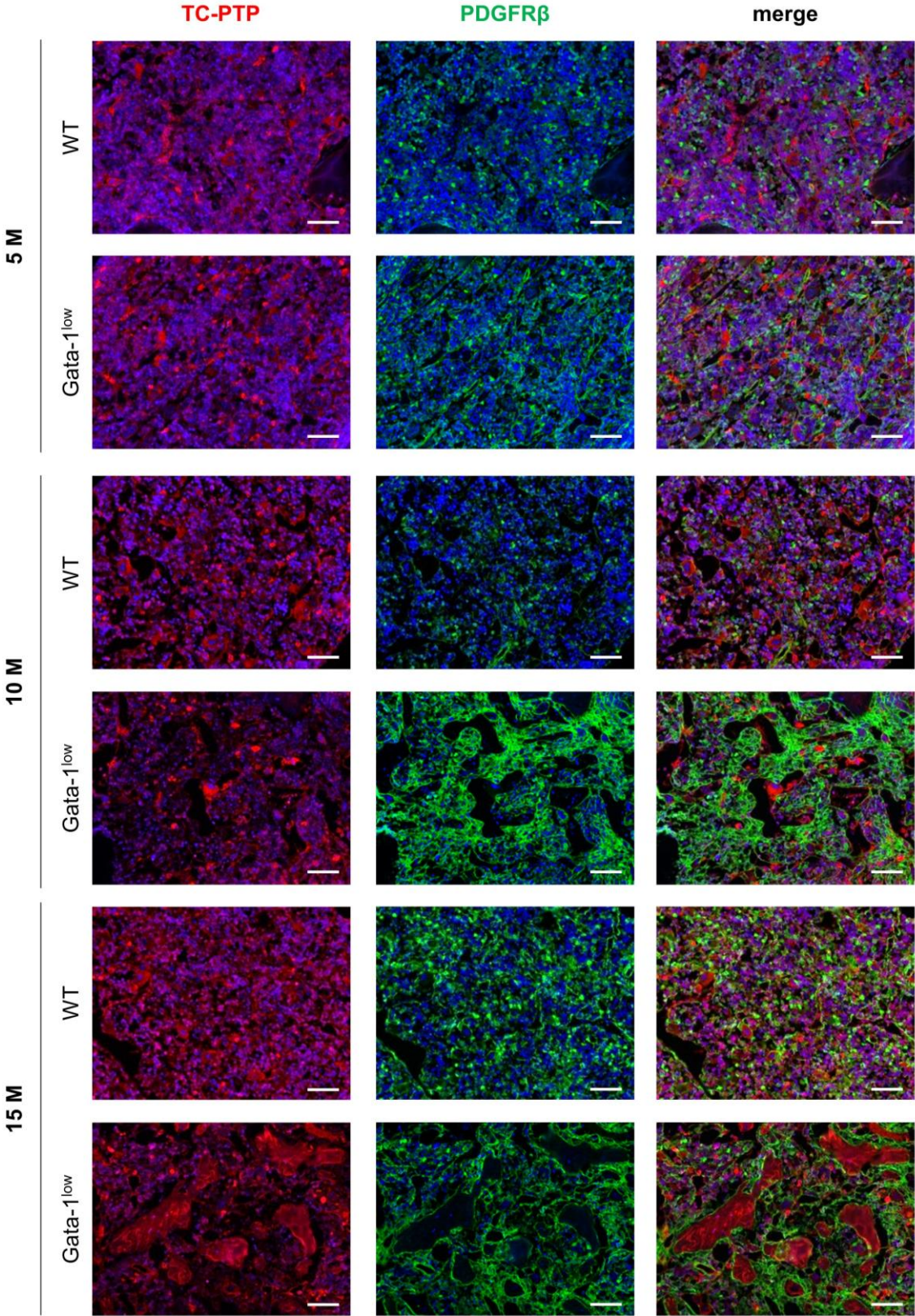
Figure 3.16: Multiplexed immunohistochemical (IHC) staining of TC-PTP and platelet-derived growth factor β (PDGFRβ) in the bone marrow of Gata-1^{low} mice at 5 months (5 M), 10 months (10 M) and 15 months (15 M) of age. Representative images showing femoral bone marrow of Gata-1^{low} mice stained for TC-PTP (red) and PDGFRβ (green). Nuclei were counterstained with DAPI (blue), scale bars = 50 µm. Images show the same sections which are depicted in Figure 3.7.

The fact that TC-PTP is expressed in a variety of different cells in the bone marrow, as shown in Figure 3.16, further raised the question, if TC-PTP expression in fibroblasts potentially enables direct regulation of PDGFRβ by TC-PTP in fibrosis-driving cells. Again, unmixed imaging data from multiplexed IHC were used to generate high magnification pseudo-brightfield IHC images from bone marrow sections of Gata-1^{low} mice (Figure 3.17). These images accentuate ubiquitous expression of TC-PTP in the bone marrow, and further, TC-PTP positivity was detected in spindle-shaped cells which were likewise positive for PDGFRβ expression (black arrowheads). The validity of this finding is strengthened by direct comparison to expression patterns of PTP1B. PTP1B and TC-PTP are two tightly related class I PTPs and structurally highly homolog.[238] Nonetheless, there is a striking difference in expression of these two PTPs in the bone marrow. PTP1B expression was virtually absent in spindle-shaped stromal cells and TC-PTP clearly discriminated as a potential regulatory PTP in bone marrow stromal cells.
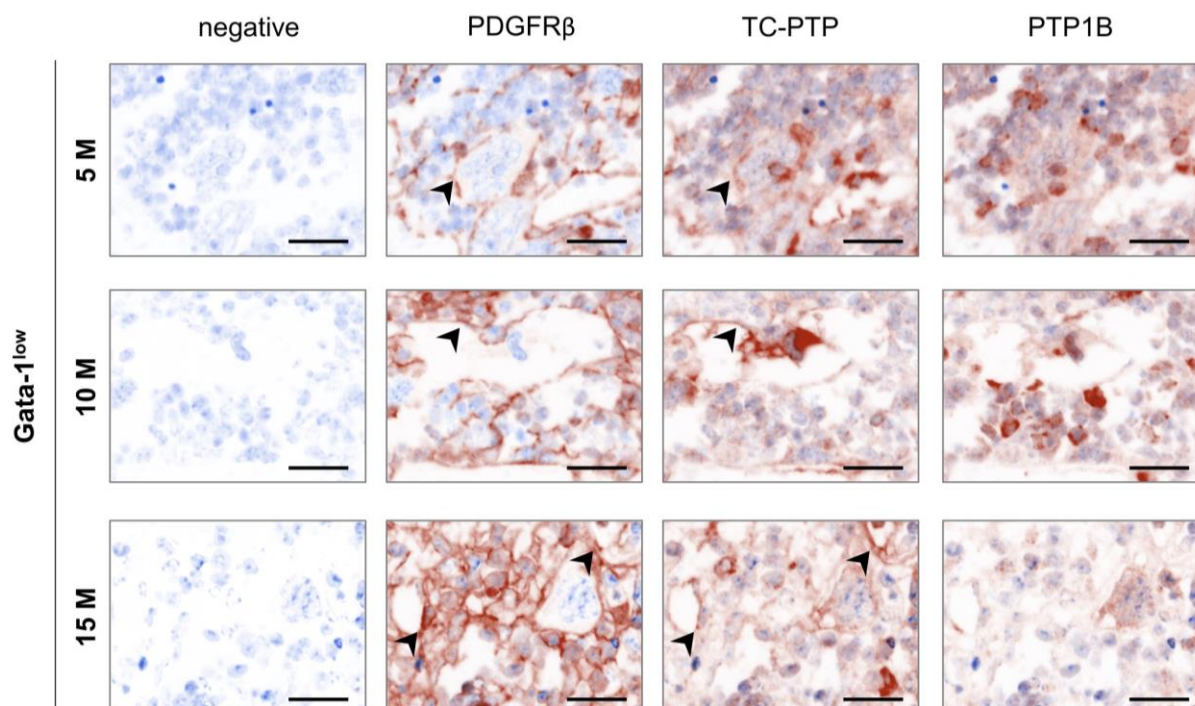
Figure 3.17: Pseudo-brightfield immunohistochemical (IHC) images of platelet-derived growth factor receptor β (PDGFRβ), TC-PTP and PTP1B. Positive staining in spindle-shaped stromal cells is indicated by black arrowhead. Scale bars = 20 µm.

Subsequently, TC-PTP protein expression was analyzed and quantified by single recognition PLA (Figure 3.18A). Quantitative analysis of confirmed an increased TC-PTP protein expression in early myelofibrosis (Figure 3.18C). The increased expression of PDGFRβ and TC-PTP in the bone marrow of Gata-1^{low} mice and the immunohistochemical detection indicating expression of both proteins in the same cell type further raised the question, if there is a profound interaction of both components in fibrotic bone marrow.

To analyze the interaction of PDGFRβ and TC-PTP, a PLA was applied using a combination of PDGFRβ and TC-PTP primary antibodies (see Figure 2.2D in the 'Methods' section for assay principle). Interestingly, there indeed was an increased interaction of PDGFRβ and TC-PTP in early and overt fibrotic bone marrow of Gata-1^{low} mice (Figure 3.18B and D).
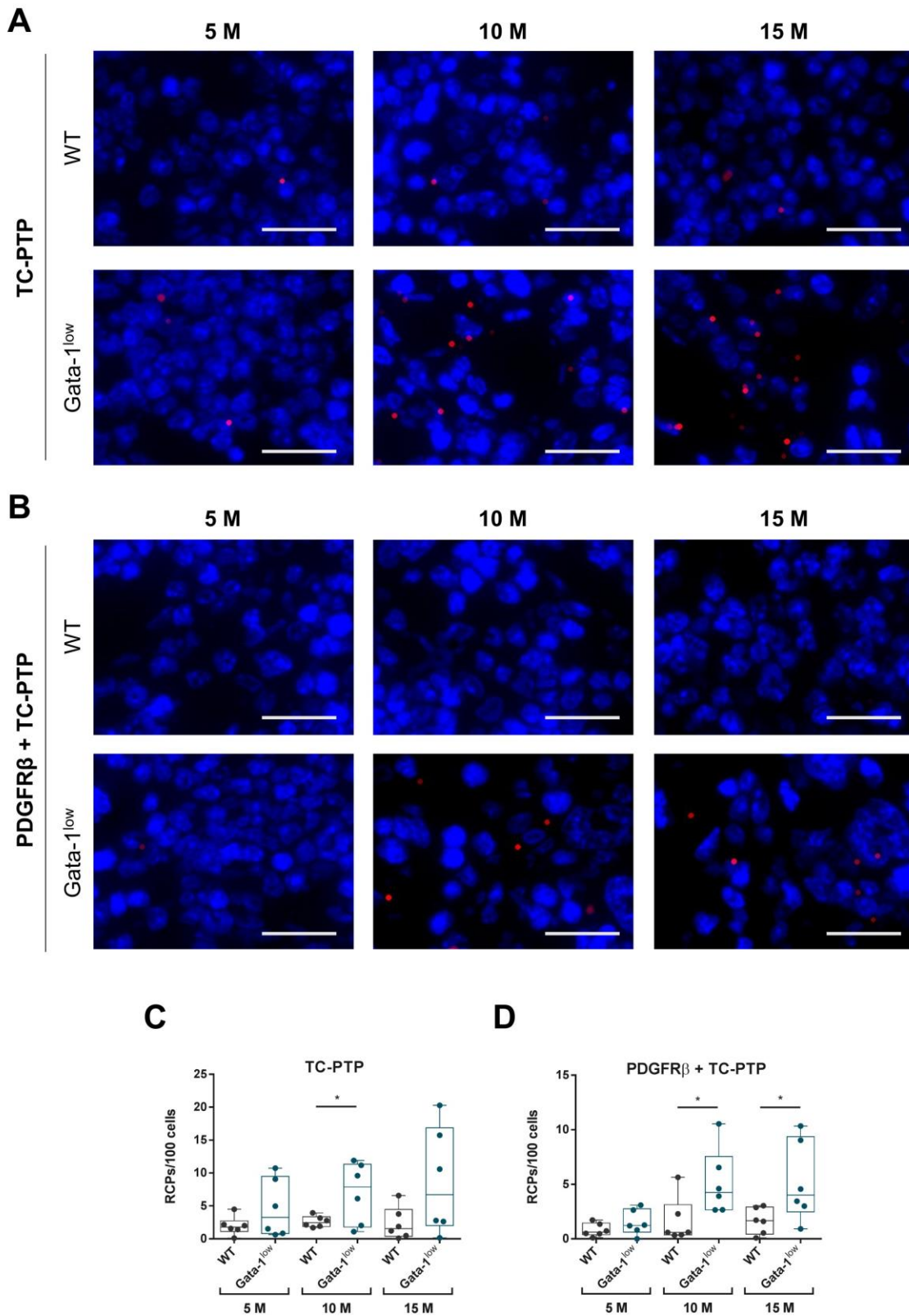
Figure 3.18: Analyses of TC-PTP protein expression and interaction with platelet-derived growth factor receptor β (PDGFRβ) in the bone marrow of Gata-1^low mice and wild type (WT) controls at 5 months (5 M), 10 months (10 M) and 15 months (15 M) of age. Representative images showing a proximity ligation assay (PLA) for analyses of **A** TC-PTP protein expression **B** PDGFRβ–TC-PTP interaction in femoral bone marrow of Gata-1^low mice and WT controls. **C** Quantitative analyses of TC-PTP protein expression and **D** PDGFRβ–TC-PTP interaction. Scale bars = 20 μm, RCPs: rolling circle products.

3.7 TC-PTP expression in fibroblasts *in vitro*

The findings of increased PDGFRβ and TC-PTP expression and interaction in bone marrow fibrosis led to further analyze the regulation of PDGFRβ by TC-PTP in fibroblasts. To enable functional analyses of both components, a murine fibroblast cell line (NIH-3T3 cells) was used for *in vitro* experiments. Expression of many proteins is influenced by cell-cell-contacts, a well-characterized example is the increased expression of the eponymous density-enhanced phosphatase 1 (DEP-1) in dense cells.[239] Therefore, PDGFRβ and TC-PTP protein expression and PDGFRβ tyrosine phosphorylation was investigated in different cell densities (Figure 3.19A). There was no difference in protein expression of PDGFRβ and TC-PTP in 40% vs. 100% confluent NIH-3T3 cells (Figure 3.19B and C). However, activation of PDGFRβ by PDGF-BB was decreased in dense cells (Figure 3.19D), but without significant effect on downstream AKT signaling (Figure 3.19E).
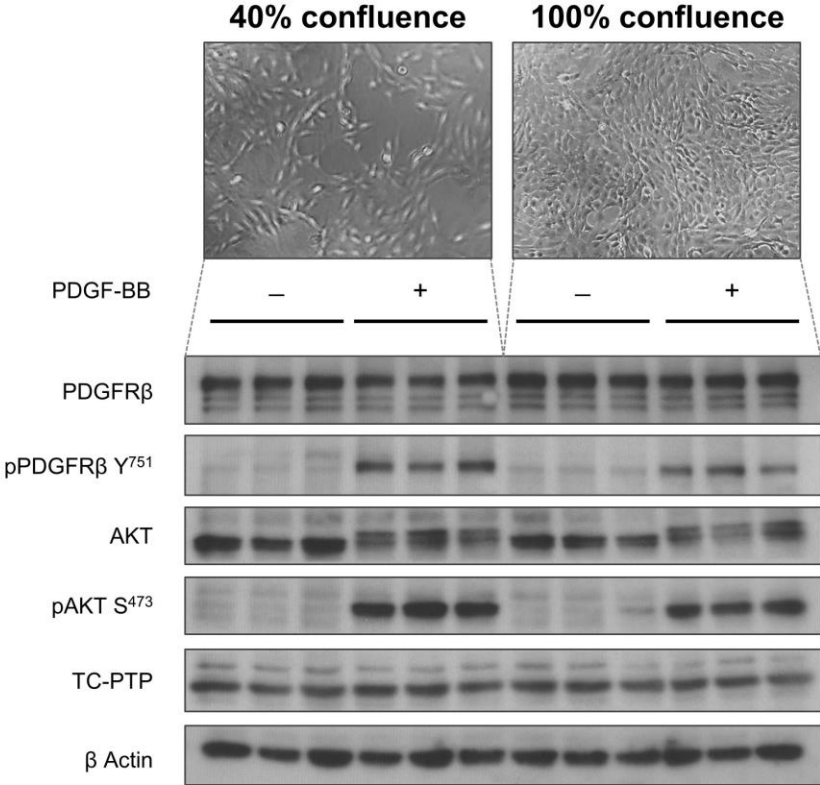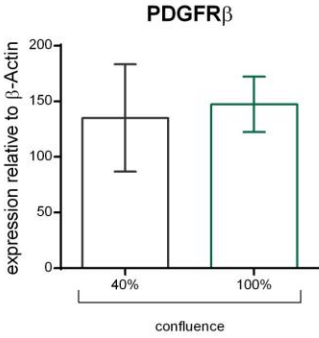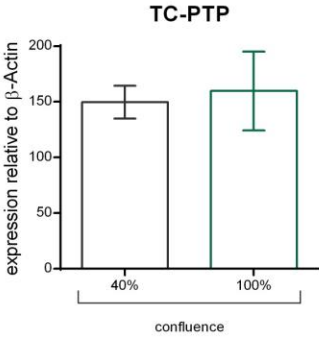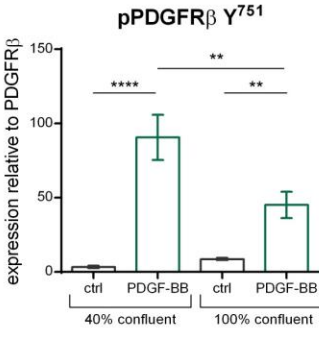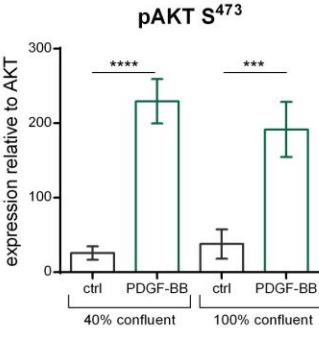
Figure 3.19: Effect of cell density on platelet-derived growth factor receptor β (PDGFRβ) activation in NIH-3T3 cells. Immunoblot of 40% and 100% confluent cells, untreated (–) and stimulated with 50 ng/ml PDGF-BB (+) for 5 min. **B** Densitometric analyses of PDGFRβ, **C** TC-PTP, **D** pPDGFRβ Y^{751} and **E** pAKT S^{473}.

These cell density-dependent differences in activation of PDGFRβ emphasize the importance of ensuring consistent growth statuses among different experiments and hence, all subsequent experiments were performed using equivalent cell densities (50-60%).

3.8   TC-PTP in PDGFRβ signaling and proliferation *in vitro*

To investigate the regulation of PDGFRβ by TC-PTP, *Ptpn2* expression was knocked down in NIH-3T3 fibroblasts (Figure 3.20A). Transfection with *Ptpn2*-targeting siRNA resulted in a moderate but significant knockdown compared to cells transfected with nontargeting siRNA (100% TC-PTP protein expression relative to GAPDH in nontargeting control cells vs. 61.2% relative TC-PTP protein expression in *Ptpn2* knockdown cells, Figure 3.20B). Cells were stimulated with PDGF-BB, leading to PDGFRβ tyrosine phosphorylation and activation of downstream signaling pathways such as AKT, ERK and PLCγ1 signaling. *Ptpn2* knockdown increased PDGF-BB-mediated PDGFRβ phosphorylation at tyrosine sites Y^{751} and Y^{1021}, signifying PDGFRβ dephosphorylation by TC-PTP at both sites (Figure 3.20C and D). Consecutive to increased PDGFRβ phosphorylation at Y^{751}, increased downstream AKT signaling was observed in *Ptpn2* knockdown cells (Figure 3.20E). However, there was no substantial effect on downstream ERK signaling (Figure 3.20F). In accordance with enhanced PDGFRβ phosphorylation at Y^{1021}, downstream PLCγ1 activation was increased in *Ptpn2* knockdown cells (Figure 3.20G).
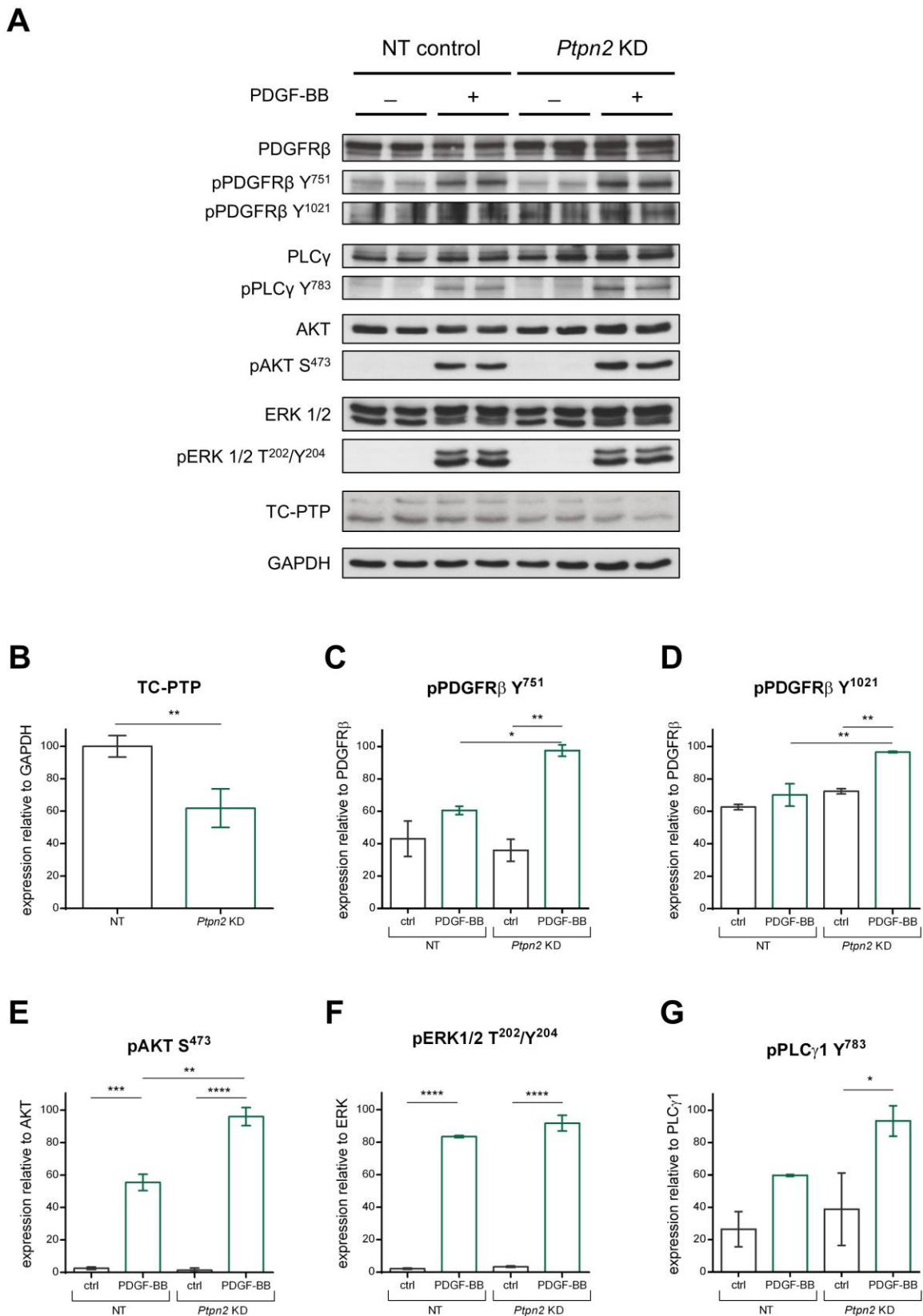
Figure 3.20: Regulation of platelet-derived growth factor receptor β (PDGFRβ) signaling by TC-PTP in NIH-3T3 cells. **A** Immunoblot of *Ptpn2* knockdown (KD) and nontargeting (NT) control cells, untreated (–) and stimulated with 50 ng/ml PDGF-BB (+) for 5 min. **B** Densitometric analyses of TC-PTP, **C** pPDGFRβ Y^{751}, **D** pPDGFRβ Y^{1021}, **E** pPLCγ1 Y^{783}, **F** pAKT S^{473}, **G** pERK1/2 T^{202}/Y^{204}.

An increased activation of signaling pathways which are typically implicated in cell survival and proliferation was observed in *Ptpn2* knockdown cells. Hence, proliferation of *Ptpn2* knockdown cells subjected to different growth conditions was analyzed (Figure 3.21). Interestingly, monitoring cells for 6 days did not reveal evident differences in proliferation of cells cultured in complete growth medium containing 10% FBS. However, when cells were exposed to serum-reduced medium (1% FBS), *Ptpn2* knockdown cells showed increased growth rates compared to control cells. Whereas control cells reached a maximum confluence of 60.6% in medium with 1% FBS, *Ptpn2* knockdown cells reached 74.9% confluence and maintained higher cell densities in serum-reduced medium.
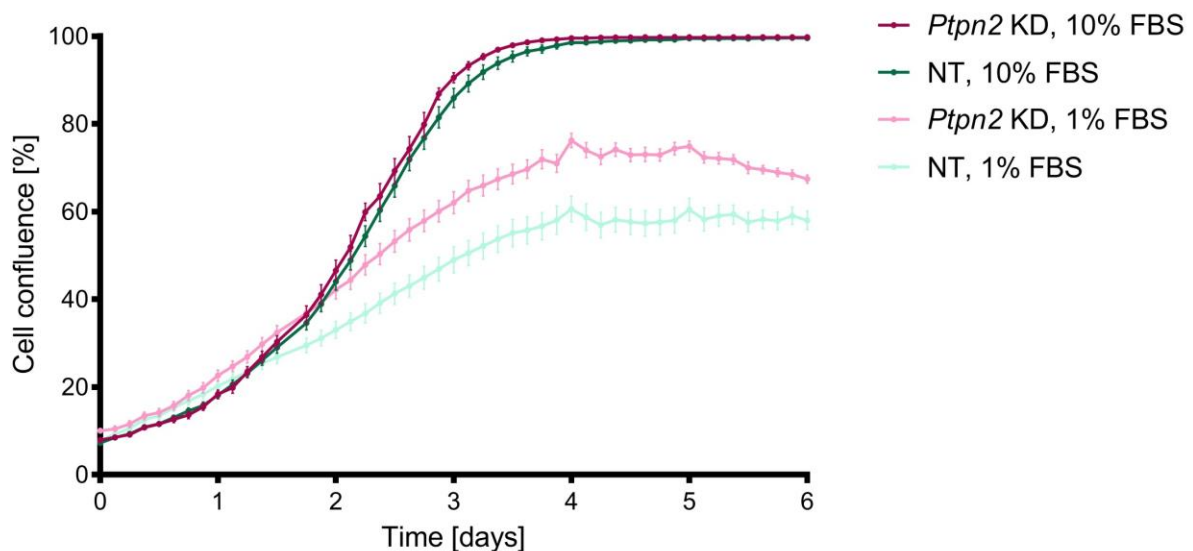
Figure 3.21: Proliferation of *Ptpn2* knockdown (KD) and nontareting (NT) control cells. Proliferation curves of NIH-3T3 cells cultured in medium containing 1% and 10% fetal bovine serum (FBS).

Finally, elaborating on the interaction of both proteins within cells, the subcellular location of PDGFRβ and TC-PTP in fibroblasts was investigated by immunofluorescent staining of PDGFRβ and TC-PTP (Figure 3.22). As a transmembrane RTK, PDGFRβ (green) localized mainly to the plasma membrane as well as to endosomal vesicles in proximity to the nucleus, whereas TC-PTP (red) located to nucleus and cytoplasm.
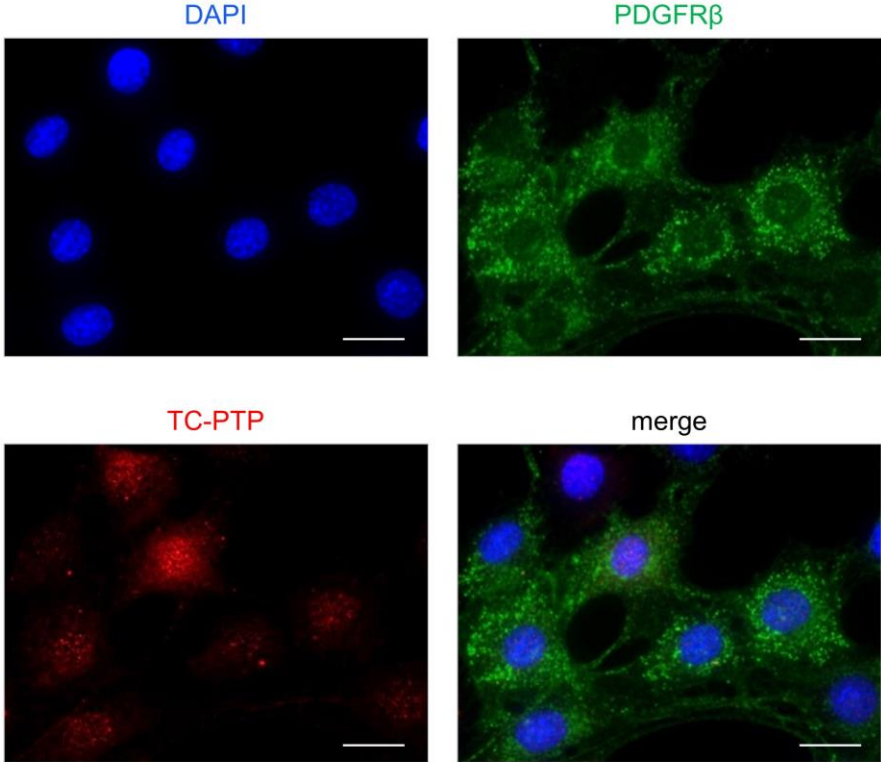
Figure 3.22: Immunofluorescence (IF) staining of platelet-derived growth factor receptor β (PDGFRβ, green) and TC-PTP (red) in NIH-3T3 cells. Nuclei were counterstained with DAPI (blue), scale bars = 20 μm.

4 DISCUSSION

Among the classical, BCR-ABL-negative MPNs, PMF is the most fatal disease with eminently unfavorable prognosis.[240] There have been intensive efforts to understand the mechanisms leading to PMF, largely focusing on genetic analyses. However, the PMF-associated driver mutations (*JAK2*, *CALR* and *MPL*), which lead to aberrant activation of JAK-STAT signaling, are not unique for PMF but also occur in the other two classical, BCR-ABL-negative MPNs (ET and PV). There is currently no distinct molecular marker available for these MPNs, emphasizing that the underlying mechanisms directing the different MPNs are not yet completely understood, and pointing towards the need for further diagnostic tools.

In this study, detailed analyses of the expression patterns of PDGFRβ signaling components in a mouse model for PMF at different fibrotic disease stages was provided using RNAseq, qPCR, multiplexed IHC, as well as *in situ* protein expression and interaction analyses by PLA. Early and overt fibrotic bone marrow was characterized by significant upregulation of PDGF signaling components and overt fibrosis by an increase in PDGFRβ–PDGF-B interaction. Since PDGFRβ tyrosine phosphorylation levels were not elevated, the regulation of PDGFRβ by counter-acting PTPs was investigated. In particular, *Ptpn2* gene as well as TC-PTP protein expression was increased in overt fibrotic bone marrow of Gata-1^{low} mice. Furthermore, enhanced PDGFRβ–TC-PTP interaction was observed in early and overt myelofibrosis, presumably counteracting PDGFRβ phosphorylation. Likewise, *Ptpn2* knockdown increased PDGFRβ tyrosine phosphorylation at Y^{751} and Y^{1021}, and resulted in enhanced downstream AKT and PLCγ1 signaling in fibroblasts. Finally, *Ptpn2* knockdown cells showed a growth condition-dependent increase in cell expansion rate.

4.1 Mouse models for myelofibrosis

PMF progression is marked by thrombocytopenia, the presence of dysplastic megakaryocytes and proliferation of fibroblasts with excessive production of ECM in the bone marrow of patients. To elucidate mechanisms of PMF, there have been different approaches to mimic the disease in mouse models. The number of

megakaryocytes can e.g. be raised by altering thrombopoietin levels in mice.[241-243] Thrombopoietin controls megakaryopoiesis[244] and increased levels of thrombopoietin lead to a quick development of myelofibrosis in mice within 2 to 3 months.[242] Other mouse models employ the mutations which can frequently be found in PMF patients. However, mice harboring the most commonly occurring JAK2[V617F] mutation develop a PV phenotype, which does not evolve into myelofibrosis.[245] In contrast, mice with a calreticulin mutation that can frequently be detected in PMF patients, show symptoms of ET.[246] In the mutant *CALR* model, heterozygous mice, in contrast to homozygous mice, do not develop myelofibrosis. The phenotype in homozygous mice, however, recapitulates a secondary myelofibrosis. The most common human mutation in the thrombopoietin receptor (MPL[W515L]) induced a myeloproliferative phenotype in murine bone marrow transplant assays with a rapid development of myelofibrosis, however, mice died between 17 and 32 days after transplantation.[72] Thus, these mouse models display discrepancies to human PMF and partly resemble features of the other classical, BCR-ABL-negative MPNs.

GATA-1, encoded by the X-chromosomal *GATA1* gene, is a transcription factor that plays a crucial role in differentiation of various hematopoietic lineages such as in erythroid and megakaryocytic differentiation.[247] Although *GATA1* is not mutated in PMF patients, megakaryocytes of PMF patients show decreased GATA-1 expression.[235] The reasons for this have not been elucidated yet, although it is hypothesized that reduced GATA-1 expression is a consequence of ribosomal deficiency as a result of increased JAK-STAT signaling.[248] *Gata1* knockout mice die *in utero* due to severe anemia.[249,250] Gata-1^{low} mice were originally generated by a deletion in the upstream promotor region of the murine *Gata1* gene in C57Bl/6 mice, however, mice showed high mortality around birth.[251,252] When those mice were backcrossed to CD1 mice, viability greatly improved.[229] This suggests an important contribution of the genetic background to disease phenotype. Gata-1^{low} mice show decreased expression of Gata-1 in megakaryocytes, thrombocytopenia and develop myelofibrosis in a time span of 2 years.[230] Importantly, Gata-1^{low} mice do not feature ET of PV symptoms and the slow disease progression resembles the development of a chronic disease in patients, and therefore Gata-1^{low} mice are suitable for the study of PMF development in mice.

4.2   Development of myelofibrosis in Gata-1^{low} mice

This study aimed at characterizing Gata-1^{low} mice at different stages of disease development and hence mice were analyzed at 5, 10 and 15 months of age. A marked thrombocytopenia and splenomegaly was observed in mice of all analyzed ages. Further, mice displayed a mild, but progressive leukocytosis and progressive anemia. A high number of dysplastic megakaryocytes was present in the bone marrow of Gata-1^{low} mice, and starting from 10 months of age, reticulum fibers accumulated in the bone marrow. At 15 months of age, there was a pronounced fibrosis in the bone marrow of Gata-1^{low} mice. Hence, Gata-1^{low} mice recapitulate the key features of disease development as seen in PMF patients. Interestingly, an impaired survival in female, homozygous Gata-1^{low} mice was observed. Other studies using the Gata-1^{low} mouse model did not report any sex-specific differences during the onset of myelofibrosis, however, the increased mortality of homozygous females in this study suggests a harsher phenotype in females. Indeed, it must be noted that mutation in the *Gata1* promotor region is X-linked. Hence, hematological parameters of male and female mice were compared in this study to reveal potential sex-specific discrepancies. Nevertheless, the small number of available female, homozygous Gata-1^{low} mice weakened plausibility of statistical analyses, and for female Gata-1^{low} mice at 15 months of age (n=1), statistical analysis was not applicable. However, there were slight differences in red blood cell counts of both sexes in 10-month-old Gata-1^{low} mice and 15-month-old WT mice, as well as in white blood cell and platelet counts in 15-month-old WT mice. Thus, in addition to potential differences in disease progression in female Gata-1^{low} mice, the sex-specific discrepancies in WT mice suggest age-dependent differences in hematological parameters in male and female mice. Conclusively, to reduce heterogeneity in this age-dependent study, male mice were used for experiments. In regard to sex-specific differences in PMF disease progression, patients do not resemble the same gender-specific discrepancies seen in the Gata-1^{low} mouse model. Although decreased GATA-1 expression can also be observed in PMF patients, a model using an X-linked mutation is substantially different in its underlying disease-inducing mechanism compared to the PMF-initiating mutations in *JAK2*, *CALR* or *MPL*. Interestingly, PMF is slightly more prevalent in men than in women,[51] without knowledge on the underlying causes for this difference.

4.3 Transcriptomic alterations in myelofibrosis

The transcription analyses in early fibrotic bone marrow of Gata-1^{low} mice revealed 1503 up-, and 1604 downregulated genes. Among the different RTKs, a general trend towards an upregulation was observed. This is in line with the established role of many RTKs in proliferative and cancerous diseases.[253] However, among the ligands for those RTKs, many genes were not differentially regulated. Given the hypothesis of an increased production of cytokines and growth factors in the bone marrow of PMF patients, which in the literature is often referred to as a 'cytokine storm',[56,76,254,255] it seems rather surprising not to find a more striking increase in gene expression of those ligands. Nevertheless, this highlights the importance of RTKs as well as other components contributing to the tightly orchestrated regulation of signaling components.

GO enrichment analyses further revealed that genes implicated in PDGF binding were most overrepresented within the 1503 upregulated genes in the bone marrow of 10-month-old Gata-1^{low} mice. Given the implication of the PDGF system in the development of myelofibrosis and the lack of information about the role of PDGF signaling dynamics in pre-fibrotic stages, this study further aimed at characterizing the PDGF signaling components in the different stages of myelofibrosis.

4.4 PDGF signaling components in bone marrow fibrosis

The data in this study showed an induction in gene expression of PDGF receptors and ligands in the bone marrow of Gata-1^{low} mice at 10 months of age. Interestingly, collagen gene expression in the bone marrow of Gata-1^{low} mice was highest in an early fibrotic stage. Hence, there was an evident overlap of the induction of PDGF signaling components with a major increase in collagen type I and type III gene expression during the early stage of bone marrow fibrosis. Collagen and PDGF signaling component gene expression remained enhanced in overt fibrotic bone marrow, although less pronounced compared to early fibrotic bone marrow of Gata-1^{low} mice, showing that collagen expression and PDGF signaling are clearly concurrent events. This is in agreement with the fact that collagens bind PDGF-A and -B homo- and heterodimers, and modulate stability and long-term activation of

the ligands, thus enhancing mitogenic activity.[256] *Vice versa*, however, PDGF-A and -B homo- and heterodimers do not stimulate the production of collagens in fibroblasts *in vitro*, although effects on collagen gene expression seem to be highly dose-dependent.[257,258]

At protein level, a steady increase in both PDGFRα and PDGFRβ protein expression was observed during the development of myelofibrosis, whereas expression in WT mice remained steady. A significantly enhanced PDGFRβ protein expression was detected in Gata-1^{low} mice at 15 month-of-age. There was no increase in PDGF-A expression, but PDGF-B protein expression was increased in overt fibrotic bone marrow of 15-month-old Gata-1^{low} mice compared to WT controls.

Within this study, multiplexed IHC was further used to evaluate cell-specific expression of PDGF receptors and ligands. There was a pronounced expression of PDGF-A, -B and PDGFRα in megakaryocytes, whereas PDGFRβ expression was absent in megakaryocytes. PDGFRβ was mainly expressed in long and spindle-like cells with elongated nuclei, which represent bone marrow stromal cells. The primary antibodies used for immunohistochemical detection in this study are specific for the different PDGF ligand and receptor isoforms, still, those antibodies detect peptide sequences within protein monomers. PDGF ligands are synthesized as dimers (PDGF-AA and -BB homo, and PDGF-AB heterodimers, see Figure 1.3 in the 'Introduction') and, physiologically, do not exist as functional monomers.[109-113] PDGF receptors, which are transmembrane RTKs, reside in the plasma membrane and dimerize upon ligand binding.[116,128] Hence, the antibody-based methods in this study might detect homo- as well as heterodimers. Since both PDGF-A and -B were located to megakaryocytes, those ligands can very well be present as PDGF-AA and -BB homo-, and PDGF-AB heterodimers. Since PDGFRα expression was limited to megakaryocytes and PDGFRβ expression to stromal cells, it can be reasoned that PDGFRαβ heterodimers do not play a measurable role in the pathology of bone marrow fibrosis. Conclusively, PDGFRα signals mainly through PDGFRαα homodimers in megakaryocytes. Localization data further indicates that PDGF-AA exerts its effects on PDGFRαα in an autocrine manner from megakaryocytes, but also in paracrine fashion from other hematopoietic cells in the bone marrow which evidently expressed PDGF-A. Still, activation of PDGFRαα by megakaryocyte-derived PDGF-AB heterodimers might also play a role. An increase in PDGFRα

expression in megakaryocytes is particularly interesting, since it is emerging in HSC-derived, clonal cells. In contrast to Gata-1^{low} mice, these cells are typically harboring one of three driver mutations (*JAK2*, *CALR* or *MPL*) in PMF patients. Despite the differences in the mouse model, where HSCs do not harbor any of these driver mutations, PDGFRα expression is indeed increased in the bone marrow of PMF patients.[89] It is therefore highly interesting that, as recently published, PDGF-AA and -BB production is not decreased after treatment with ruxolitinib in an MPN mouse model. Further, PDGFRα signaling remained active despite JAK1/2 inhibition by ruxolitinib.[103]

In this study, PDGF-B expression was detected in megakaryocytes and consequently, PDGF-BB signals on PDGFRββ homodimers, expressed in bone marrow fibroblasts, in a paracrine manner. In contrast to PDGFRαα, PDGFRββ is not activated by PDGF-AB heterodimers (see Figure 1.3 in the 'Introduction'). The data generated within this study therefore strongly supports the notion that paracrine signaling of PDGF-BB on PDGFRββ drives fibroblast proliferation in bone marrow fibrosis. Hence, this study further placed special focus on these PDGF ligand and receptor isoforms.

It has previously been described that PDGFRβ expression in PMF bone marrow fibroblasts correlates with the grade of myelofibrosis and that immunohistochemical staining of PDGFRβ in bone marrow of PMF patients might serve as a marker for PMF progression.[90,187,188] It should further be noted that selective inhibition of PDGFRβ in PMF patients might still be a promising treatment option. Inhibition of PDGFRβ by imatinib has been largely dismissed after marginal effects in three different studies.[193-195] However, none of the patients within these small scale studies (11 - 23 PMF patients) have been selected for enhanced PDGFRβ expression in the bone marrow, and a subset of patients could benefit from PDGFRβ inhibition. The gradual increase of PDGFRβ protein expression, which can be observed in PMF patients, was also present in Gata-1^{low} mice. Thus, the data generated within this study are supportive of the findings in PMF patients. Henceforth, PDGFRβ expression during PMF development in mice was investigated in-depth using sophisticated and sensitive methods.

Yet, insights into whether PDGFRβ expression is upregulated at a transcriptional level in these cells or if increased PDGFRβ expression is a result of an increased

number of fibroblasts in fibrotic bone marrow are still lacking and should be further investigated. While the latter seems straightforward, it is reasonable that fibroblasts and other stromal cells in PMF display altered function and expression patterns. Fibroblasts in PMF are not considered malignant, since they do not harbor driver mutations.[49] This rationale is strongly supported by the fact, that allogenic stem cell transplantation, and thus elimination of the clonal HSC population, is curative for PMF and can reverse fibrosis.[259] Nevertheless, fibroblasts in PMF can feature other genetic abberations,[260] and chronic inflammation and a dysfunctional microenvironment can effect expression of PDGF signaling components.[185] Hence, transcriptional, translational or epigenetic alterations are conceivable in PMF fibroblasts. Experiments using induced pluripotent stem cells further show that PDGFRβ expression underlies epigenetic regulation by DNA methylation, and that the PDGFRβ-associated methylation landscape largely changes after differentiation.[261] Moreover, surface levels of PDGFRβ can be altered by recycling and degradation mechanisms. PDGF receptors are internalized upon ligand binding and then recycled to the plasma membrane, or ubiquitinated and degraded.[200] The phosphatase TC-PTP, for example, does not only alter PDGFRβ function by dephosphorylation, but also influences intracellular trafficking and degradation, directing PDGFRβ towards Rab4-dependent recycling pathways.[262] This is especially interesting in the context of increased TC-PTP expression and PDGFRβ–TC-PTP interaction observed in this study.

4.5 Activation and regulation of PDGFRβ in myelofibrosis

Along with an increase in PDGFRβ and PDGF-B protein expression, an increase in PDGFRβ–PDGF-B interaction was observed in overt fibrotic bone marrow of Gata-1^{low} mice, analyzed by PLA. This finding seems self-evident, given the increased protein expression in this stage of the disease. When analyzing PDGFRβ tyrosine phosphorylation, however, no increase was detected. There are a number of possible explanations for this finding.

a) PDGFRβ tyrosine phosphorylation is a rare event

Tyrosine phosphorylation is a rare event. The ratio of phosphorylated serine, threonine vs. phosphorylated tyrosine residues are approximately 90%, 10% vs. 0.05% in the overall cellular phosphoproteom.[263,264] Furthermore, PDGFRβ is a relatively low abundant receptor. Differences in PDGFRβ tyrosine phosphorylation state might be subtle. Other detection methods (e.g. IB) use an amplified signal (e.g. enhanced chemiluminescence), which can be used to visualize phosphorylated tyrosine residues in blotted proteins. The PLA creates one signal per accessible PDGFRβ tyrosine phosphorylation site, and formalin-fixed, paraffin-embedded tissue presents a thin section of a respective tissue. In 1 µm bone marrow sections, the overall number of signals might not be sufficient to display subtle differences in phosphorylation states. However, the high cellularity of hematopoietic cells, which typically have a rather small proportion of cytoplasmic area but are comprised mostly of nucleus, did not allow for the use of thicker sections, otherwise cells would not have been microscopically distinguishable.

b) Methodology

In the wider context of a), the detection of PDGFRβ tyrosine phosphorylation might further be impeded by the accessibility of antibody epitopes. According to manufacturer's information, the monoclonal PDGFRβ antibody used (Y92) recognizes an epitope between amino acid position 1050 and the C-terminus. There are no tyrosine residues within this part of the sequence and hence, binding of this antibody to the receptor should *a priori* not interfere with the binding of phosphotyrosine-targeting antibodies. However, it cannot be ruled out that specific conformation and tertiary structure might influence detection of certain phosphorylation sites. In order to address this issue, three widely used phosphotyrosine-targeting antibodies were used (pY100, pY20 and 4G10) in combination with the PDGFRβ antibody. Although it is generally assumed that these antibodies bind phosphotyrosine residues rather unspecifically, there is evidence that they differ in their sequence preference.[265] Therefore, a combination of these three antibodies was used to detect a maximum range of phosphorylated PDGFRβ tyrosine residues.

c) Physiological situation is not unambiguous

Tyrosine phosphorylation in cells within tissues is not a straightforward event, especially compared to *in vitro* experiments. Under physiological conditions, the simplified but artificial switch-off (unstimulated, unphosphorylated) and switch-on (stimulated, phosphorylated) does not exist in such an unambiguous, mutually exclusive manner.

d) Upregulation of PTPs

Receptor phosphorylation is tightly regulated by presence of PTPs, which dephosphorylate PDGFRβ. A number of PTPs, which site-selectively dephosphorylate PDGFRβ, have previously been identified: PTP1B,[118,211-213] TC-PTP,[212,214] SHP-1,[215,216] SHP-2,[212,217-221] PTP-PEST,[212,222] DEP-1,[223] PTEN[224] and LMW-PTP.[225] An increased expression of these PTPs might be responsible for the absence of an increased PDGFRβ phosphorylation. Using RNAseq data from early fibrotic bone marrow of Gata-1^{low} mice, PTPs were analyzed for differential expression and it was observed that the majority of PTPs was not differentially regulated in this stage of bone marrow fibrosis. The above mentioned, PDGFRβ-dephosphorylating PTPs were not differentially expressed within the RNAseq data. To overcome drawbacks by small numbers of mice analyzed by RNAseq, and to include all three disease stages in the analyses, gene expression of the six classical, class I PTPs, which are known to target PDGFRβ, was analyzed by qPCR. The results showed different expression dynamics among gene expression of *Ptpn1* (encoding PTP1B), *Ptpn2* (encoding TC-PTP), *Ptpn6* (encoding SHP-1), *Ptpn11* (encoding SHP-2), *Ptpn12* (encoding PTP-PEST) and *Ptprj* (encoding DEP-1).

Interestingly, all analyzed PTPs showed tendencies towards an upregulation in early fibrotic bone marrow of 10-month-old Gata-1^{low} mice, supporting the hypothesis that increased PTP expression contributes to PDGFRβ dephosphorylation. Only *Ptpn2* and *Ptpn11* gene expression remained increased in overt fibrotic bone marrow. This study further focused on *Ptpn2* (TC-PTP), since the increased *Ptpn2* gene expression could conclusively explain the previously described results. Importantly, there are several lines of evidence showing an implication of TC-PTP in a number of bone marrow alterations (discussed more in detail in section 4.6).[236,237,266,267]

4.6   A potential role of TC-PTP in bone marrow fibrosis

Ptpn2 gene expression, as well as TC-PTP protein expression was increased in overt fibrotic bone marrow of Gata-1^low mice. As TC-PTP is ubiquitously expressed, PDGFRβ regulation by TC-PTP might play an important role in myelofibrosis. The multiplexed imaging of TC-PTP and PDGFRβ showed expression of both proteins in stromal cells, and indeed, an increased PDGFRβ–TC-PTP interaction in early and overt fibrotic bone marrow was detected by PLA.

TC-PTP, which was first identified in a T cell cDNA library,[268] is closely related to PTP1B. Both PTPs share 54% sequence identity, and even 69% in their PTP domain (sequences collected from UniProt database and aligned using NCBI blastp® tool). Due to a splicing site in the *Ptpn2* gene, the primary transcript is spliced and can give rise to two TC-PTP isoforms. Both isoforms differ in their C-terminal part, isoform 1 contains a hydrophobic ER-anchoring sequence, whereas isoform 2 contains a nuclear localization signal.[269-271] Hence, isoform 1, a 48 kDa protein, is predicted to be located primarily to the ER, whereas isoform 2, a 45 kDa protein and more abundant than isoform 1, can shuttle between cytoplasm and nucleus.[272] There has been evidence that TC-PTP isoform 1 dephosphorylates several RTK precursor proteins during their synthesis in the ER, e.g. the epidermal growth factor receptor (EGFR) and the adapter protein Shc.[273,274] Possibly, TC-PTP supports proper protein processing by counteracting the autophosphorylation of RTKs during synthesis and posttranslational modification. In addition, TC-PTP dephosphorylates JAK-STAT signaling components,[275] colony-stimulating factor 1 receptor (CSF1R)[276] and PDGFRβ.[212,214]

Homozygous TC-PTP knockout mice die 3 to 5 weeks after birth and display severe defects in hematopoiesis.[237] Those defects were present mainly in erythropoiesis, and in T and B cell development, whereas myeloid and macrophage development were not impaired. Interestingly, transplantation of WT HSCs into lethally irradiated TC-PTP knockout did not rescue hematopoiesis. *Vice versa*, transplantation of TC-PTP knockout HSCs into WT mice did not result in comparable hematopoietic defects.[237] This indicates that TC-PTP knockout leads to changes in the bone marrow microenvironment which prevents normal HSC function. In line with this, the number of stromal cells in the bone marrow of TC-PTP knockout mice was reduced when

compared to WT control mice.[237] This is highly interesting in the context of the findings in this study, which provided evidence for the expression of TC-PTP in bone marrow stromal cells in myelofibrosis and the interaction with PDGFRβ.

In accordance with predicted subcellular location of the two TC-PTP isoforms, TC-PTP expression was observed in nucleus and cytoplasm, as shown by immunofluorescence staining in NIH-3T3 fibroblasts. Neither PDGFRβ nor TC-PTP protein expression was influenced by cell density, but PDGFRβ tyrosine phosphorylation was reduced in dense fibroblasts *in vitro. Ptpn2* expression was knocked down in NIH-3T3 fibroblasts and cells were stimulated with PDGF-BB. Consistent with other studies,[212,214] IB analyses showed a counter-regulation of PDGFRβ by TC-PTP in fibroblasts *in vitro.* In contrast to a study suggesting that TC-PTP preferentially dephosphorylates PDGFRβ Y^{1021} site,[214] however, a greater effect of *Ptpn2* knockdown on phosphorylation at Y^{751} was observed in this study, suggesting cell-type specific dephosphorylation patterns of TC-PTP. *Ptpn2* knockdown resulted in increased PDGFRβ phosphorylation at Y^{751}, which serves as a binding site for PI3K.[134] Conclusively, an increase in downstream AKT activation as a central mediator of cell proliferation was detected. PDGFRβ phosphorylation also activates Ras and downstream ERK signaling,[135] however, there was no increase in ERK signaling in *Ptpn2* knockdown cells. The fact that PDGFRβ-mediated PI3K activation negatively regulates the ERK signaling might be a plausible explanation for this finding.[141] *Ptpn2* knockdown further led to increased PDGFRβ tyrosine phosphorylation at Y^{1021}, resulting in enhanced downstream PLCγ1 activation, suggesting a possible role of downstream protein kinase C and Ca^{2+} signaling.

Ptpn2 knockdown fibroblasts cultured in complete growth medium containing 10% FBS did not have an apparent superiority in proliferation. However, increased growth rates in *Ptpn2* knockdown cells exposed to reduced-serum media containing 1% FBS were detected. This suggests that under conditions of high abundance of growth factors, differences in proliferation in *Ptpn2* knockdown cells are abolished, while apparent during serum-deprivation, possibly being closer to actual circumstances in the bone marrow. Other studies using murine skin cancer models showed that TC-PTP controls proliferation and survival via AKT and STAT3 activation.[277,278] Further, emphasizing the role of TC-PTP in hematopoietic cells, TC-PTP controls

T cell proliferation.[266] The data in this study, based on a moderate knockdown, indicate that more discrete changes in TC-PTP expression controls cell growth mainly when the availability of growth components is limited. Furthermore, AKT and PLCγ1 were identified as contributing pathways.

4.7 Methodology - considerations and limitations

Diagnosis of PMF largely relies on histopathological assessment of bone marrow sections. Nevertheless, reproducibly in the evaluation of megakaryocyte morphology, which is essential to discriminate pre-PMF from ET, is modest among hematopathologists.[58] The limitations in diagnostics and the lack of a specific molecular marker for PMF underlines the need for new molecular markers and diagnostic approaches. Within this study, multiplexed IHC and an *in situ* PLA were applied as sensitive means to analyze protein expression, interaction and phosphorylation. To our knowledge, this is the first study that utilized multiplexed IHC and PLA in bone marrow tissue.

The bone marrow consists of a great number of different cell types in a strictly organized microenvironment. PMF is an excellent example for a disease, where it is essential to understand the cellular responses of different cell populations. Other widely used methods to phenotype and quantify cell populations, such as fluorescence-activated cell sorting (FACS) rarely reflect the physiological situation and hence, *in situ* analyses can provide helpful information. Further, even when analyzing cell populations deriving from the same clone *in vitro*, there can often be striking differences in protein expression between single cells. Widely used gene (i.e. RNAseq and qPCR) and protein expression analyses (i.e. IB) are population-averaging methods, but useful information can get lost when cell-to-cell variations are masked.[279,280]

PLA is an assay that is based on dual antibody recognition and local signal amplification when the two used antibodies are in close proximity. The method was first described in 2002,[281] and later applied for *in situ* interaction analyses[282] and to detect protein phosphorylation.[283] Applied in a single recognition approach, PLA can visualize single molecules using microscopy.[284] This is especially useful when

detecting low abundant proteins and within this study, single recognition PLA was used to quantify protein expression of PDGFs and their receptors.

This method has definite advantages; it is a highly sensitive and quantitative method, relatively inexpensive and does not require special equipment. Furthermore, PLA is the only method which is applicable to analyze protein-protein interactions and posttranslational modifications *in situ*, whereas immunoprecipation and IB are *per se* population-averaging approaches. The main limitation of the method is the need for tissue fixation, which can have effects on epitope integrity. In bone marrow tissue, processing includes decalcification of the bone to make the tissue applicable for sectioning. In this study, decalcification by EDTA was used as a mild approach to keep epitopes largely intact. However, in routine pathology, bone marrow biopsies are decalcified using acidic solutions. Furthermore, archiving conditions might contribute to epitope integrity.[285] Finally, antibodies used for an *in situ* PLA must be specific, suitable for formalin-fixed samples, and for combination the antibodies must be raised in different species. Particularly in bone marrow tissue, fluorescent signals which are distinct from the clearly recognizable RCPs were observed during data generation in this study. These are most likely not ascribed to primary antibody binding but are caused by binding of the oligonucleotides which are conjugated to secondary antibodies (PLA probes). Such signals have also been observed using DNA probes in fluorescence *in situ* hybridization (FISH) approaches in bone marrow tissue and are associated with eosinophils.[286] Although these signals are clearly disguisable in size and shape, and hence did not affect quantification, they could impact PLA eligibility in tissues which are rich in eosinophils.

In conclusion, the use of PLA as a diagnostic approach to detect bone marrow alterations needs further optimization and must be individually adapted for the detection of defined and well-established markers. Nevertheless, sensitive *in situ* detection of interacting proteins or the activation status of receptors (e.g. phosphorylation) is highly interesting in diseases, which classically rely on utilization of histopathological methods. Further, monitoring of activation statuses is an interesting means to monitor disease progression and response to targeted therapies as a 'companion diagnostics' tool.

4.8   Perspectives of PTPs in the context of primary myelofibrosis

Early diagnosis of pre-PMF is challenging due to its similarity to ET, nevertheless, correct distinction of both MPNs is clinically highly relevant.[57] To date, the precise mechanisms causing myelofibrosis in PMF patients have still not been fully elucidated. The discovery of JAK-STAT-associated mutations led to the development of JAK inhibitors and since its FDA approval in 2011, the JAK1/2 inhibitor ruxolitinib has become part of combined standard therapy for PMF patients. Long-term treatment with ruxolitinib reduces spleen size and prolongs the overall survival of PMF patients.[100] However, there is no improvement or reversal of bone marrow fibrosis, efficacy of ruxolitinib is limited by drug resistances,[101] and JAK inhibition does not abrogate clonal proliferation.[102] To date, allogeneic stem cell transplantation remains the only curative treatment for PMF, however, transplantation is only suitable for a subset of high-risk patients and limited by comorbidities and donor availability.[96,97] The limitations in diagnosis and efficient treatment of PMF in particular emphasize the need for:

(1) new molecular markers for an early diagnosis

(2) new therapeutic approaches

Referring to (1), it is highly relevant that the gene expression data generated in this study show very distinct expression patterns among the different PTPs during the development of PMF in mice. Expression of all analyzed PTPs showed trends towards an upregulation in early fibrotic bone marrow, although high biological variance diminished statistical significance in most cases. These data nonetheless indicate a clear implication of PTPs in early bone marrow fibrosis in mice. Indeed, a number of PTPs are associated with different types of human diseases, and several PTPs have previously been implicated in cancer. For instance, the class I dual-specific phosphatase PTEN has a well-established role as a tumor suppressor and is mutated in different cancers, such as breast and prostate cancer.[287] Furthermore, SHP-2 has been ascribed a pivotal role in many cancer types, e.g. breast, lung, liver, gastric cancer and leukemia.[288] Another noteworthy example is PTPN13, which has emerged as a potential tumor suppressor in non-small cell lung cancer.[289] Prospectively, differentially expressed PTPs might be potential molecular markers with ability to facilitate early diagnosis of PMF. In this study, *Ptpn1* (encoding PTP1B)

and *Ptprj* (encoding DEP-1) gene expression were downregulated in pre-fibrotic bone marrow of 5-month-old Gata-1^{low} mice. In a stage where a commencing fibrosis can be detected in the bone marrow of Gata-1^{low} mice at 10 months of age, both genes, reversely, showed tendencies of increased gene expression. It would be highly interesting if these expression patterns correspond to the situation in PMF patients and potentially discriminate pre-PMF from ET. It would further be worthwhile to evaluate PTPs in context with clinical data from PMF patients. Correlations with progression, beneficial or adverse survival, for example, might identify individual PTPs of relevance and enable further studies to clarify their function in fibrotic bone marrow.

In this study, increased TC-PTP expression and PDGFRβ–TC-PTP interaction was detected during the progression of myelofibrosis in a PMF mouse model. Which functional consequences this interaction has *in vivo* remains to be clarified. As a negative regulator of PDGFRβ signaling, increased PDGFRβ phosphorylation and downstream signaling was observed in *Ptpn2* knockdown cells *in vitro*. Conclusively, higher cell growth rates were observed in *Ptpn2* knockdown cells, although only evident under reduced-serum conditions. Reversely, increased TC-PTP expression and PDGFRβ–TC-PTP interaction *in vivo* presumably implies a counter-regulation of PDGFRβ signaling in fibroblasts and reduced fibroblast proliferation. Since this notion is not directly conferrable relating to the fibroblast proliferation present in bone marrow fibrosis, further analyses are needed to elucidate the precise role of TC-PTP during disease progression. It is conceivable that increased TC-PTP expression and PDGFRβ–TC-PTP interaction are plainly a result of increased numbers of fibroblasts in the bone marrow. Apart from this, it is very well possible that increased TC-PTP expression in fibrotic bone marrow has more pronounced effects on other *in vivo* targets, such as EGFR, STATs or CSF1R.[273-276] After all, multiplexed IHC revealed TC-PTP expression in various different cell types within the bone marrow. Furthermore, there are numerous regulatory mechanisms which orchestrate intracellular events, which makes attribution of cause and effect intricate. PTPs themselves are regulated by different mechanisms, for example by reversible oxidation of cysteine residues in the catalytic domain of PTPs.[290] Intriguingly, PDGF stimulation in cells was shown to result in the production of reactive oxygen species, which leads to cysteine oxidation.[291,292] In addition, several PTPs (e.g. PTP1B, CD45 and PTP-PEST) harbor regulatory serine phosphorylation sites.[293-295]

It has long been recognized that altered RTK expression plays a pivotal role in different types of cancer, well characterized examples are EGFR in glioblastoma, breast, lung, colorectal, ovarian and other cancers,[296] or the BCR-ABL fusion protein in CML.[190] It is a more recent finding that also deregulation of PTPs contributes to the progression of cancer and other diseases, which makes PTPs - in respect of (2) - especially interesting as potential molecular targets.[297] In addition to an implication of different PTPs in cancer, PTP1B has gained special interest as a negative regulator of the insulin receptor. PTP1B knockout mice are more sensitive to insulin and resistant to obesity.[298,299] These findings brought about efforts in the development of PTP1B inhibitors for the treatment of type II diabetes, insulin resistance and obesity.[300,301]

However, development of therapeutic drugs targeting PTPs is considered rather difficult, and the work on the development on specific PTP1B inhibitors are ongoing.[302] The phosphotyrosine binding sites are highly conserved among the different PTPs, hence, PTP inhibitors are usually not very selective. Nevertheless, this is also a common problem in kinase inhibitors, which block structural homologue ATP binding sites in multiple RTKs. Still, kinase inhibitors are being successfully used in therapy, a well-established example is imatinib for CML treatment.[190,303] In addition to potentially evolving progress in the development of specific PTP inhibitors, other mechanisms for targeting PTPs could present interesting options. For PTPRs, blocking the extracellular domain using antibodies or antibody-fragments would be a conceivable approach. Another problem which persists is that most PTPs regulate more than one RTK and hence, PTP inhibition influences different pathways. Thus, targeting of PTPs must be carefully adopted and evaluated in the biological context of the respective PTP.

TC-PTP is PTP1B's closest homologue, although, both PTPs have very distinct functions. Clear implications of PTP1B in diabetes and obesity and targeting of PTP1B raise the question, if TC-PTP qualifies as an equally interesting therapeutic target for drug discovery. In the context of PMF fibroblasts, enhanced TC-PTP expression is *a priori* hypothesized to repress cell proliferation, and hence TC-PTP inhibition is not reasonable as a treatment option for PMF. Still, therapeutic inhibition of TC-PTP is generally relevant in case of overexpression in a pathological context. To date, different compounds have been tested for TC-PTP inhibition. A PTP inhibitor

('PTP inhibitor XIX'), for example, targets TC-PTP but also inhibits CD45 and PTEN.[304] However, there have been successful attempts to develop a selective TC-PTP inhibitor ('compound 8'), which was also shown to be 8-fold more selective for TC-PTP over PTP1B.[305]

4.9 Conclusion

This study aimed at investigating expression, activation and regulation of PDGFRβ during the development of PMF in mice. Hence, the bone marrow of Gata-1^{low} mice was assessed in a **pre-**, an **early** and an **overt fibrotic stage.** Among the PDGF signaling components, especially PDGFRβ and PDGF-B displayed a major increase in expression and interaction in early and overt bone marrow fibrosis, with a distinct role of PDGFRβ in bone marrow stromal cells. For a comprehensive characterization, a PLA was applied as a novel technique to analyze the PDGFRβ activation status *in situ.* With further tissue- and marker-specific optimization, PLA might prospectively be a promising tool in diagnosis. Furthermore, the role of PTPs during PMF development was assessed in this study, and numerous PTPs were found to be differentially regulated in the bone marrow of Gata-1^{low} mice. In particular, TC-PTP was identified as a regulator of PDGFRβ signaling during disease development in mice. Hence, PTPs represent previously unrecognized contributors to disease development in bone marrow fibrosis and might be novel molecular markers in PMF.

5 REFERENCES

1.   Orkin SH, Zon LI. Hematopoiesis: an evolving paradigm for stem cell biology. Cell. 2008;132(4):631-644.

2.   Travlos GS. Normal structure, function, and histology of the bone marrow. Toxicol Pathol. 2006;34(5):548-565.

3.   Lorenz E, Uphoff D, Reid TR, Shelton E. Modification of irradiation injury in mice and guinea pigs by bone marrow injections. J Natl Cancer Inst. 1951;12(1):197-201.

4.   Doulatov S, Notta F, Laurenti E, Dick JE. Hematopoiesis: a human perspective. Cell Stem Cell. 2012;10(2):120-136.

5.   Ferrari G, Cusella-De Angelis G, Coletta M, et al. Muscle regeneration by bone marrow-derived myogenic progenitors. Science. 1998;279(5356):1528-1530.

6.   Pittenger MF, Mackay AM, Beck SC, et al. Multilineage potential of adult human mesenchymal stem cells. Science. 1999;284(5411):143-147.

7.   Mackay AM, Beck SC, Murphy JM, Barry FP, Chichester CO, Pittenger MF. Chondrogenic differentiation of cultured human mesenchymal stem cells from marrow. Tissue Eng. 1998;4(4):415-428.

8.   Lindner U, Kramer J, Rohwedel J, Schlenke P. Mesenchymal Stem or Stromal Cells: Toward a Better Understanding of Their Biology? Transfus Med Hemother. 2010;37(2):75-83.

9.   Caplan AI. Mesenchymal Stem Cells: Time to Change the Name! Stem Cells Transl Med. 2017;6(6):1445-1451.

10.   Sipp D, Robey PG, Turner L. Clear up this stem-cell mess. Nature. 2018;561(7724):455-457.

11.   Dennis JE, Charbord P. Origin and differentiation of human and murine stroma. Stem Cells. 2002;20(3):205-214.

12.   Medvinsky A, Rybtsov S, Taoudi S. Embryonic origin of the adult hematopoietic system: advances and questions. Development. 2011;138(6):1017-1031.

13.   Maximow A. Der Lymphozyt als gemeinsame Stammzelle der verschiedenen Blutelemente in der embryonalen Entwicklung und im postfetalen Leben der Säugetiere. Folia Haematologica. 1909;8:125-134.

14.   Friedenstein AJ, Gorskaja JF, Kulagina NN. Fibroblast precursors in normal and irradiated mouse hematopoietic organs. Exp Hematol. 1976;4(5):267-274.

15.   Haniffa MA, Collin MP, Buckley CD, Dazzi F. Mesenchymal stem cells: the fibroblasts' new clothes? Haematologica. 2009;94(2):258-263.

16.   Shirai K, Sera Y, Bulkeley W, et al. Hematopoietic stem cell origin of human fibroblasts: cell culture studies of female recipients of gender-mismatched stem cell transplantation and patients with chronic myelogenous leukemia. Exp Hematol. 2009;37(12):1464-1471.

17. Riddell J, Gazit R, Garrison BS, et al. Reprogramming committed murine blood cells to induced hematopoietic stem cells with defined factors. Cell. 2014;157(3):549-564.

18. Li Y, Adomat H, Guns ET, et al. Identification of a Hematopoietic Cell Dedifferentiation-Inducing Factor. J Cell Physiol. 2016;231(6):1350-1363.

19. Kanji S, Pompili VJ, Das H. Plasticity and maintenance of hematopoietic stem cells during development. Recent Pat Biotechnol. 2011;5(1):40-53.

20. Wagner W, Saffrich R, Wirkner U, et al. Hematopoietic progenitor cells and cellular microenvironment: behavioral and molecular changes upon interaction. Stem Cells. 2005;23(8):1180-1191.

21. King AG, Wierda D, Landreth KS. Bone marrow stromal cell regulation of B-lymphopoiesis. I. The role of macrophages, IL-1, and IL-4 in pre-B cell maturation. J Immunol. 1988;141(6):2016-2026.

22. Moore KA, Lemischka IR. Stem cells and their niches. Science. 2006;311(5769):1880-1885.

23. Zhang J, Niu C, Ye L, et al. Identification of the haematopoietic stem cell niche and control of the niche size. Nature. 2003;425(6960):836-841.

24. Ding L, Morrison SJ. Haematopoietic stem cells and early lymphoid progenitors occupy distinct bone marrow niches. Nature. 2013;495(7440):231-235.

25. Coskun S, Hirschi KK. Establishment and regulation of the HSC niche: Roles of osteoblastic and vascular compartments. Birth Defects Res C Embryo Today. 2010;90(4):229-242.

26. Doan PL, Chute JP. The vascular niche: home for normal and malignant hematopoietic stem cells. Leukemia. 2012;26(1):54-62.

27. Arber DA, Orazi A, Hasserjian R, et al. The 2016 revision to the World Health Organization classification of myeloid neoplasms and acute leukemia. Blood. 2016;127(20):2391-2405.

28. Faderl S, Talpaz M, Estrov Z, O'Brien S, Kurzrock R, Kantarjian HM. The biology of chronic myeloid leukemia. N Engl J Med. 1999;341(3):164-172.

29. Lundberg P, Karow A, Nienhold R, et al. Clonal evolution and clinical correlates of somatic mutations in myeloproliferative neoplasms. Blood. 2014;123(14):2220-2228.

30. Campbell PJ, Green AR. The myeloproliferative disorders. N Engl J Med. 2006;355(23):2452-2466.

31. Maxson JE, Gotlib J, Pollyea DA, et al. Oncogenic CSF3R mutations in chronic neutrophilic leukemia and atypical CML. N Engl J Med. 2013;368(19):1781-1790.

32. Wang SA, Tam W, Tsai AG, et al. Targeted next-generation sequencing identifies a subset of idiopathic hypereosinophilic syndrome with features similar to chronic eosinophilic leukemia, not otherwise specified. Mod Pathol. 2016;29(8):854-864.

33. Dolgikh TY, Domnikova NP, Tornuev YV, Vinogradova EV, Krinitsyna YM. Incidence of Myelofibrosis in Chronic Myeloid Leukemia, Multiple Myeloma,

and Chronic Lymphoid Leukemia during Various Phases of Diseases. Bull Exp Biol Med. 2017;162(4):483-487.

34. Tefferi A, Lasho TL, Guglielmelli P, et al. Targeted deep sequencing in polycythemia vera and essential thrombocythemia. Blood Adv. 2016;1(1):21-30.

35. Yogarajah M, Tefferi A. Leukemic Transformation in Myeloproliferative Neoplasms: A Literature Review on Risk, Characteristics, and Outcome. Mayo Clin Proc. 2017;92(7):1118-1128.

36. Scott LM, Tong W, Levine RL, et al. JAK2 exon 12 mutations in polycythemia vera and idiopathic erythrocytosis. N Engl J Med. 2007;356(5):459-468.

37. Vannucchi AM, Lasho TL, Guglielmelli P, et al. Mutations and prognosis in primary myelofibrosis. Leukemia. 2013;27(9):1861-1869.

38. Tefferi A, Lasho TL, Finke CM, et al. Targeted deep sequencing in primary myelofibrosis. Blood Adv. 2016;1(2):105-111.

39. Gianelli U, Cattaneo D, Bossi A, et al. The myeloproliferative neoplasms, unclassifiable: clinical and pathological considerations. Mod Pathol. 2017;30(2):169-179.

40. Lundberg P, Takizawa H, Kubovcakova L, et al. Myeloproliferative neoplasms can be initiated from a single hematopoietic stem cell expressing JAK2-V617F. J Exp Med. 2014;211(11):2213-2230.

41. Delhommeau F, Dupont S, Tonetti C, et al. Evidence that the JAK2 G1849T (V617F) mutation occurs in a lymphomyeloid progenitor in polycythemia vera and idiopathic myelofibrosis. Blood. 2007;109(1):71-77.

42. Jamieson CH, Gotlib J, Durocher JA, et al. The JAK2 V617F mutation occurs in hematopoietic stem cells in polycythemia vera and predisposes toward erythroid differentiation. Proc Natl Acad Sci U S A. 2006;103(16):6224-6229.

43. Nangalia J, Massie CE, Baxter EJ, et al. Somatic CALR mutations in myeloproliferative neoplasms with nonmutated JAK2. N Engl J Med. 2013;369(25):2391-2405.

44. Mead AJ, Mullally A. Myeloproliferative neoplasm stem cells. Blood. 2017;129(12):1607-1616.

45. Kendall RT, Feghali-Bostwick CA. Fibroblasts in fibrosis: novel roles and mediators. Front Pharmacol. 2014;5:123.

46. Thannickal VJ, Zhou Y, Gaggar A, Duncan SR. Fibrosis: ultimate and proximate causes. J Clin Invest. 2014;124(11):4673-4677.

47. Wynn TA. Common and unique mechanisms regulate fibrosis in various fibroproliferative diseases. J Clin Invest. 2007;117(3):524-529.

48. Li X, Zhu L, Wang B, Yuan M, Zhu R. Drugs and Targets in Fibrosis. Front Pharmacol. 2017;8:855.

49. Greenberg BR, Woo L, Veomett IC, Payne CM, Ahmann FR. Cytogenetics of bone marrow fibroblastic cells in idiopathic chronic myelofibrosis. Br J Haematol. 1987;66(4):487-490.

50. Moulard O, Mehta J, Fryzek J, Olivares R, Iqbal U, Mesa RA. Epidemiology of myelofibrosis, essential thrombocythemia, and polycythemia vera in the European Union. Eur J Haematol. 2014;92(4):289-297.

51.   Tefferi A, Lasho TL, Jimma T, et al. One thousand patients with primary myelofibrosis: the mayo clinic experience. Mayo Clin Proc. 2012;87(1):25-33.

52.   O'Sullivan JM, Harrison CN. Myelofibrosis: clinicopathologic features, prognosis, and management. Clin Adv Hematol Oncol. 2018;16(2):121-131.

53.   Tefferi A. Pathogenesis of myelofibrosis with myeloid metaplasia. J Clin Oncol. 2005;23(33):8520-8530.

54.   Kvasnicka HM, Beham-Schmid C, Bob R, et al. Problems and pitfalls in grading of bone marrow fibrosis, collagen deposition and osteosclerosis - a consensus-based study. Histopathology. 2016;68(6):905-915.

55.   Barosi G. Essential thrombocythemia vs. early/prefibrotic myelofibrosis: why does it matter. Best Pract Res Clin Haematol. 2014;27(2):129-140.

56.   Vainchenker W, Constantinescu SN, Plo I. Recent advances in understanding myelofibrosis and essential thrombocythemia. F1000Res. 2016;5.

57.   Barbui T, Thiele J, Passamonti F, et al. Survival and disease progression in essential thrombocythemia are significantly influenced by accurate morphologic diagnosis: an international study. J Clin Oncol. 2011;29(23):3179-3184.

58.   Wilkins BS, Erber WN, Bareford D, et al. Bone marrow pathology in essential thrombocythemia: interobserver reliability and utility for identifying disease subtypes. Blood. 2008;111(1):60-70.

59.   Kleppe M, Kwak M, Koppikar P, et al. JAK-STAT pathway activation in malignant and nonmalignant cells contributes to MPN pathogenesis and therapeutic response. Cancer Discov. 2015;5(3):316-331.

60.   Baxter EJ, Scott LM, Campbell PJ, et al. Acquired mutation of the tyrosine kinase JAK2 in human myeloproliferative disorders. Lancet. 2005;365(9464):1054-1061.

61.   Saharinen P, Silvennoinen O. The pseudokinase domain is required for suppression of basal activity of Jak2 and Jak3 tyrosine kinases and for cytokine-inducible activation of signal transduction. J Biol Chem. 2002;277(49):47954-47963.

62.   Kralovics R, Passamonti F, Buser AS, et al. A gain-of-function mutation of JAK2 in myeloproliferative disorders. N Engl J Med. 2005;352(17):1779-1790.

63.   Levine RL, Wadleigh M, Cools J, et al. Activating mutation in the tyrosine kinase JAK2 in polycythemia vera, essential thrombocythemia, and myeloid metaplasia with myelofibrosis. Cancer Cell. 2005;7(4):387-397.

64.   Klampfl T, Gisslinger H, Harutyunyan AS, et al. Somatic mutations of calreticulin in myeloproliferative neoplasms. N Engl J Med. 2013;369(25):2379-2390.

65.   Molinari M, Eriksson KK, Calanca V, et al. Contrasting functions of calreticulin and calnexin in glycoprotein folding and ER quality control. Mol Cell. 2004;13(1):125-135.

66.   Michalak M, Groenendyk J, Szabo E, Gold LI, Opas M. Calreticulin, a multi-process calcium-buffering chaperone of the endoplasmic reticulum. Biochem J. 2009;417(3):651-666.

67. Kollmann K, Warsch W, Gonzalez-Arias C, et al. A novel signalling screen demonstrates that CALR mutations activate essential MAPK signalling and facilitate megakaryocyte differentiation. Leukemia. 2017;31(4):934-944.

68. Lau WW, Hannah R, Green AR, Gottgens B. The JAK-STAT signaling pathway is differentially activated in CALR-positive compared with JAK2V617F-positive ET patients. Blood. 2015;125(10):1679-1681.

69. Chachoua I, Pecquet C, El-Khoury M, et al. Thrombopoietin receptor activation by myeloproliferative neoplasm associated calreticulin mutants. Blood. 2016;127(10):1325-1335.

70. Marty C, Pecquet C, Nivarthi H, et al. Calreticulin mutants in mice induce an MPL-dependent thrombocytosis with frequent progression to myelofibrosis. Blood. 2016;127(10):1317-1324.

71. Nivarthi H, Chen D, Cleary C, et al. Thrombopoietin receptor is required for the oncogenic function of CALR mutants. Leukemia. 2016;30(8):1759-1763.

72. Pikman Y, Lee BH, Mercher T, et al. MPLW515L is a novel somatic activating mutation in myelofibrosis with myeloid metaplasia. PLoS Med. 2006;3(7):e270.

73. Grinfeld J, Nangalia J, Baxter EJ, et al. Classification and Personalized Prognosis in Myeloproliferative Neoplasms. N Engl J Med. 2018;379(15):1416-1430.

74. Abdel-Wahab O, Manshouri T, Patel J, et al. Genetic analysis of transforming events that convert chronic myeloproliferative neoplasms to leukemias. Cancer Res. 2010;70(2):447-452.

75. Lasho TL, Mudireddy M, Finke CM, et al. Targeted next-generation sequencing in blast phase myeloproliferative neoplasms. Blood Adv. 2018;2(4):370-380.

76. Desterke C, Martinaud C, Ruzehaji N, Le Bousse-Kerdiles MC. Inflammation as a Keystone of Bone Marrow Stroma Alterations in Primary Myelofibrosis. Mediators Inflamm. 2015;2015:415024.

77. Wynn TA. Cellular and molecular mechanisms of fibrosis. J Pathol. 2008;214(2):199-210.

78. Tefferi A, Vaidya R, Caramazza D, Finke C, Lasho T, Pardanani A. Circulating interleukin (IL)-8, IL-2R, IL-12, and IL-15 levels are independently prognostic in primary myelofibrosis: a comprehensive cytokine profiling study. J Clin Oncol. 2011;29(10):1356-1363.

79. Roberts AB, Sporn MB, Assoian RK, et al. Transforming growth factor type beta: rapid induction of fibrosis and angiogenesis in vivo and stimulation of collagen formation in vitro. Proc Natl Acad Sci U S A. 1986;83(12):4167-4171.

80. Nakerakanti S, Trojanowska M. The Role of TGF-beta Receptors in Fibrosis. Open Rheumatol J. 2012;6:156-162.

81. Prud'homme GJ. Pathobiology of transforming growth factor beta in cancer, fibrosis and immunologic disease, and therapeutic considerations. Lab Invest. 2007;87(11):1077-1091.

82. Taylor LM, Khachigian LM. Induction of platelet-derived growth factor B-chain expression by transforming growth factor-beta involves transactivation by Smads. J Biol Chem. 2000;275(22):16709-16716.

83. Andrianifahanana M, Wilkes MC, Gupta SK, et al. Profibrotic TGFbeta responses require the cooperative action of PDGF and ErbB receptor tyrosine kinases. FASEB J. 2013;27(11):4444-4454.

84. Lataillade JJ, Pierre-Louis O, Hasselbalch HC, et al. Does primary myelofibrosis involve a defective stem cell niche? From concept to evidence. Blood. 2008;112(8):3026-3035.

85. Le Bousse-Kerdiles MC. Primary myelofibrosis and the "bad seeds in bad soil" concept. Fibrogenesis Tissue Repair. 2012;5(Suppl 1):S20.

86. Zhao M, Perry JM, Marshall H, et al. Megakaryocytes maintain homeostatic quiescence and promote post-injury regeneration of hematopoietic stem cells. Nat Med. 2014;20(11):1321-1326.

87. Caenazzo A, Pietrogrande F, Polato G, et al. Changes in the mitogenic activity of platelet-derived growth factor(s) in patients with myeloproliferative disease. Acta Haematol. 1989;81(3):131-135.

88. Reilly JT. Pathogenesis of idiopathic myelofibrosis: role of growth factors. J Clin Pathol. 1992;45(6):461-464.

89. Bock O, Loch G, Busche G, von Wasielewski R, Schlue J, Kreipe H. Aberrant expression of platelet-derived growth factor (PDGF) and PDGF receptor-alpha is associated with advanced bone marrow fibrosis in idiopathic myelofibrosis. Haematologica. 2005;90(1):133-134.

90. Bedekovics J, Kiss A, Beke L, Karolyi K, Mehes G. Platelet derived growth factor receptor-beta (PDGFRbeta) expression is limited to activated stromal cells in the bone marrow and shows a strong correlation with the grade of myelofibrosis. Virchows Arch. 2013;463(1):57-65.

91. Le Bousse-Kerdiles MC, Martyre MC, French IrnoIM. Involvement of the fibrogenic cytokines, TGF-beta and bFGF, in the pathogenesis of idiopathic myelofibrosis. Pathol Biol (Paris). 2001;49(2):153-157.

92. Martyre MC. TGF-beta and megakaryocytes in the pathogenesis of myelofibrosis in myeloproliferative disorders. Leuk Lymphoma. 1995;20(1-2):39-44.

93. Chagraoui H, Komura E, Tulliez M, Giraudier S, Vainchenker W, Wendling F. Prominent role of TGF-beta 1 in thrombopoietin-induced myelofibrosis in mice. Blood. 2002;100(10):3495-3503.

94. Di Raimondo F, Azzaro MP, Palumbo GA, et al. Elevated vascular endothelial growth factor (VEGF) serum levels in idiopathic myelofibrosis. Leukemia. 2001;15(6):976-980.

95. Steurer M, Zoller H, Augustin F, et al. Increased angiogenesis in chronic idiopathic myelofibrosis: vascular endothelial growth factor as a prominent angiogenic factor. Hum Pathol. 2007;38(7):1057-1064.

96. Kroger NM, Deeg JH, Olavarria E, et al. Indication and management of allogeneic stem cell transplantation in primary myelofibrosis: a consensus process by an EBMT/ELN international working group. Leukemia. 2015;29(11):2126-2133.

97. McLornan DP, Yakoub-Agha I, Robin M, Chalandon Y, Harrison CN, Kroger N. State-of-the-art review: allogeneic stem cell transplantation for myelofibrosis in 2019. Haematologica. 2019;104(4):659-668.

98. Guglielmelli P, Rotunno G, Bogani C, et al. Ruxolitinib is an effective treatment for CALR-positive patients with myelofibrosis. Br J Haematol. 2016;173(6):938-940.

99. Pacilli A, Rotunno G, Mannarelli C, et al. Mutation landscape in patients with myelofibrosis receiving ruxolitinib or hydroxyurea. Blood Cancer J. 2018;8(12):122.

100. Verstovsek S, Mesa RA, Gotlib J, et al. Long-term treatment with ruxolitinib for patients with myelofibrosis: 5-year update from the randomized, double-blind, placebo-controlled, phase 3 COMFORT-I trial. J Hematol Oncol. 2017;10(1):55.

101. Harrison CN, Vannucchi AM, Kiladjian JJ, et al. Long-term findings from COMFORT-II, a phase 3 study of ruxolitinib vs best available therapy for myelofibrosis. Leukemia. 2016;30(8):1701-1707.

102. Deininger M, Radich J, Burn TC, Huber R, Paranagama D, Verstovsek S. The effect of long-term ruxolitinib treatment on JAK2p.V617F allele burden in patients with myelofibrosis. Blood. 2015;126(13):1551-1554.

103. Stivala S, Codilupi T, Brkic S, et al. Targeting compensatory MEK/ERK activation increases JAK inhibitor efficacy in myeloproliferative neoplasms. J Clin Invest. 2019;130:1596-1611.

104. Cervantes F. How I treat myelofibrosis. Blood. 2014;124(17):2635-2642.

105. Kohler N, Lipton A. Platelets as a source of fibroblast growth-promoting activity. Exp Cell Res. 1974;87(2):297-301.

106. Ross R, Glomset J, Kariya B, Harker L. A platelet-dependent serum factor that stimulates the proliferation of arterial smooth muscle cells in vitro. Proc Natl Acad Sci U S A. 1974;71(4):1207-1210.

107. Westermark B, Wasteson A. A platelet factor stimulating human normal glial cells. Exp Cell Res. 1976;98(1):170-174.

108. Fredriksson L, Li H, Eriksson U. The PDGF family: four gene products form five dimeric isoforms. Cytokine Growth Factor Rev. 2004;15(4):197-204.

109. Heldin CH, Westermark B, Wasteson A. Platelet-derived growth factor: purification and partial characterization. Proc Natl Acad Sci U S A. 1979;76(8):3722-3726.

110. Antoniades HN, Scher CD. Radioimmunoassay of a human serum growth factor for Balb/c-3T3 cells: derivation from platelets. Proc Natl Acad Sci U S A. 1977;74(5):1973-1977.

111. Vogel A, Raines E, Kariya B, Rivest MJ, Ross R. Coordinate control of 3T3 cell proliferation by platelet-derived growth factor and plasma components. Proc Natl Acad Sci U S A. 1978;75(6):2810-2814.

112. Heldin CH, Wasteson A, Westermark B. Partial purification and characterization of platelet factors stimulating the multiplication of normal human glial cells. Exp Cell Res. 1977;109(2):429-437.

113. Oefner C, D'Arcy A, Winkler FK, Eggimann B, Hosang M. Crystal structure of human platelet-derived growth factor BB. EMBO J. 1992;11(11):3921-3926.

114. Bergsten E, Uutela M, Li X, et al. PDGF-D is a specific, protease-activated ligand for the PDGF beta-receptor. Nat Cell Biol. 2001;3(5):512-516.

115. Li X, Ponten A, Aase K, et al. PDGF-C is a new protease-activated ligand for the PDGF alpha-receptor. Nat Cell Biol. 2000;2(5):302-309.

116. Heldin CH, Westermark B. Mechanism of action and in vivo role of platelet-derived growth factor. Physiol Rev. 1999;79(4):1283-1316.

117. Gilbertson DG, Duff ME, West JW, et al. Platelet-derived growth factor C (PDGF-C), a novel growth factor that binds to PDGF alpha and beta receptor. J Biol Chem. 2001;276(29):27406-27414.

118. Wickenhauser C, Hillienhof A, Jungheim K, et al. Detection and quantification of transforming growth factor beta (TGF-beta) and platelet-derived growth factor (PDGF) release by normal human megakaryocytes. Leukemia. 1995;9(2):310-315.

119. Hoch RV, Soriano P. Roles of PDGF in animal development. Development. 2003;130(20):4769-4784.

120. Leveen P, Pekny M, Gebre-Medhin S, Swolin B, Larsson E, Betsholtz C. Mice deficient for PDGF B show renal, cardiovascular, and hematological abnormalities. Genes Dev. 1994;8(16):1875-1887.

121. Soriano P. Abnormal kidney development and hematological disorders in PDGF beta-receptor mutant mice. Genes Dev. 1994;8(16):1888-1896.

122. Lindahl P, Johansson BR, Leveen P, Betsholtz C. Pericyte loss and microaneurysm formation in PDGF-B-deficient mice. Science. 1997;277(5323):242-245.

123. Bostrom H, Willetts K, Pekny M, et al. PDGF-A signaling is a critical event in lung alveolar myofibroblast development and alveogenesis. Cell. 1996;85(6):863-873.

124. Soriano P. The PDGF alpha receptor is required for neural crest cell development and for normal patterning of the somites. Development. 1997;124(14):2691-2700.

125. Ding H, Wu X, Bostrom H, et al. A specific requirement for PDGF-C in palate formation and PDGFR-alpha signaling. Nat Genet. 2004;36(10):1111-1116.

126. Gladh H, Folestad EB, Muhl L, et al. Mice Lacking Platelet-Derived Growth Factor D Display a Mild Vascular Phenotype. PLoS One. 2016;11(3):e0152276.

127. Heldin CH, Lennartsson J. Structural and functional properties of platelet-derived growth factor and stem cell factor receptors. Cold Spring Harb Perspect Biol. 2013;5(8):a009100.

128. Heldin CH, Ostman A, Ronnstrand L. Signal transduction via platelet-derived growth factor receptors. Biochim Biophys Acta. 1998;1378(1):F79-113.

129. Srinivasan D, Kaetzel DM, Plattner R. Reciprocal regulation of Abl and receptor tyrosine kinases. Cell Signal. 2009;21(7):1143-1150.

130. Hansen K, Johnell M, Siegbahn A, et al. Mutation of a Src phosphorylation site in the PDGF beta-receptor leads to increased PDGF-stimulated chemotaxis but decreased mitogenesis. EMBO J. 1996;15(19):5299-5313.

131. Baxter RM, Secrist JP, Vaillancourt RR, Kazlauskas A. Full activation of the platelet-derived growth factor beta-receptor kinase involves multiple events. J Biol Chem. 1998;273(27):17050-17055.

132. Twamley-Stein GM, Pepperkok R, Ansorge W, Courtneidge SA. The Src family tyrosine kinases are required for platelet-derived growth factor-mediated signal transduction in NIH 3T3 cells. Proc Natl Acad Sci U S A. 1993;90(16):7696-7700.

133. Mori S, Ronnstrand L, Yokote K, et al. Identification of two juxtamembrane autophosphorylation sites in the PDGF beta-receptor; involvement in the interaction with Src family tyrosine kinases. EMBO J. 1993;12(6):2257-2264.

134. Panayotou G, Bax B, Gout I, et al. Interaction of the p85 subunit of PI 3-kinase and its N-terminal SH2 domain with a PDGF receptor phosphorylation site: structural features and analysis of conformational changes. EMBO J. 1992;11(12):4261-4272.

135. Kashishian A, Kazlauskas A, Cooper JA. Phosphorylation sites in the PDGF receptor with different specificities for binding GAP and PI3 kinase in vivo. EMBO J. 1992;11(4):1373-1382.

136. Nishimura R, Li W, Kashishian A, et al. Two signaling molecules share a phosphotyrosine-containing binding site in the platelet-derived growth factor receptor. Mol Cell Biol. 1993;13(11):6889-6896.

137. Arvidsson AK, Rupp E, Nanberg E, et al. Tyr-716 in the platelet-derived growth factor beta-receptor kinase insert is involved in GRB2 binding and Ras activation. Mol Cell Biol. 1994;14(10):6715-6726.

138. Yokote K, Margolis B, Heldin CH, Claesson-Welsh L. Grb7 is a downstream signaling component of platelet-derived growth factor alpha- and beta-receptors. J Biol Chem. 1996;271(48):30942-30949.

139. Fantl WJ, Escobedo JA, Martin GA, et al. Distinct phosphotyrosines on a growth factor receptor bind to specific molecules that mediate different signaling pathways. Cell. 1992;69(3):413-423.

140. Kazlauskas A, Kashishian A, Cooper JA, Valius M. GTPase-activating protein and phosphatidylinositol 3-kinase bind to distinct regions of the platelet-derived growth factor receptor beta subunit. Mol Cell Biol. 1992;12(6):2534-2544.

141. Jurek A, Heldin CH, Lennartsson J. Platelet-derived growth factor-induced signaling pathways interconnect to regulate the temporal pattern of Erk1/2 phosphorylation. Cell Signal. 2011;23(1):280-287.

142. Ridefelt P, Siegbahn A. Tyr1009 and Tyr1021 in the platelet-derived growth factor beta-receptor mediate agonist triggered calcium signalling. Anticancer Res. 1998;18(3A):1819-1825.

143. Ronnstrand L, Mori S, Arridsson AK, et al. Identification of two C-terminal autophosphorylation sites in the PDGF beta-receptor: involvement in the interaction with phospholipase C-gamma. EMBO J. 1992;11(11):3911-3919.

144. Eriksson A, Nanberg E, Ronnstrand L, et al. Demonstration of functionally different interactions between phospholipase C-gamma and the two types of platelet-derived growth factor receptors. J Biol Chem. 1995;270(13):7773-7781.

145. Klinghoffer RA, Mueting-Nelsen PF, Faerman A, Shani M, Soriano P. The two PDGF receptors maintain conserved signaling in vivo despite divergent embryological functions. Mol Cell. 2001;7(2):343-354.

146. Barst RJ. PDGF signaling in pulmonary arterial hypertension. J Clin Invest. 2005;115(10):2691-2694.

147. Ten Freyhaus H, Berghausen EM, Janssen W, et al. Genetic Ablation of PDGF-Dependent Signaling Pathways Abolishes Vascular Remodeling and Experimental Pulmonary Hypertension. Arterioscler Thromb Vasc Biol. 2015;35(5):1236-1245.

148. Kappert K, Paulsson J, Sparwel J, et al. Dynamic changes in the expression of DEP-1 and other PDGF receptor-antagonizing PTPs during onset and termination of neointima formation. FASEB J. 2007;21(2):523-534.

149. George SJ, Williams A, Newby AC. An essential role for platelet-derived growth factor in neointima formation in human saphenous vein in vitro. Atherosclerosis. 1996;120(1-2):227-240.

150. Clarke ID, Dirks PB. A human brain tumor-derived PDGFR-alpha deletion mutant is transforming. Oncogene. 2003;22(5):722-733.

151. Ozawa T, Brennan CW, Wang L, et al. PDGFRA gene rearrangements are frequent genetic events in PDGFRA-amplified glioblastomas. Genes Dev. 2010;24(19):2205-2218.

152. Verhaak RG, Hoadley KA, Purdom E, et al. Integrated genomic analysis identifies clinically relevant subtypes of glioblastoma characterized by abnormalities in PDGFRA, IDH1, EGFR, and NF1. Cancer Cell. 2010;17(1):98-110.

153. Heinrich MC, Corless CL, Duensing A, et al. PDGFRA activating mutations in gastrointestinal stromal tumors. Science. 2003;299(5607):708-710.

154. Golub TR, Barker GF, Lovett M, Gilliland DG. Fusion of PDGF receptor beta to a novel ets-like gene, tel, in chronic myelomonocytic leukemia with t(5;12) chromosomal translocation. Cell. 1994;77(2):307-316.

155. Cools J, DeAngelo DJ, Gotlib J, et al. A tyrosine kinase created by fusion of the PDGFRA and FIP1L1 genes as a therapeutic target of imatinib in idiopathic hypereosinophilic syndrome. N Engl J Med. 2003;348(13):1201-1214.

156. Simon MP, Pedeutour F, Sirvent N, et al. Deregulation of the platelet-derived growth factor B-chain gene via fusion with collagen gene COL1A1 in dermatofibrosarcoma protuberans and giant-cell fibroblastoma. Nat Genet. 1997;15(1):95-98.

157. Patel KU, Szabo SS, Hernandez VS, et al. Dermatofibrosarcoma protuberans COL1A1-PDGFB fusion is identified in virtually all dermatofibrosarcoma protuberans cases when investigated by newly developed multiplex reverse transcription polymerase chain reaction and fluorescence in situ hybridization assays. Hum Pathol. 2008;39(2):184-193.

158. Ghanem M, Nijman R, Safan M, van der Kwast T, Vansteenbrugge G. Expression and prognostic value of platelet-derived growth factor-AA and its receptor alpha in nephroblastoma. BJU Int. 2010;106(9):1389-1393.

159. Carvalho I, Milanezi F, Martins A, Reis RM, Schmitt F. Overexpression of platelet-derived growth factor receptor alpha in breast cancer is associated with tumour progression. Breast Cancer Res. 2005;7(5):R788-795.

160. Kawai T, Hiroi S, Torikata C. Expression in lung carcinomas of platelet-derived growth factor and its receptors. Lab Invest. 1997;77(5):431-436.

161. Henriksen R, Funa K, Wilander E, Backstrom T, Ridderheim M, Oberg K. Expression and prognostic significance of platelet-derived growth factor and its receptors in epithelial ovarian neoplasms. Cancer Res. 1993;53(19):4550-4554.

162. Zhao J, Roth J, Bode-Lesniewska B, Pfaltz M, Heitz PU, Komminoth P. Combined comparative genomic hybridization and genomic microarray for detection of gene amplifications in pulmonary artery intimal sarcomas and adrenocortical tumors. Genes Chromosomes Cancer. 2002;34(1):48-57.

163. Arai H, Ueno T, Tangoku A, et al. Detection of amplified oncogenes by genome DNA microarrays in human primary esophageal squamous cell carcinoma: comparison with conventional comparative genomic hybridization analysis. Cancer Genet Cytogenet. 2003;146(1):16-21.

164. Fischer AN, Fuchs E, Mikula M, Huber H, Beug H, Mikulits W. PDGF essentially links TGF-beta signaling to nuclear beta-catenin accumulation in hepatocellular carcinoma progression. Oncogene. 2007;26(23):3395-3405.

165. Farooqi AA, Siddik ZH. Platelet-derived growth factor (PDGF) signalling in cancer: rapidly emerging signalling landscape. Cell Biochem Funct. 2015;33(5):257-265.

166. Di Rocco F, Carroll RS, Zhang J, Black PM. Platelet-derived growth factor and its receptor expression in human oligodendrogliomas. Neurosurgery. 1998;42(2):341-346.

167. Smith JS, Wang XY, Qian J, et al. Amplification of the platelet-derived growth factor receptor-A (PDGFRA) gene occurs in oligodendrogliomas with grade IV anaplastic features. J Neuropathol Exp Neurol. 2000;59(6):495-503.

168. Ko YJ, Small EJ, Kabbinavar F, et al. A multi-institutional phase ii study of SU101, a platelet-derived growth factor receptor inhibitor, for patients with hormone-refractory prostate cancer. Clin Cancer Res. 2001;7(4):800-805.

169. Ustach CV, Huang W, Conley-LaComb MK, et al. A novel signaling axis of matriptase/PDGF-D/ss-PDGFR in human prostate cancer. Cancer Res. 2010;70(23):9631-9640.

170. Ostman A. PDGF receptors in tumor stroma: Biological effects and associations with prognosis and response to treatment. Adv Drug Deliv Rev. 2017;121:117-123.

171. Pietras K, Ostman A. Hallmarks of cancer: interactions with the tumor stroma. Exp Cell Res. 2010;316(8):1324-1331.

172. Lindmark G, Sundberg C, Glimelius B, Pahlman L, Rubin K, Gerdin B. Stromal expression of platelet-derived growth factor beta-receptor and platelet-derived growth factor B-chain in colorectal cancer. Lab Invest. 1993;69(6):682-689.

173. Donnem T, Al-Saad S, Al-Shibli K, Andersen S, Busund LT, Bremnes RM. Prognostic impact of platelet-derived growth factors in non-small cell lung cancer tumor and stromal cells. J Thorac Oncol. 2008;3(9):963-970.

174. Shaw RJ, Benedict SH, Clark RA, King TE, Jr. Pathogenesis of pulmonary fibrosis in interstitial lung disease. Alveolar macrophage PDGF(B) gene activation and up-regulation by interferon gamma. Am Rev Respir Dis. 1991;143(1):167-173.

175. Bonner JC, Lindroos PM, Rice AB, Moomaw CR, Morgan DL. Induction of PDGF receptor-alpha in rat myofibroblasts during pulmonary fibrogenesis in vivo. Am J Physiol. 1998;274(1):L72-80.

176. Hoyle GW, Li J, Finkelstein JB, et al. Emphysematous lesions, inflammation, and fibrosis in the lungs of transgenic mice overexpressing platelet-derived growth factor. Am J Pathol. 1999;154(6):1763-1775.

177. Pinzani M, Milani S, Herbst H, et al. Expression of platelet-derived growth factor and its receptors in normal human liver and during active hepatic fibrogenesis. Am J Pathol. 1996;148(3):785-800.

178. Ikura Y, Morimoto H, Ogami M, Jomura H, Ikeoka N, Sakurai M. Expression of platelet-derived growth factor and its receptor in livers of patients with chronic liver disease. J Gastroenterol. 1997;32(4):496-501.

179. Borkham-Kamphorst E, van Roeyen CR, Ostendorf T, Floege J, Gressner AM, Weiskirchen R. Pro-fibrogenic potential of PDGF-D in liver fibrosis. J Hepatol. 2007;46(6):1064-1074.

180. Yoshimura A, Gordon K, Alpers CE, et al. Demonstration of PDGF B-chain mRNA in glomeruli in mesangial proliferative nephritis by in situ hybridization. Kidney Int. 1991;40(3):470-476.

181. Floege J, Johnson RJ, Alpers CE, et al. Visceral glomerular epithelial cells can proliferate in vivo and synthesize platelet-derived growth factor B-chain. Am J Pathol. 1993;142(2):637-650.

182. Pandolfi A, Florita M, Altomare G, Pigatto P, Donati MB, Poggi A. Increased plasma levels of platelet-derived growth factor activity in patients with progressive systemic sclerosis. Proc Soc Exp Biol Med. 1989;191(1):1-4.

183. Klareskog L, Gustafsson R, Scheynius A, Hallgren R. Increased expression of platelet-derived growth factor type B receptors in the skin of patients with systemic sclerosis. Arthritis Rheum. 1990;33(10):1534-1541.

184. Buhl EM, Djudjaj S, Babickova J, et al. The role of PDGF-D in healthy and fibrotic kidneys. Kidney Int. 2016;89(4):848-861.

185. Bonner JC. Regulation of PDGF and its receptors in fibrotic diseases. Cytokine Growth Factor Rev. 2004;15(4):255-273.

186. Klinkhammer BM, Floege J, Boor P. PDGF in organ fibrosis. Mol Aspects Med. 2018;62:44-62.

187. Bedekovics J, Szeghalmy S, Beke L, Fazekas A, Mehes G. Image analysis of platelet derived growth factor receptor-beta (PDGFRbeta) expression to determine the grade and dynamics of myelofibrosis in bone marrow biopsy samples. Cytometry B Clin Cytom. 2014;86(5):319-328.

188. Mehes G, Tzankov A, Hebeda K, Anagnostopoulos I, Krenacs L, Bedekovics J. Platelet-derived growth factor receptor beta (PDGFRbeta) immunohistochemistry highlights activated bone marrow stroma and is potentially predictive for fibrosis progression in prefibrotic myeloproliferative neoplasia. Histopathology. 2015;67(5):617-624.

189. Heldin CH. Targeting the PDGF signaling pathway in tumor treatment. Cell Commun Signal. 2013;11:97.

190. Moen MD, McKeage K, Plosker GL, Siddiqui MA. Imatinib: a review of its use in chronic myeloid leukaemia. Drugs. 2007;67(2):299-320.

191. Helbig G, Stella-Holowiecka B, Majewski M, et al. A single weekly dose of imatinib is sufficient to induce and maintain remission of chronic eosinophilic leukaemia in FIP1L1-PDGFRA-expressing patients. Br J Haematol. 2008;141(2):200-204.

192. Cheah CY, Burbury K, Apperley JF, et al. Patients with myeloid malignancies bearing PDGFRB fusion genes achieve durable long-term remissions with imatinib. Blood. 2014;123(23):3574-3577.

193. Tefferi A, Mesa RA, Gray LA, et al. Phase 2 trial of imatinib mesylate in myelofibrosis with myeloid metaplasia. Blood. 2002;99(10):3854-3856.

194. Hasselbalch HC, Bjerrum OW, Jensen BA, et al. Imatinib mesylate in idiopathic and postpolycythemic myelofibrosis. Am J Hematol. 2003;74(4):238-242.

195. Cortes J, Giles F, O'Brien S, et al. Results of imatinib mesylate therapy in patients with refractory or recurrent acute myeloid leukemia, high-risk myelodysplastic syndrome, and myeloproliferative disorders. Cancer. 2003;97(11):2760-2766.

196. Hawthorne T, Giot L, Blake L, et al. A phase I study of CR002, a fully-human monoclonal antibody against platelet-derived growth factor-D. Int J Clin Pharmacol Ther. 2008;46(5):236-244.

197. Jayson GC, Parker GJ, Mullamitha S, et al. Blockade of platelet-derived growth factor receptor-beta by CDP860, a humanized, PEGylated di-Fab', leads to fluid accumulation and is associated with increased tumor vascularized volume. J Clin Oncol. 2005;23(5):973-981.

198. Pender A, Jones RL. Olaratumab: a platelet-derived growth factor receptor-alpha-blocking antibody for the treatment of soft tissue sarcoma. Clin Pharmacol. 2017;9:159-164.

199. Hao ZM, Fan XB, Li S, et al. Vaccination with platelet-derived growth factor B kinoids inhibits CCl(4)-induced hepatic fibrosis in mice. J Pharmacol Exp Ther. 2012;342(3):835-842.

200. Sorkin A, Westermark B, Heldin CH, Claesson-Welsh L. Effect of receptor kinase inactivation on the rate of internalization and degradation of PDGF and the PDGF beta-receptor. J Cell Biol. 1991;112(3):469-478.

201. Chiarugi P, Cirri P, Taddei ML, et al. New perspectives in PDGF receptor downregulation: the main role of phosphotyrosine phosphatases. J Cell Sci. 2002;115(Pt 10):2219-2232.

202. Wang Y, Pennock SD, Chen X, Kazlauskas A, Wang Z. Platelet-derived growth factor receptor-mediated signal transduction from endosomes. J Biol Chem. 2004;279(9):8038-8046.

203. Mustelin T, Feng GS, Bottini N, et al. Protein tyrosine phosphatases. Front Biosci. 2002;7:d85-142.

204. Ostman A, Bohmer FD. Regulation of receptor tyrosine kinase signaling by protein tyrosine phosphatases. Trends Cell Biol. 2001;11(6):258-266.

205. Schlessinger J. Cell signaling by receptor tyrosine kinases. Cell. 2000;103(2):211-225.

206. Alonso A, Sasin J, Bottini N, et al. Protein tyrosine phosphatases in the human genome. Cell. 2004;117(6):699-711.

207. Tonks NK. Protein tyrosine phosphatases: from genes, to function, to disease. Nat Rev Mol Cell Biol. 2006;7(11):833-846.

208. Zhang ZY, Maclean D, McNamara DJ, Sawyer TK, Dixon JE. Protein tyrosine phosphatase substrate specificity: size and phosphotyrosine positioning requirements in peptide substrates. Biochemistry. 1994;33(8):2285-2290.

209. Neel BG, Tonks NK. Protein tyrosine phosphatases in signal transduction. Curr Opin Cell Biol. 1997;9(2):193-204.

210. Julien SG, Dube N, Hardy S, Tremblay ML. Inside the human cancer tyrosine phosphatome. Nat Rev Cancer. 2011;11(1):35-49.

211. Haj FG, Markova B, Klaman LD, Bohmer FD, Neel BG. Regulation of receptor tyrosine kinase signaling by protein tyrosine phosphatase-1B. J Biol Chem. 2003;278(2):739-744.

212. Markova B, Herrlich P, Ronnstrand L, Bohmer FD. Identification of protein tyrosine phosphatases associating with the PDGF receptor. Biochemistry. 2003;42(9):2691-2699.

213. Venkatesan B, Ghosh-Choudhury N, Das F, et al. Resveratrol inhibits PDGF receptor mitogenic signaling in mesangial cells: role of PTP1B. FASEB J. 2008;22(10):3469-3482.

214. Persson C, Savenhed C, Bourdeau A, et al. Site-selective regulation of platelet-derived growth factor beta receptor tyrosine phosphorylation by T-cell protein tyrosine phosphatase. Mol Cell Biol. 2004;24(5):2190-2201.

215. Yu Z, Su L, Hoglinger O, Jaramillo ML, Banville D, Shen SH. SHP-1 associates with both platelet-derived growth factor receptor and the p85 subunit of phosphatidylinositol 3-kinase. J Biol Chem. 1998;273(6):3687-3694.

216. Tibaldi E, Zonta F, Bordin L, et al. The tyrosine phosphatase SHP-1 inhibits proliferation of activated hepatic stellate cells by impairing PDGF receptor signaling. Biochim Biophys Acta. 2014;1843(2):288-298.

217. Klinghoffer RA, Kazlauskas A. Identification of a putative Syp substrate, the PDGF beta receptor. J Biol Chem. 1995;270(38):22208-22217.

218. Dechert U, Adam M, Harder KW, Clark-Lewis I, Jirik F. Characterization of protein tyrosine phosphatase SH-PTP2. Study of phosphopeptide substrates and possible regulatory role of SH2 domains. J Biol Chem. 1994;269(8):5602-5611.

219. Lechleider RJ, Sugimoto S, Bennett AM, et al. Activation of the SH2-containing phosphotyrosine phosphatase SH-PTP2 by its binding site, phosphotyrosine 1009, on the human platelet-derived growth factor receptor. J Biol Chem. 1993;268(29):21478-21481.

220. Bennett AM, Tang TL, Sugimoto S, Walsh CT, Neel BG. Protein-tyrosine-phosphatase SHPTP2 couples platelet-derived growth factor receptor beta to Ras. Proc Natl Acad Sci U S A. 1994;91(15):7335-7339.

221. Ronnstrand L, Arvidsson AK, Kallin A, et al. SHP-2 binds to Tyr763 and Tyr1009 in the PDGF beta-receptor and mediates PDGF-induced activation of

the Ras/MAP kinase pathway and chemotaxis. Oncogene. 1999;18(25):3696-3702.

222. Sun T, Aceto N, Meerbrey KL, et al. Activation of multiple proto-oncogenic tyrosine kinases in breast cancer via loss of the PTPN12 phosphatase. Cell. 2011;144(5):703-718.

223. Kovalenko M, Denner K, Sandstrom J, et al. Site-selective dephosphorylation of the platelet-derived growth factor beta-receptor by the receptor-like protein-tyrosine phosphatase DEP-1. J Biol Chem. 2000;275(21):16219-16226.

224. Takahashi Y, Morales FC, Kreimann EL, Georgescu MM. PTEN tumor suppressor associates with NHERF proteins to attenuate PDGF receptor signaling. EMBO J. 2006;25(4):910-920.

225. Chiarugi P, Cirri P, Taddei ML, et al. Insight into the role of low molecular weight phosphotyrosine phosphatase (LMW-PTP) on platelet-derived growth factor receptor (PDGF-r) signaling. LMW-PTP controls PDGF-r kinase activity through TYR-857 dephosphorylation. J Biol Chem. 2002;277(40):37331-37338.

226. Dance M, Montagner A, Salles JP, Yart A, Raynal P. The molecular functions of Shp2 in the Ras/Mitogen-activated protein kinase (ERK1/2) pathway. Cell Signal. 2008;20(3):453-459.

227. Bioukar EB, Marricco NC, Zuo D, Larose L. Serine phosphorylation of the ligand-activated beta-platelet-derived growth factor receptor by casein kinase I-gamma2 inhibits the receptor's autophosphorylating activity. J Biol Chem. 1999;274(30):21457-21463.

228. Ye J, Coulouris G, Zaretskaya I, Cutcutache I, Rozen S, Madden TL. Primer-BLAST: a tool to design target-specific primers for polymerase chain reaction. BMC Bioinformatics. 2012;13:134.

229. Vannucchi AM, Bianchi L, Cellai C, et al. Accentuated response to phenylhydrazine and erythropoietin in mice genetically impaired for their GATA-1 expression (GATA-1(low) mice). Blood. 2001;97(10):3040-3050.

230. Vannucchi AM, Bianchi L, Cellai C, et al. Development of myelofibrosis in mice genetically impaired for GATA-1 expression (GATA-1(low) mice). Blood. 2002;100(4):1123-1132.

231. Ashburner M, Ball CA, Blake JA, et al. Gene ontology: tool for the unification of biology. The Gene Ontology Consortium. Nat Genet. 2000;25(1):25-29.

232. Livak KJ, Schmittgen TD. Analysis of relative gene expression data using real-time quantitative PCR and the 2(-Delta Delta C(T)) Method. Methods. 2001;25(4):402-408.

233. Toth ZE, Mezey E. Simultaneous visualization of multiple antigens with tyramide signal amplification using antibodies from the same species. J Histochem Cytochem. 2007;55(6):545-554.

234. Bradford MM. A rapid and sensitive method for the quantitation of microgram quantities of protein utilizing the principle of protein-dye binding. Anal Biochem. 1976;72:248-254.

235. Vannucchi AM, Pancrazzi A, Guglielmelli P, et al. Abnormalities of GATA-1 in megakaryocytes from patients with idiopathic myelofibrosis. Am J Pathol. 2005;167(3):849-858.

236. Wiede F, Chew SH, van Vliet C, et al. Strain-dependent differences in bone development, myeloid hyperplasia, morbidity and mortality in ptpn2-deficient mice. PLoS One. 2012;7(5):e36703.

237. You-Ten KE, Muise ES, Itie A, et al. Impaired bone marrow microenvironment and immune function in T cell protein tyrosine phosphatase-deficient mice. J Exp Med. 1997;186(5):683-693.

238. Stuible M, Doody KM, Tremblay ML. PTP1B and TC-PTP: regulators of transformation and tumorigenesis. Cancer Metastasis Rev. 2008;27(2):215-230.

239. Ostman A, Yang Q, Tonks NK. Expression of DEP-1, a receptor-like protein-tyrosine-phosphatase, is enhanced with increasing cell density. Proc Natl Acad Sci U S A. 1994;91(21):9680-9684.

240. Tefferi A, Guglielmelli P, Larson DR, et al. Long-term survival and blast transformation in molecularly annotated essential thrombocythemia, polycythemia vera, and myelofibrosis. Blood. 2014;124(16):2507-2513; quiz 2615.

241. Yan XQ, Lacey D, Fletcher F, et al. Chronic exposure to retroviral vector encoded MGDF (mpl-ligand) induces lineage-specific growth and differentiation of megakaryocytes in mice. Blood. 1995;86(11):4025-4033.

242. Villeval JL, Cohen-Solal K, Tulliez M, et al. High thrombopoietin production by hematopoietic cells induces a fatal myeloproliferative syndrome in mice. Blood. 1997;90(11):4369-4383.

243. Kakumitsu H, Kamezaki K, Shimoda K, et al. Transgenic mice overexpressing murine thrombopoietin develop myelofibrosis and osteosclerosis. Leuk Res. 2005;29(7):761-769.

244. Kaushansky K. Thrombopoietin: the primary regulator of platelet production. Blood. 1995;86(2):419-431.

245. Mullally A, Lane SW, Ball B, et al. Physiological Jak2V617F expression causes a lethal myeloproliferative neoplasm with differential effects on hematopoietic stem and progenitor cells. Cancer Cell. 2010;17(6):584-596.

246. Li J, Prins D, Park HJ, et al. Mutant calreticulin knockin mice develop thrombocytosis and myelofibrosis without a stem cell self-renewal advantage. Blood. 2018;131(6):649-661.

247. Romeo PH, Prandini MH, Joulin V, et al. Megakaryocytic and erythrocytic lineages share specific transcription factors. Nature. 1990;344(6265):447-449.

248. Gilles L, Arslan AD, Marinaccio C, et al. Downregulation of GATA1 drives impaired hematopoiesis in primary myelofibrosis. J Clin Invest. 2017;127(4):1316-1320.

249. Pevny L, Simon MC, Robertson E, et al. Erythroid differentiation in chimaeric mice blocked by a targeted mutation in the gene for transcription factor GATA-1. Nature. 1991;349(6306):257-260.

250. Fujiwara Y, Browne CP, Cunniff K, Goff SC, Orkin SH. Arrested development of embryonic red cell precursors in mouse embryos lacking transcription factor GATA-1. Proc Natl Acad Sci U S A. 1996;93(22):12355-12358.

251. McDevitt MA, Shivdasani RA, Fujiwara Y, Yang H, Orkin SH. A "knockdown" mutation created by cis-element gene targeting reveals the dependence of erythroid cell maturation on the level of transcription factor GATA-1. Proc Natl Acad Sci U S A. 1997;94(13):6781-6785.

252. Shivdasani RA, Fujiwara Y, McDevitt MA, Orkin SH. A lineage-selective knockout establishes the critical role of transcription factor GATA-1 in megakaryocyte growth and platelet development. EMBO J. 1997;16(13):3965-3973.

253. Du Z, Lovly CM. Mechanisms of receptor tyrosine kinase activation in cancer. Mol Cancer. 2018;17(1):58.

254. Hoermann G, Greiner G, Valent P. Cytokine Regulation of Microenvironmental Cells in Myeloproliferative Neoplasms. Mediators Inflamm. 2015;869242.

255. Malara A, Abbonante V, Zingariello M, Migliaccio A, Balduini A. Megakaryocyte Contribution to Bone Marrow Fibrosis: many Arrows in the Quiver. Mediterr J Hematol Infect Dis. 2018;10(1):e2018068.

256. Somasundaram R, Schuppan D. Type I, II, III, IV, V, and VI collagens serve as extracellular ligands for the isoforms of platelet-derived growth factor (AA, BB, and AB). J Biol Chem. 1996;271(43):26884-26891.

257. Tan EM, Qin H, Kennedy SH, Rouda S, Fox JWt, Moore JH, Jr. Platelet-derived growth factors-AA and -BB regulate collagen and collagenase gene expression differentially in human fibroblasts. Biochem J. 1995;310 (Pt 2):585-588.

258. Lepisto J, Peltonen J, Vaha-Kreula M, Niinikoski J, Laato M. Platelet-derived growth factor isoforms PDGF-AA, -AB and -BB exert specific effects on collagen gene expression and mitotic activity of cultured human wound fibroblasts. Biochem Biophys Res Commun. 1995;209(2):393-399.

259. Kroger N, Thiele J, Zander A, et al. Rapid regression of bone marrow fibrosis after dose-reduced allogeneic stem cell transplantation in patients with primary myelofibrosis. Exp Hematol. 2007;35(11):1719-1722.

260. Wang JC, Lang HD, Lichter S, Weinstein M, Benn P. Cytogenetic studies of bone marrow fibroblasts cultured from patients with myelofibrosis and myeloid metaplasia. Br J Haematol. 1992;80(2):184-188.

261. Hewitt KJ, Shamis Y, Knight E, et al. PDGFRbeta expression and function in fibroblasts derived from pluripotent cells is linked to DNA demethylation. J Cell Sci. 2012;125(Pt 9):2276-2287.

262. Karlsson S, Kowanetz K, Sandin A, et al. Loss of T-cell protein tyrosine phosphatase induces recycling of the platelet-derived growth factor (PDGF) beta-receptor but not the PDGF alpha-receptor. Mol Biol Cell. 2006;17(11):4846-4855.

263. Hunter T. The Croonian Lecture 1997. The phosphorylation of proteins on tyrosine: its role in cell growth and disease. Philos Trans R Soc Lond B Biol Sci. 1998;353(1368):583-605.

264. Mann M, Ong SE, Gronborg M, Steen H, Jensen ON, Pandey A. Analysis of protein phosphorylation using mass spectrometry: deciphering the phosphoproteome. Trends Biotechnol. 2002;20(6):261-268.

265. Tinti M, Nardozza AP, Ferrari E, et al. The 4G10, pY20 and p-TYR-100 antibody specificity: profiling by peptide microarrays. N Biotechnol. 2012;29(5):571-577.

266. Wiede F, La Gruta NL, Tiganis T. PTPN2 attenuates T-cell lymphopenia-induced proliferation. Nat Commun. 2014;5:3073.

267. Bourdeau A, Trop S, Doody KM, Dumont DJ, Tremblay ML. Inhibition of T cell protein tyrosine phosphatase enhances interleukin-18-dependent hematopoietic stem cell expansion. Stem Cells. 2013;31(2):293-304.

268. Cool DE, Tonks NK, Charbonneau H, Walsh KA, Fischer EH, Krebs EG. cDNA isolated from a human T-cell library encodes a member of the protein-tyrosine-phosphatase family. Proc Natl Acad Sci U S A. 1989;86(14):5257-5261.

269. Champion-Arnaud P, Gesnel MC, Foulkes N, Ronsin C, Sassone-Corsi P, Breathnach R. Activation of transcription via AP-1 or CREB regulatory sites is blocked by protein tyrosine phosphatases. Oncogene. 1991;6(7):1203-1209.

270. Mosinger B, Jr., Tillmann U, Westphal H, Tremblay ML. Cloning and characterization of a mouse cDNA encoding a cytoplasmic protein-tyrosine-phosphatase. Proc Natl Acad Sci U S A. 1992;89(2):499-503.

271. Reddy RS, Swarup G. Alternative splicing generates four different forms of a non-transmembrane protein tyrosine phosphatase mRNA. DNA Cell Biol. 1995;14(12):1007-1015.

272. Lorenzen JA, Dadabay CY, Fischer EH. COOH-terminal sequence motifs target the T cell protein tyrosine phosphatase to the ER and nucleus. J Cell Biol. 1995;131(3):631-643.

273. Lammers R, Bossenmaier B, Cool DE, et al. Differential activities of protein tyrosine phosphatases in intact cells. J Biol Chem. 1993;268(30):22456-22462.

274. Tiganis T, Bennett AM, Ravichandran KS, Tonks NK. Epidermal growth factor receptor and the adaptor protein p52Shc are specific substrates of T-cell protein tyrosine phosphatase. Mol Cell Biol. 1998;18(3):1622-1634.

275. Pike KA, Tremblay ML. TC-PTP and PTP1B: Regulating JAK-STAT signaling, controlling lymphoid malignancies. Cytokine. 2016;82:52-57.

276. Simoncic PD, Bourdeau A, Lee-Loy A, et al. T-cell protein tyrosine phosphatase (Tcptp) is a negative regulator of colony-stimulating factor 1 signaling and macrophage differentiation. Mol Cell Biol. 2006;26(11):4149-4160.

277. Lee H, Kim M, Baek M, et al. Targeted disruption of TC-PTP in the proliferative compartment augments STAT3 and AKT signaling and skin tumor development. Sci Rep. 2017;7:45077.

278. Lee H, Morales LD, Slaga TJ, Kim DJ. Activation of T-cell protein-tyrosine phosphatase suppresses keratinocyte survival and proliferation following UVB irradiation. J Biol Chem. 2015;290(1):13-24.

279. Huang S. Non-genetic heterogeneity of cells in development: more than just noise. Development. 2009;136(23):3853-3862.

280. Levsky JM, Singer RH. Gene expression and the myth of the average cell. Trends Cell Biol. 2003;13(1):4-6.

281. Fredriksson S, Gullberg M, Jarvius J, et al. Protein detection using proximity-dependent DNA ligation assays. Nat Biotechnol. 2002;20(5):473-477.

282. Soderberg O, Leuchowius KJ, Gullberg M, et al. Characterizing proteins and their interactions in cells and tissues using the in situ proximity ligation assay. Methods. 2008;45(3):227-232.

283. Jarvius M, Paulsson J, Weibrecht I, et al. In situ detection of phosphorylated platelet-derived growth factor receptor beta using a generalized proximity ligation method. Mol Cell Proteomics. 2007;6(9):1500-1509.

284. Liu Y, Gu J, Hagner-McWhirter A, et al. Western blotting via proximity ligation for high performance protein analysis. Mol Cell Proteomics. 2011;10(11):O111 011031.

285. Xie R, Chung JY, Ylaya K, et al. Factors influencing the degradation of archival formalin-fixed paraffin-embedded tissue sections. J Histochem Cytochem. 2011;59(4):356-365.

286. Patterson S, Gross J, Webster AD. DNA probes bind non-specifically to eosinophils during in situ hybridization: carbol chromotrope blocks binding to eosinophils but does not inhibit hybridization to specific nucleotide sequences. J Virol Methods. 1989;23(2):105-109.

287. Di Cristofano A, Pandolfi PP. The multiple roles of PTEN in tumor suppression. Cell. 2000;100(4):387-390.

288. Zhang J, Zhang F, Niu R. Functions of Shp2 in cancer. J Cell Mol Med. 2015;19(9):2075-2083.

289. Scrima M, De Marco C, De Vita F, et al. The nonreceptor-type tyrosine phosphatase PTPN13 is a tumor suppressor gene in non-small cell lung cancer. Am J Pathol. 2012;180(3):1202-1214.

290. den Hertog J, Ostman A, Bohmer FD. Protein tyrosine phosphatases: regulatory mechanisms. FEBS J. 2008;275(5):831-847.

291. Sundaresan M, Yu ZX, Ferrans VJ, Irani K, Finkel T. Requirement for generation of H2O2 for platelet-derived growth factor signal transduction. Science. 1995;270(5234):296-299.

292. Bae YS, Sung JY, Kim OS, et al. Platelet-derived growth factor-induced H(2)O(2) production requires the activation of phosphatidylinositol 3-kinase. J Biol Chem. 2000;275(14):10527-10531.

293. Flint AJ, Gebbink MF, Franza BR, Jr., Hill DE, Tonks NK. Multi-site phosphorylation of the protein tyrosine phosphatase, PTP1B: identification of cell cycle regulated and phorbol ester stimulated sites of phosphorylation. EMBO J. 1993;12(5):1937-1946.

294. Ostergaard HL, Trowbridge IS. Negative regulation of CD45 protein tyrosine phosphatase activity by ionomycin in T cells. Science. 1991;253(5026):1423-1425.

295. Garton AJ, Tonks NK. PTP-PEST: a protein tyrosine phosphatase regulated by serine phosphorylation. EMBO J. 1994;13(16):3763-3771.

296. Sigismund S, Avanzato D, Lanzetti L. Emerging functions of the EGFR in cancer. Mol Oncol. 2018;12(1):3-20.

297. Zhang ZY. Protein tyrosine phosphatases: prospects for therapeutics. Curr Opin Chem Biol. 2001;5(4):416-423.

298. Elchebly M, Payette P, Michaliszyn E, et al. Increased insulin sensitivity and obesity resistance in mice lacking the protein tyrosine phosphatase-1B gene. Science. 1999;283(5407):1544-1548.

299. Klaman LD, Boss O, Peroni OD, et al. Increased energy expenditure, decreased adiposity, and tissue-specific insulin sensitivity in protein-tyrosine phosphatase 1B-deficient mice. Mol Cell Biol. 2000;20(15):5479-5489.

300. Moller NP, Iversen LF, Andersen HS, McCormack JG. Protein tyrosine phosphatases (PTPs) as drug targets: inhibitors of PTP-1B for the treatment of diabetes. Curr Opin Drug Discov Devel. 2000;3(5):527-540.

301. Zhang ZY, Lee SY. PTP1B inhibitors as potential therapeutics in the treatment of type 2 diabetes and obesity. Expert Opin Investig Drugs. 2003;12(2):223-233.

302. Tamrakar AK, Maurya CK, Rai AK. PTP1B inhibitors for type 2 diabetes treatment: a patent review (2011 - 2014). Expert Opin Ther Pat. 2014;24(10):1101-1115.

303. Bhullar KS, Lagaron NO, McGowan EM, et al. Kinase-targeted cancer therapies: progress, challenges and future directions. Mol Cancer. 2018;17(1):48.

304. Le HTT, Cho YC, Cho S. Inhibition of protein tyrosine phosphatase non-receptor type 2 by PTP inhibitor XIX: Its role as a multiphosphatase inhibitor. BMB Rep. 2017;50(6):329-334.

305. Zhang S, Chen L, Luo Y, Gunawan A, Lawrence DS, Zhang ZY. Acquisition of a potent and selective TC-PTP inhibitor via a stepwise fluorophore-tagged combinatorial synthesis and screening strategy. J Am Chem Soc. 2009;131(36):13072-13079.

6   DECLARATION

I hereby declare that this thesis has been composed solely by myself and that the work presented within is my original research. This study does not contain, in whole or in part, material that has previously been submitted to obtain any academic degree.

7 PUBLICATIONS

MANUSCRIPT FROM THIS STUDY

Kramer F, Dernedde J, Mezheyeuski A, Tauber R, Micke P and Kappert K. Platelet-derived growth factor receptor β activation and regulation in murine myelofibrosis. Haematologica, in press.

OTHER MANUSCRRIPTS

Lorenz M, Blaschke B, Benn A, Hammer E, Witt E, Kirwan J, Fritsche-Guenther R, Gloaguen Y, Bartsch C, Vietzke A, **Kramer F**, Kappert K, Brunner P, Nguyen HG, Dreger H, Stangl K, Knaus P and Stangl V. Sex-specific metabolic and functional differences in human umbilical vein endothelial cells from twin pairs. Atherosclerosis, in press.

Krueger F, Kappert K, Foryst-Ludwig A, **Kramer F**, Clemenz M, Grzesiak A, Sommerfeld M, Paul Frese J, Greiner A, Kintscher U, Unger T, Kaschina E. AT1-receptor blockade attenuates outward aortic remodeling associated with diet-induced obesity in mice. Clin Sci (Lond). 2017;131(15):1989-2005.

8 CURRICULUM VITAE

Due to data protection, the Curriculum Vitae is not included in the published online version.